LUND UNIVERSITY

Global sequence and dispersion of ventricular repolarization: In vivo validation of non-invasive parameters using monophasic action potential mapping technique

Xia, Yunlong

2007

GLOBAL SEQUENCE AND DISPERSION OF VENTRICULAR REPOLARIZATION

In vivo validation of non-invasive parameters using monophasic action potential mapping technique

YUNLONG XIA, M.D.

夏 云 龙

DEPARTMENT OF CARDIOLOGY

LUND UNIVERSITY, SWEDEN

2007

Yunlong Xia

Printed at KFS AB, Lund, Sweden
April 2007
Lund University, Faculty of Medicine Doctoral Dissertation Series 2007:96
ISBN 978-91-85559-74-9 ISSN 1652-8220

To My Wife, Ling

My Parents, Hua and Guizhen

My Brother's Family: Yunping, Chunrong and Ji

CONTENTS

ABSTRACT

Objective: To validate the noninvasive parameters, QT interval, QT dispersion, T_{peak}-T_{end} interval, and the activation recovery time (ART) from the unipolar electrograms for estimation of global dispersion of ventricular repolarization (DVR). Also to investigate the changes of repolarization sequence and DVR by altered ventricular pacing sites.

Methods: The material consisted of one series of 12 patients (Study I) and two series with 10 healthy pigs in each (Studies II and III; Studies IV and V).

Endocardial MAPs and unipolar electrograms were simultaneously recorded using the CARTO system from left (LV) and/or right ventricles (RV) in 12 patients. End of repolarization (EOR) times from the MAPs and ART from the unipolar electrograms were acquired and 3-dimensional maps of global EOR and ART were reconstructed (Study I).

Using the CARTO system, MAP mapping was performed over both the endocardium and the epicardium of the LV and RV in 10 open-chest pigs, from which the EOR times over the epicardium (EOR_{epi}), endocardium (EOR_{endo}) and over both (EOR_{total}) were obtained. The minimum and maximum EOR, and the global dispersion of EOR times were calculated and compared to the QT_{peak} and QT_{end} intervals, QT_{peak} and QT_{end} dispersions, and T_{peak}-T_{end} interval measured from simultaneously recorded 12-lead ECG (Studies II and III).

Global MAPs were also recorded from the LV and RV endocardium during right atrial (RA) pacing, RV apex endocardial (RV_{Endo}) pacing and LV laterobasal epicardial (LV_{Epi}) pacing in 10 close-chest pigs. Three-dimensional maps of the activation time (AT) and EOR were constructed, and global sequence and dispersion of ventricular repolarization were evaluated under the above mentioned pacing protocols, and also the QT interval, QT dispersion and T_{peak}-T_{end} interval from the simultaneously recorded 12-lead ECG (Studies IV and V).

Results:

ART mapping for evaluation of global repolarization sequence

In the 12 patients, MAPs were obtained from 34±12 left (n = 6) or right (n = 9) ventricular sites, and 15 sets of 3-dimensional maps of global EOR and ART

sequences were reconstructed. The ART sequence was consistent with the EOR sequence in 14 of 15 maps. In the total 473-paired measurements, the differences between the ART and the EOR time were 2±22 ms (NS). A significant, positive correlation between the ART and the EOR time was found in all maps (r = 0.58±0.22). Agreement analysis showed that the differences between these two measurements were almost all within the range of mean difference ± 2 standard deviations for each individual map, and for all the 473 recordings. The global dispersion of ART was 79±35 ms, and that of EOR time 78±35 ms (NS) (Study I).

Coincidence of the QT_{peak} and QT_{end} with the global EOR times

MAPs were recorded from 51±10 epi- and 64±9 endocardial sites of the LV in the 10 open-chest pigs, and from 41±4 epicardial and 53±2 endocardial sites of the RV in 2 of the 10 pigs, from which the EOR_{epi}, EOR_{endo} and EOR_{total} were obtained, and dispersions of EOR-epi, EOR-endo and EOR-total calculated. The minimal EOR_{total} was on the epicardium in 5 pigs, and the maximal EOR_{total} was on the endocardium in 9 pigs. The minimal, mean and maximal QT_{peak} intervals were all significantly smaller than the maximal EOR_{epi} (322±23 ms, $p < 0.01$). No significant difference was found between the maximal QT_{end} interval (338±30 ms) and the maximal EOR_{endo} (339±24 ms, difference = 1±19 ms, $p = 0.92$), between the maximal QT_{end} interval and the maximal EOR_{total} (341±24 ms, difference = 2±18 ms, $p = 0.69$) nor between the minimal QT_{peak} interval (283±28 ms) and the minimal EOR_{total} (282±20 ms, difference = 0±15 ms, $p = 0.95$) (Study II).

Global dispersion of EOR times and T_{peak}-T_{end} interval

In the 10 open-chest pigs, the maximal T_{peak}-T_{end} intervals (57±7 ms) were consistent with the dispersion of EOR-total (58±11 ms, $p > 0.05$), and significantly correlated with the dispersion of EOR-total (r = 0.64, $p < 0.05$). However, the mean T_{peak}-T_{end} intervals (44±5 ms), and T_{peak}-T_{end} intervals from lead II (41±6 ms) and V_5 (43±5 ms) were all significantly smaller than and poorly correlated with the dispersion of EOR-total, as were the QT_{peak} and QT_{end} dispersions (15±2 ms *vs.* 21±4 ms) (Study III).

Global repolarization sequence under altered ventricular pacing protocols

In the 10 close-chest pigs, MAPs were recorded from 112±16 endocardial sites of both ventricles during RA pacing in 5 pigs (Group I), from 122±23 sites during RV_{Endo} pacing in 10 pigs (Groups I and II), and from 126±26 sites during

LV_{Epi} pacing in 5 pigs (Group II), based on which 20 sets of 3-dimensional maps of AT and EOR over the endocardium of both ventricles were reconstructed. During RA pacing, the EOR sequence followed the AT sequence in both ventricles. Strikingly, the EOR sequence was also consistent with the AT sequence in both ventricles during RV_{Endo} and LV_{Epi} pacing, even though the mapping was performed after an abrupt change of the pacing site. In all maps, there was a negative correlation between the MAP duration and the AT and a positive correlation between the EOR time and the AT under each pacing protocol ($p <$ 0.05-0.001) (Study IV).

Global DVR under different ventricular pacing protocols

In the 10 close-chest pigs, the global dispersion of AT increased from 55±12 ms during RA pacing to 69±15 ms during RV_{Endo} pacing, and to 87±15 ms during LV_{Epi} pacing. The global dispersion of EOR times during LV_{Epi} pacing (94±17 ms) was significantly greater than those during RA (63±12 ms, $p < 0.05$) and RV_{Endo} pacing (72±18 ms, $p < 0.05$), whereas no significant difference was found between those during RA and RV_{Endo} pacing ($p > 0.05$). In addition, the QT intervals, QT dispersion and T_{peak}-T_{end} intervals during LV_{Epi} pacing were all significantly greater than those during RA and RV_{Endo} pacing ($p < 0.05$) (Study V).

Conclusions:

1. The ART from unipolar electrograms is a good estimate of EOR time measured from MAPs, suggesting the usefulness of the former in evaluation of global sequence and dispersion of ventricular repolarization.

2. In *in vivo* pig models, the T_{peak} does not coincide with the full repolarization of the epicardium, but coincides well with the earliest EOR, while the T_{end} corresponds with the latest EOR. These findings suggest that not only the transmural gradients, but also the apico-basal repolarization gradients contribute to the genesis of the T wave.

3. The maximal T_{peak}-T_{end} interval may be used as a noninvasive estimate of the global DVR, but not the QT_{peak} and QT_{end} dispersions, nor the mean T_{peak}-T_{end} interval and that from a single lead.

4. The ventricular repolarization sequence followed the activation sequence not only during RA pacing, but also during RV_{Endo} pacing and LV_{Epi} pacing,

suggesting the importance of activation sequence in governing repolarization patterns. Significant changes in repolarization from an altered activation sequence may happen within a few hours *in vivo*, implying that electrical remodeling of the ventricles may be rapidly induced by altered activation sequence.

5. Compared to RA and RV_{Endo} pacing, LV_{Epi} pacing increases QT interval, QT dispersion, T_{peak}-T_{end} interval and the global DVR. These findings provide *in vivo* evidence supporting the involvement of increased DVR in the incidence of malignant ventricular arrhythmias in a subgroup of patients with biventricular pacing.

Key words: Ventricular repolarization, dispersion, monophasic action potential, electroanatomical mapping, T wave, epicardial pacing.

LIST OF PAPERS

This dissertation is based on the following papers, which will be referred to in the text as Studies I - V.

Study I.

Xia Y, Kongstad O, Hertervig E, Holm M, Olsson B, Yuan S. Activation Recovery Time Measurements in Evaluation of Global Sequence and Dispersion of Ventricular Repolarization. J Electrocardiol. 2005;38(1):28-35.

Study II.

Xia Y, Liang Y, Kongstad O, Liao Q, Holm M, Olsson B, Yuan S. *In Vivo* Validation of the Coincidence of the Peak and End of the T Wave with the Full Repolarization of the Epicardium and Endocardium in Swine. Heart Rhythm 2005;2(2):162-169.

Study III.

Xia Y, Liang Y, Kongstad O, Liao Q, Holm M, Olsson B, Yuan S. T(peak)-T(end) Interval as an Index of Global Dispersion of Ventricular Repolarization: Evaluations Using Monophasic Action Potential Mapping of the Epi- and Endocardium in Swine. J Interv Card Electrophysiol. 2005;14(2):79-87.

Study IV.

Xia Y, Kongstad O, Platonov P, Olsson B, Yuan S. Ventricular Repolarization Sequence During Right Ventricular Endocardial and Left Ventricular Epicardial Pacing: Monophasic Action Potential Mapping in Swine. J Card Electrophysiol. (Submitted)

Study V.

Xia Y, Kongstad O, Platonov P, Olsson B, Yuan S. Increased Global Dispersion of Ventricular Repolarization during Left Ventricular Epicardial Pacing: *In Vivo* Evaluation by Monophasic Action Potential Mapping in Swine. Heart Rhythm (Submitted)

OTHER RELATED WORKS
(NOT INCLUDED IN THIS THESIS)

I. **Yunlong Xia,** Shiwen Yuan. *In vivo* validation of the T-peak to T-end interval: Implications for genesis of the T wave (Editorial). Heart Rhythm 2007;4:349–350.

II. Pyotr Platonov, **Yunlong Xia,** Shiwen Yuan, Rolf Johansson. Non-fluoroscopic Catheter-based Mapping Systems in Cardiac Electrophysiology: From Approved Clinical Indications to Novel Research Usage (Review). The International Journal of Medical Robotics and Computer Assisted Surgery. 2006;2(1): 26-27.

III. Ole Kongstad，**Yunlong Xia**，Yanchun Liang, Eric Ljungstrom, Eva Hertervig, Bertil Olsson, Shiwen Yuan. Epicardial and endocardial dispersion of ventricular repolarization: A study of monophasic action potential mapping in healthy pigs. Scand Cardiovasc J. 2005;39(6):342-7.

IV. Ole Kongstad, **Yunlong Xia,** Pyotr Platonov, Magnus Holm, Bertil Olsson, Shiwen Yuan. Ventricular repolarization sequence on the epicardium and endocardium: monophasic action potential mapping in swine during atrial and ventricular pacing (Submitted).

V. **Yunlong Xia**, Ole Kongstad, Pyotr Platonov P, Bertil Olsson, Shiwen Yuan. T_{peak} to T_{end} interval as an index of global but not local dispersion of ventricular repolarization during right and left ventricular pacing: a monophasic action potential mapping in swine (In manuscript).

VI. **Yunlong Xia,** Bertil Olsson, Shiwen Yuan. Global sequence and dispersion of cardiac repolarization evaluated by integration of monophasic action potential recording and electroanatomic mapping techniques (Review) (In manuscript).

ABBREVIATIONS

ART	activation recovery time
AT	activation time
AP	action potential
CRT	cardiac resynchronization therapy
DVR	dispersion of ventricular repolarization
ECG	electrocardiogram
EOR	end of repolarization time
LV	left ventricle or left ventricular
$LV_{Epi}P$	left ventricular epicardial pacing
MAP	monophasic action potential
MAPd	monophasic action potential duration
RA	right atrium or right atrial
RAP	right atrial pacing
RV	right ventricle or right ventricular
$RV_{Endo}P$	right ventricular endocardial pacing
VF	ventricular fibrillation
VT	ventricular tachycardia

BACKGROUND

Cardiovascular disease remains the leading cause of death in the industrialized world, and sudden cardiac death is the main cause of death in patients with cardiovascular disease. Sudden cardiac death refers to a sudden loss of consciousness caused by cardiac arrest and cessation of cardiac function. It can result in death within 1 hour of the onset of symptoms, and claims at least 300,000 lives annually in the United States (1-3). Ventricular tachycardia (VT) and ventricular fibrillation (VF) are the most common causes of out-of-hospital cardiac arrest, accounting for approximately three quarters of cases (4). The diagnosis and management of ventricular tachyarrhythmias remains one of the most formidable tasks faced by the medical community. The importance of recognizing ventricular tachyarrhythmias, identifying patients at risk, establishing an appropriate work-up, and determining therapy is a challenging task and continues to evolve as data from clinical studies alter the management of VT and VF.

Intensive research during the last few decades has provided us with detailed information about the cell membrane and the ionic channels and currents that form the molecular basis of the membrane potential and the AP, and thereby the changes by the interventions (5-12). However, this knowledge has been gained mainly from experimental studies on single cells or isolated slices of heart muscle, mostly using sophisticated methods that can only be performed in experimental settings. There is very limited information on characteristics of ventricular repolarization in the intact heart and its relationship with clinical ventricular arrhythmias. Thus, development of new methods in this field and further experimental studies are certainly warranted.

To give a better understanding of the various features of ventricular repolarization, several aspects of cardiac repolarization are reviewed below, ranging from ion channels to the inscription of the T wave on the body surface electrogram (ECG), their related methodological aspects, and their relation to arrhythmogenesis.

1. Cell membrane potential and currents

During the resting phase myocardial cells have a negative transmembrane potential of 60-90 mV inside the cell, which is derived from an unequal distribution of sodium ions (Na^+), with a greater concentration outside the cell, and potassium ions (K^+), with a greater concentration inside the cell, across the semipermeable membrane (5, 13).

Cardiac excitation and repolarization are based on the consecutive activation of many membrane currents, which have different roles during different phases of the action potential (AP) (phases 0-4) (Fig. 1). Differences in current densities result in variability in AP configuration in the different cardiac tissues.

Depolarization is a robust and relatively simple process that is universal for almost all excitable tissues. It is mainly produced by sodium influx through a single channel, giving rise to the upstroke of the AP, and the inward L-type calcium current, underlying the plateau phase (Fig. 1). After repolarization, the sodium channel normally recovers rapidly from inactivation (within 10 ms) and is ready to open again (14).

In contrast, repolarization is a very complex process involving fluxes of several different ions through numerous different ionic channels with complex interactions even in a single cell (13) (Fig. 1). Three main repolarizing currents are the transient outward current I_{to}, and the rapid (I_{Kr}) and the slow components (I_{Ks}) of the delayed rectifier current. The transient outward current I_{to} is responsible for the fast early repolarization phase 1 of the AP， giving the AP a “spike and dome” appearance. Activation of I_{to} is very fast, 2-10 ms, but inactivation and recovery show differing rates, and two subpopulations of channels (fast and slow) encoded by different genes are recognizable (6). I_{kr} and I_{ks} are characterized by delayed activations kinetics, and they are the major contributors to repolarization phases 2 and 3. In particular, the slow deactivation of I_{Kr} and I_{Ks} allows potassium currents to contribute to the late phase of phase 3 repolarization (15, 16). There are important differences in kinetics between I_{kr} and I_{ks}. I_{Kr} normally results from rapid activation and very rapid inactivation. At positive membrane potentials, inactivation proceeds at a rate faster than channel activation. However, at membrane potentials below 0 mV, the channel recovers from inactivation and reopens. Consequently, I_{Kr} has a relatively low conductance during the AP plateau (phase 2) but increases during phase 3 repolarization (16), which gives it relatively

strong rectification properties. In contrast, I_{Ks} increases gradually during the plateau phase of the AP because of its slow activation kinetics，but remains activated during phase 3 of repolarization as a result of slow deactivation (15).

The inward calcium $I_{Ca(L)}$ current channels are worth mentioning here, because they are essential contributor to the electrophysiological properties of the heart, and they also act as critical initiator of cardiac excitation-contraction coupling. Cardiac $I_{Ca(L)}$ is rapidly activated by depolarization, reaching a peak in 2-7 ms, and triggers Ca^{2+} release via the type-2-ryanodine receptor (RyR2) from the sarcoplasmic reticulum to generate the calcium transient, which, in turn, carries the contraction message to the contractile elements of the cell (17-19) . It is the $I_{Ca(L)}$ together with residual I_{Na} that maintains the AP plateau (phase 2). Compared to I_{Na}, however, the early $I_{Ca(L)}$ spike contributes very little to depolarization of the normal AP upstroke in myocardium. It slowly declines as L-type calcium channel inactivation is time-, voltage-, and Ca^{2+}-dependent.

The balance between these depolarizing and repolarizing currents and their

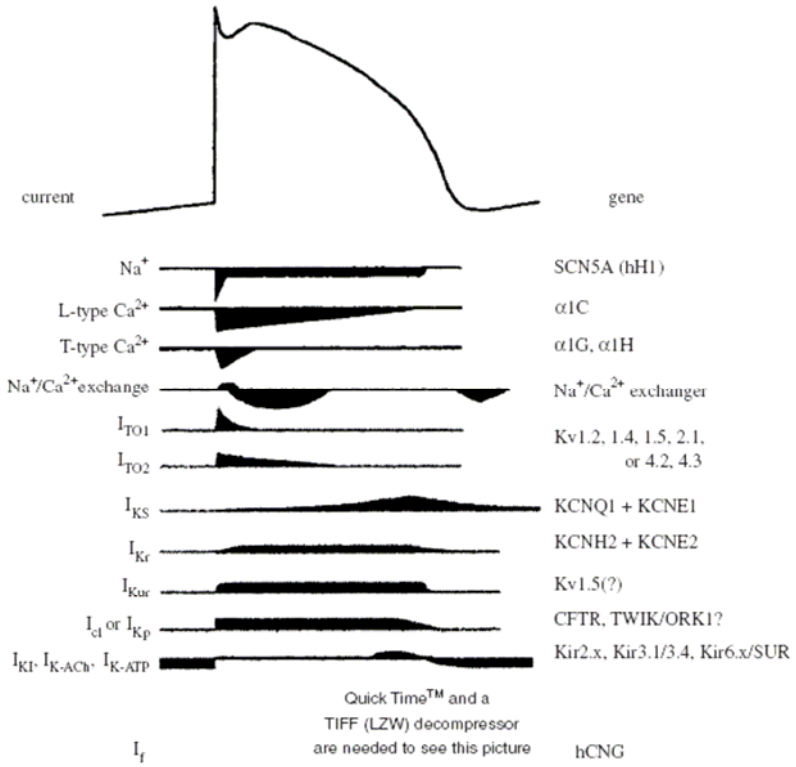

Fig. 1. The relative contribution in time of ionic currents, and the genes and/or channels underlying these currents, to the cardiac action potential. Downward deflections represent inward currents, and upward deflections represent outward currents. Reproduced with permission from Rosen MR, *et al*. (13).

time and voltage characteristics, determine the duration and shape of the AP. Various pathological situations and changes to the hormonal and/or paracrine systems changes can modulate the expression and magnitude of different channels, which could be proarrhythmogenic. Mutations in the gene encoding the sodium channel (SCN5A) (20), in the genes encoding KCNQ1 (responsible for I_{ks}) (21) and the KCNH2 (HERG gene, responsible for I_{Kr}) (22), as well as mutations in the b-subunits of the genes for KCNQ1 (23) and KCNH2 (24), are related to the Brugada and/or long QT syndrome.

The ventricular AP duration is extremely long compared to that of skeletal muscle or neural tissue. The AP duration is more or less equal to the duration of the mechanic systole, and is also adapted to cycle length over a long physiological range, which serves three important functions (25). Firstly, the long ventricular AP duration leads to a long refractory period, preventing a physiological status like tetanus in skeletal muscle. Secondly, whenever the ventricular working myocardium is activated, these cells in the wake of the activation front are refractory, which prevents possible reentry from happening. Thirdly, the AP duration is important for the amplitude and duration of the calcium transient, which can trigger the massive release of Ca^{2+} from the sarcoplasmic reticulum, and thereby provides modulation of contractility (25).

2. Heterogeneity in action potential in different ventricular cells

Heterogeneity in repolarization moment may be found at a regional level, i.e. between base and apex or between the anterior and posterior sides of the ventricles, between the two ventricles, or transmurally as known to occur among epicardium, M cells and endocardium (26-37).

Heterogeneity of AP duration in different ventricular areas

The heterogeneity of AP duration is due to the variation in current over different regions of the heart. There are very few data on current distribution in the human heart. In the rabbit, the sum of both delayed rectifier currents is larger at the base of the ventricle than at the apex. Actually, I_{Ks} at the base is larger than I_{Kr} at base and apex, and also larger than I_{Ks} at the apex, whereas I_{Ks} at the apex is

smaller than I_{Kr} at the base and apex (38). Thus, in the rabbit ventricle apical APs are significantly longer than those of the basal area. In canine hearts, apical APs appeared to be shorter than basal ones (27). Obviously, species differences are important in the AP heterogeneity. In human ventricle, the molecular data on I_{Ks} are in agreement with the functional data in the dog (27). I_{Ks} current was found to be about twice as large in the right ventricle than in the left ventricle. In the *in vivo* situation, transventricular or global gradients have also been demonstrated - in which different activation times (AT), AP durations and repolarization times over the epicardium and/or endocardium could be observed in both swine and humans (37, 39).

Transmural Heterogeneity of AP in the ventricular wall

Until the early 1990s, the cellular composition of the ventricular wall was thought to be largely homogeneous. Recently, studies using isolated tissues, cells, and ventricular wedge preparations have revealed three distinct myocardial cell types: epicardial, M, and endocardial cells. Differences in the electrophysiological characteristics and pharmacological profiles of the three myocardial cell types have been described in dog, guinea pig, rabbit, pig, and human ventricles (9-11, 28, 29, 40-51). The principal feature of the M cell is the ability of its AP to prolong more than that of epicardium or endocardium, with slowing of rate (Fig. 2) (41, 46, 50). Tissue isolated from the M region shows an AP duration that is more than 100 ms longer than those from the epicardium or endocardium at basic cycle lengths of no less than 2,000 ms.

The distribution of M cells in the ventricular wall has, however, only been investigated in detail in the canine left ventricle. M cells with the longest AP duration are typically found in the deep subepicardium to midmyocardium of the lateral wall, the deep subendocardium to midmyocardium of the anterior wall, and throughout the wall in the region of the outflow tracts. M cells are also present in the deep layers of papillary muscles, trabeculae, and interventricular septum (47, 52). The different distribution of M cells over the ventricles might also contribute to the spatial dispersion of AP, as mentioned above.

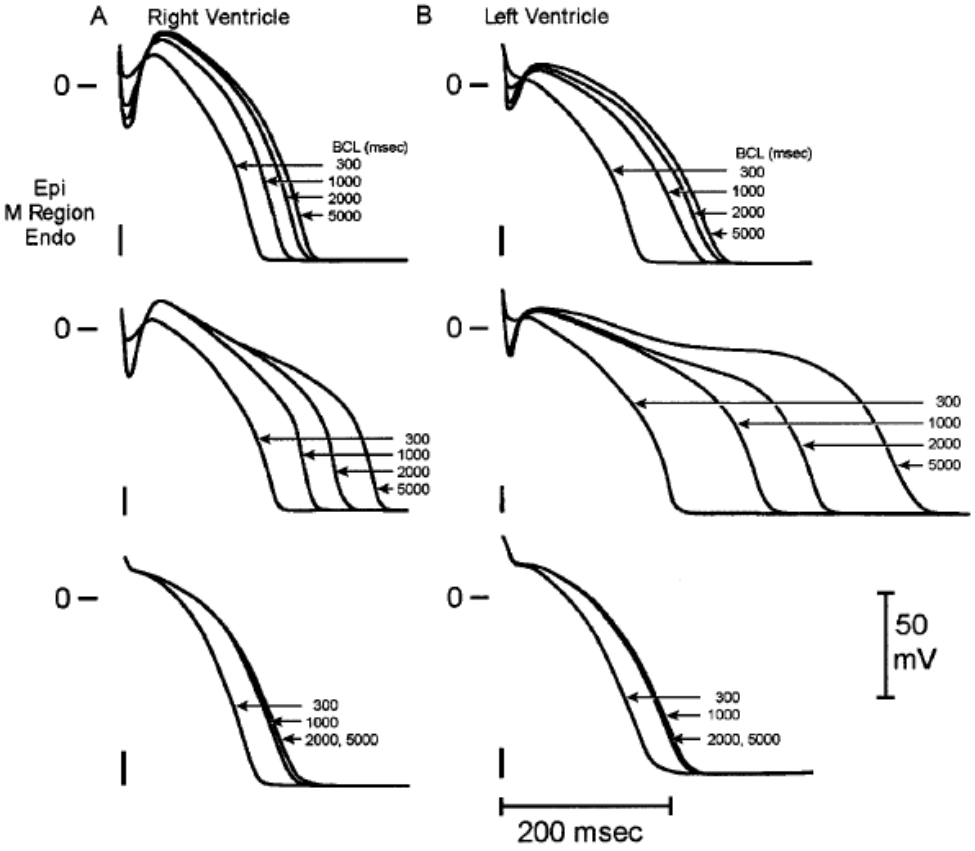

Fig. 2. Transmembrane action potentials recorded from epicardial (upper), M cell (middle), and endocardial (lower) tissue slices isolated from the canine right (A) or left (B) ventricle. The basic cycle length (BCL) used at the time of recording is indicated next to each trace. M cells display a greater prolongation of action potential duration with slowing of rate. This feature is more pronounced in the left than in the right ventricle. The epicardial and M cells display an I_{to}-mediated phase-1 notch, resulting in the classic 'spike and dome' morphology that is more pronounced in the right than in the left ventricle. Reproduced with permission from Yan GX, *et al*. (50).

The ionic basis of the prolonged AP duration of M cells includes a smaller I_{Ks} and a larger late I_{Na} (53, 54), and sodium-calcium exchange current ($I_{Na\text{-}Ca}$) (55) compared to epicardial and endocardial cells, whereas other currents are similar in these three cell types in the canine heart (53). The net result is a decrease in repolarizing current during phases 2 and 3 of the M cell AP. These ionic distinctions sensitize the M cells to a variety of pharmacological agents. For example, agents that block I_{Kr}, such as d-sotalol, erythromycin, almokalant, and quinidine produce much greater prolongation of M cell AP duration, but have a relatively small effect on the other ventricular cell types (56). Preferential prolongation of the M cell AP duration leads to exaggeration of transmural dispersion of repolarization, consequently, creating the substrate for development

of ventricular arrhythmias such as Torsades de Pointes, as seen in the long QT syndrome.

Besides the differences during AP phase 3, the three cell types also differ with respect to currents contributing to phase 1. The APs of epicardial and M cells display a prominent I_{to}-mediated phase 1 that is absent in endocardial cells (57). The early repolarization phase gives the epicardial AP a notched appearance. In the canine heart, I_{to} and the AP notch are much larger in right than in left ventricular epicardial (58) and M (44) cells. Under pathophysiological conditions, the repolarizing currents at the end of phase 1 can overwhelm the depolarizing currents, causing an all-or-none repolarization at the end of phase 1 of the epicardial AP, which leads to a markedly abbreviated epicardial AP duration and a pronounced transmural dispersion of repolarization, providing the substrate for the development of ventricular tachyarrhythmia.

Conflicting findings on transmural dispersion of repolarization recorded in vivo

Although these three different cell types with distinct AP features have been clearly described in ventricular wedge preparations of slowing rate, several *in vivo*

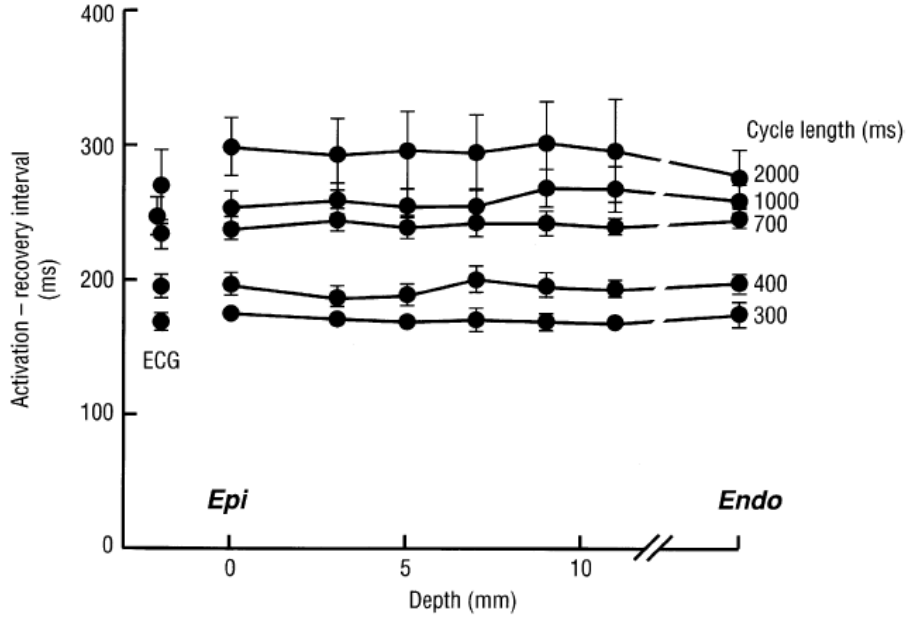

Fig. 3. Activation recovery intervals recorded transmurally between epicardium (epi) and endocardium (endo) in canine ventricle *in vivo*. No differences in transmural ARI was detected over a range of basic cycle lengths between 300 and 2,000 ms. Reproduced with permission from Anyukhovsky EP, *et al*. (41).

studies have failed to demonstrate the significant transmural dispersion of repolarization, which has caused the transmural dispersion of AP duration to be a controversial issue. Several studies have assessed repolarization transmurally in animal hearts *in vivo* using plunge electrodes and measuring refractory periods (59-62). However, none of the studies in which refractory periods were measured transmurally demonstrated any prolongation in the midmyocardium. Moreover, also in the dog, relevant dispersion in AP duration has been shown to be absent - at least at physiological cycle length (41, 63). Fig. 3 shows data from Anyukhovsky *et al*. (41) showing activation recovery intervals recorded transmurally from the canine ventricular wall *in vivo* for a range of cycle lengths. No significant transmural difference in activation recovery intervals was detectable at any cycle length. In particular, even at the longest cycle lengths, at which differences between midmyocardium and the more superficial layers are most pronounced in cell preparations, no transmural gradients were detectable. On the other hand, El-Sherif *et al*. also recorded transmural ARIs in canine ventricles *in vivo* and found longer activation recovery intervals in midmyocardium compared to endocardial and epicardial regions. However, the differences in activation recovery intervals were relatively small being in the order of 25 ms and only occurring at longer cycle lengths (43). Thus, these *in vivo* studies in animals show either no transmural repolarization gradient or only a small gradient. Importantly, in the *in vivo* human heart, mid-mural zeniths in repolarization moments have not been observed and a functional role of M-cells in transmural dispersion cannot be established at this time (Fig. 4) (25, 31, 36, 64).

Electrotonus on action potential as an explanation of the conflict

The reason for the disparity in AP duration being less pronounced in the intact ventricular wall might be explained by electrotonic coupling of cells (64). AP duration is an intrinsic feature of ventricular myocytes, but also depends on the electrotonic effect of neighboring myocardium. It is well known that local electrotonic current flow via gap junctions between cells will have a tendency to equalize any potential difference (65-68). Thus, when cells with different AP duration are juxtaposed, the longer AP duration will tend to lengthen the shorter and the shorter AP duration will tend to shorten the longer.

The presence of a transmural repolarization gradient in the arterially perfused ventricular wedge preparation has sometimes been interpreted as evidence for the presence of transmural repolarization gradients in whole hearts *in vivo*. However, these transmural gradients are only about 30-40 ms, which is significantly less than the value of about 100 ms observed in isolated cells and tissues at comparable cycle lengths (9, 31, 69). If the large repolarization gradients seen in isolated cells and tissues are due to the absence of cell coupling and electrotonic current flow, the smaller repolarization gradients seen in ventricular wedge could be explained by the partially uncoupled nature of the ventricular wedge. In the ventricular wedge AP duration is measured from the transected surface, which is at least partially uncoupled. Recent computer simulation studies based on electrophysiological characteristics of the guinea pig (the Luo-Rudy model) or humans (Priebe-Beuckelmann model) has further demonstrated a prominent reduction in AP duration of M-cells at stronger intercellular coupling (36). Thus, there has been substantial evidence to suggest that in well-coupled normal myocardium significant repolarization gradients over short distances are minimal or absent.

3. Dynamics of action potential

Electrical restitution (70)

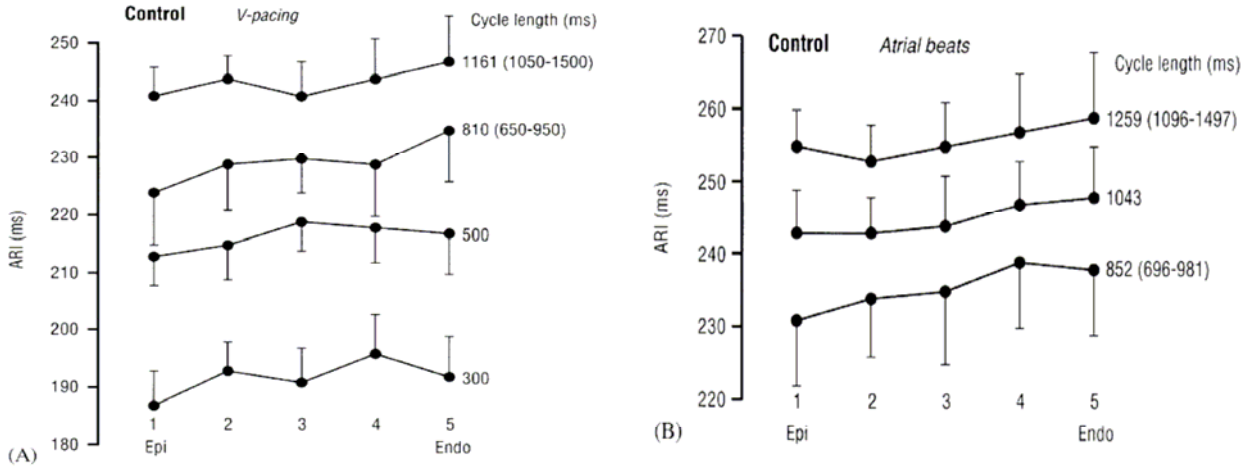

Fig. 4. Activation recovery intervals (ARI) recorded transmurally from the left ventricle in patients during cardiac surgery: during ventricular pacing (A) and during atrial pacing (B). No significant ARI gradients were seen either during ventricular pacing over a range of cycle lengths between 300 and 1,500 ms, or during atrial pacing over a range of cycle lengths between 700 and 1,500 ms. Reproduced with permission from Taggart P, *et al*. (31).

The dynamics of AP duration can be expressed by a so-called electrical restitution curve.

The electrical restitution curve (71, 72) describes the time course of recovery of AP duration as a function of the diastolic interval or cycle length between a steady-state response and an extrastimulus response – from the most premature response past the steady-state response to a postmature response. An important link between electrical restitution kinetics and arrhythmogenesis can be seen in electrical alternans and non-linear dynamics. Electrical alternans, either measured as AP duration alternans (73) or T wave alternans (74), has been shown to be a predictor of VF or sudden cardiac death. The rationale is that a slope of the electrical restitution curve of > 1 amplifies AP duration alternans and can lead to

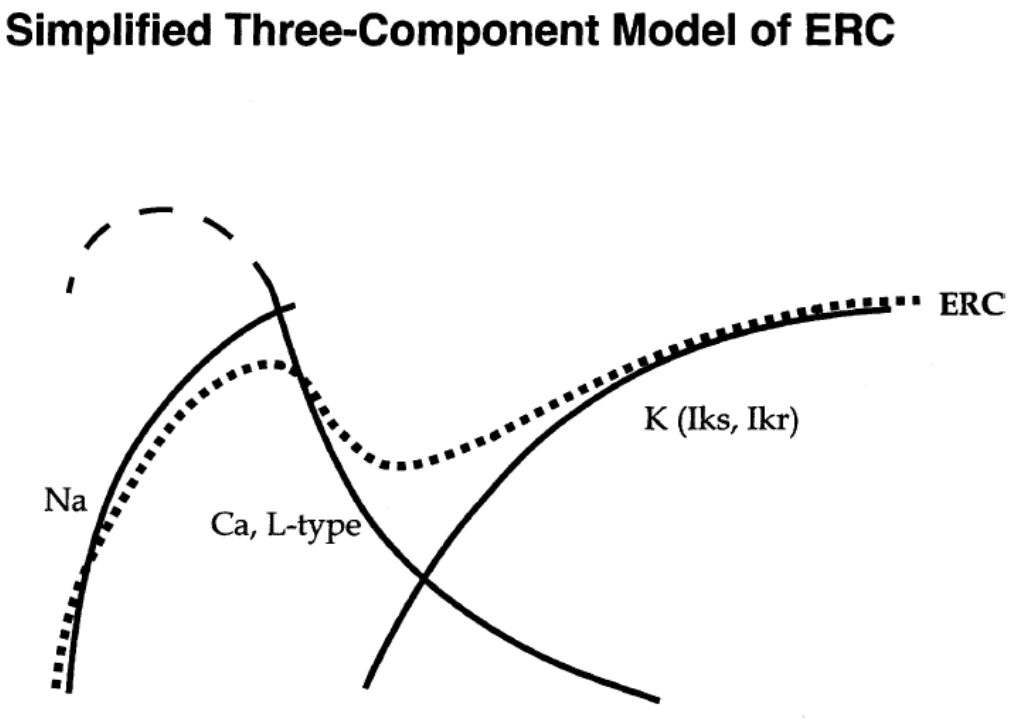

Fig. 5: Electrical restitution curve depicted as a function of the three most important ion channels governing action potential duration (APD). Upsloping solid line at left: the earliest part of APD recovery relies mainly on the fast sodium current that needs to recover sufficiently to allow for activation of $I_{Ca\text{-}L}$. Downsloping solid middle line: Due to minimal negative feedback on $I_{Ca\text{-}L}$, $I_{Ca\text{-}L}$ is maximal during early responses and declines in negative exponential fashion with increasing intervals. Maximal phase 2 APD is reached when the Na^+ and Ca^{2+} lines intersect. Upsloping solid line at right: Potassium outward currents. Increase in these currents increases APD at more terminal repolarization levels, not at the plateau. Dotted line: Composite curve reflecting the electrical restitution curve (at an approximate repolarization level of 70%) based on the three major currents. Curves are not based on actual experimental or modeling data but are hand drawn. The diagram, while going beyond a single entity of the electrical restitution curve, is still extremely simplified. Reproduced with permission from Franz MR, *et al*. (70).

wavebreak, an imminent precursor of fibrillatory rhythms, whereas a slope of < 1 reduces alternans (75). However, in contrast to this traditional theory, recent studies have suggested that it would be advantageous to lower the slope of the electrical restitution curve by drug intervention, as this might reduce the potential for electrical alternans and ventricular fibrillation. Actually, the slope of the electrical restitution curve is a complex and multifactorial function of ion channel recovery that cannot be described by a simple or mono-exponential curve. The normal ventricular electrical restitution curve can be at best be simplified as being triphasic, starting with a steep initial recovery at the shortest diastolic intervals, a transient decline, and a final asymptotic rise to a plateau phase reached at long diastolic intervals (Fig. 5) (70).

As mentioned above, the AP duration is the net result of a number of electrogenic ion channels, each of which has individual onset and offset recovery kinetics. Consequently, restitution of AP duration is governed by a multitude of different ion channel kinetics. As seen in Fig. 5, the electrical restitution curve can be better described as a triphasic time course. The earliest premature responses have a slowed upstroke, a lower amplitude, and a shorter plateau phase - all of which can be attributed to a diminished sodium inward currents (76, 77). Premature responses that occur at a diastolic interval of approximately 50-100 ms have full upstroke velocities and reach higher phase 2 amplitudes due to the blocked L-type calcium inward current, which during premature beats faces minimal sinus rhythm feedback inhibition (18, 78). This gives those premature APs an almost rectangular appearance. As the diastolic interval lengthens further, the Ca^{2+} inward current diminishes further and leads to further phase 2 shortening while potassium channels begin to delay the final repolarization. This gives delayed APs a more triangular shape.

For the initial electrical restitution curve, a steep slope may be beneficial because it allows shortening of AP duration and subsequently lengthening of diastolic interval to move AP restitution more rapidly outside the ventricular vulnerable window. In addition, a shortening of AP duration, leading to shorter electrical and hemodynamic systole, can save time for diastolic filling. Immediate shortening of AP duration after an increase in heart rate is therefore a physiological prerequisite. Furthermore, an important effect of such a triphasic electrical restitution curve is the physiological rate-adaptive shortening of AP

duration, which allows the subsequent AP duration to move more quickly from the steep initial electrical restitution phase onto the flat phase. Flattening of this phase of the electrical restitution curve may reduce AP duration alternans following immediately after a sudden increase in rate (70).

Cardiac Memory and remodeling

The term remodeling is frequently used to describe adaptational and mal-adaptational processes by which the heart responds to disease or external stimuli. Cardiac memory refers to a specialized form of remodeling, which is characterized by an altered T wave on ECG recorded during sinus rhythm (or any rhythm with normal ventricular activation) and induced by a preceding period of altered electrical activation (Fig. 6) (79, 80).

The electrophysiological changes of cardiac memory have been studied in

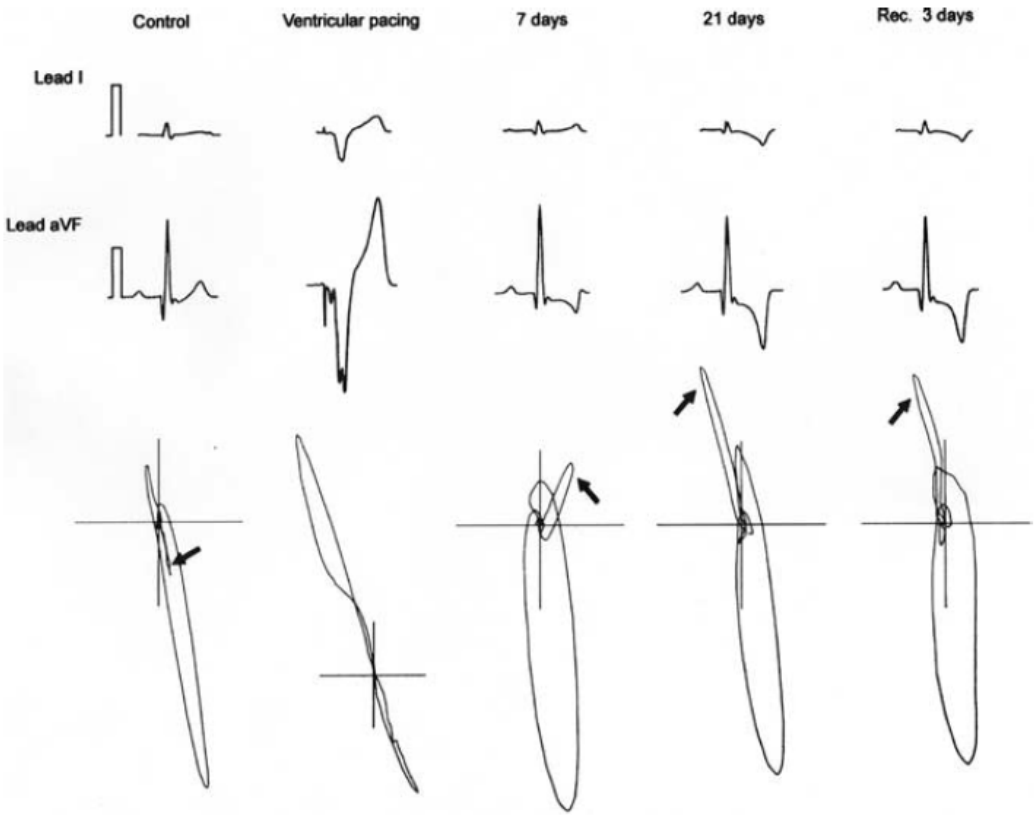

Fig. 6: Evolution of cardiac memory in the canine model. Upper panels: Leads I and aVF before ventricular pacing (control), during pacing, and 1 hour after cessation of pacing on days 7 and 21, and after 3 days of recovery after pacing was permanently discontinued. Bottom panel: frontal plane vectorcardiogram from the same animal. Cross-hairs, 0.5±0.5 mm. The T wave vector during sinus rhythm is indicated by the arrow. Reproduced with permission from Patberg KW, *et al*. (80).

intact animal models, isolated hearts, isolated tissues, and single cells (79, 81, 82). Altered activation sequence, rather than altered heart rate, has been demonstrated to be substantially responsible for ventricular remodeling (83-85). A classic example of the altered relationship between repolarization and activation was provided by Costard-Jäckle *et al*. (86). They transiently changed the ventricular activation pattern in Langendorff-perfused rabbit hearts and induced changes in repolarization that outlasted the pacing period. Resumption of atrial pacing after the heart had been paced from the right ventricle resulted in loss of the normal inverse relationship between activation time and AP duration. The duration of loss of this relationship increased with the duration of ventricular pacing, and this was considered to be a manifestation of cardiac memory.

Changes in ion currents are associated with the occurrence of cardiac memory. In the studies on the mechanisms of AP changes of long-term cardiac memory, the decreased phase 1 notch and altered repolarization of epicardial myocytes were found to be in part due to a reduced I_{to} density, as well as more positive activation and delayed recovery from inactivation of I_{to} (87). Reductions are also seen in mRNA levels for Kv4.3 and in protein and mRNA levels for KChIP2, the pore-forming unit and an accessory protein for the I_{to} channel, respectively (87, 88). Apart from the I_{to} changes, the L-type calcium current $I_{Ca,L}$, which contributes to the maintenance of the AP plateau, activates at more positive membrane potentials and remains open for a longer period of time in epicardial myocytes from dogs with long-term cardiac memory than in corresponding controls (89). This change in $I_{Ca,L}$ may contribute to the heightened and prolonged epicardial AP plateau associated with cardiac memory. In addition, the rapidly activating delayed rectifier potassium current I_{Kr} shows a reversal of its transmural gradient (90). In contrast, no significant change can be seen in the slowly activating component of the delayed rectifier I_{Ks} (90).

Transmembrane ion currents are only one important determinant of AP contour. Gap junctions, which facilitate cell-to-cell communication via low-resistance intercellular connections, also contribute significantly. In long-term cardiac memory, there is reduced expression of the gap junctional protein connexin43 (91). In addition, connexin 43, which is normally localized at the ends of adult ventricular myocytes, is redistributed to the lateral margins of the cell membrane when long-term cardiac memory is induced (91).

Thus, the molecular changes characterizing long-term cardiac memory occur mainly as consequences of cardiac pacing in the clinical setting. In other words, ventricular pacing, long thought to be a "neutral" intervention with regard to cellular and subcellular function, is actually a potent modulator of cellular processes. The extent to which and the mechanisms by which these changes influence the possible ventricular tachyarrhythmia are not yet completely clear.

Potential proarrhythmic effects of epicardial pacing (92) (93)

Cardiac resynchronization therapy (CRT), involving right ventricular endocardial pacing and left ventricular epicardial pacing, has recently become an established therapy for patients with systolic heart failure of New York Heart Association class III/IV and prolonged QRS duration (94). Although a great deal of attention has been directed at showing the mechanical benefits and in improvement the CRT configuration and protocol, little attention has been paid to the consequences of reversing the direction of activation of the left ventricular wall. Although a delayed or halted progression of cardiac dysfunction may be sufficient to prevent malignant ventricular tachyarrhythmias, there is still experimental evidence (95, 96) and also some clinical evidence (97) that left ventricular pacing may have proarrhythmic potential (98-102).

Medina-Ravell *et al*. were the first to point out that the common design for resynchronization therapy, involving LV epicardial pacing, is associated with a nonphysiological ventricular activation sequence (95). In the ventricular wedge preparation, switching from endocardial to epicardial pacing resulted in a change of activation sequence between epicardium and endocardium, which was associated with an increase in transmural dispersion and QT interval without a parallel increase in endocardial and epicardial transmembrane AP duration. Another study examined the cellular basis of QT prolongation after reversal of the direction of activation of the LV wall (96). Based on previous investigations documenting the contribution of M cells to transmural dispersion, this study

postulated that delayed activation and repolarization of M cells, coupled with earlier activation and repolarization of epicardial cells, may result in QT prolongation, development of transmural heterogeneity, and Torsades de Pointes after a shift from endocardial to epicardial activation of the LV wall in the absence and presence of rapidly activating delayed rectifier potassium current I_{Kr} blockade. This hypothesis was confirmed in a one-dimensional mathematical model of transmural conduction, and also in the perfused canine LV wedge preparation (96). Epicardial activation augments transmural dispersion because the epicardial AP activates and repolarizes earlier and the M cells with the longest AP duration located in the deep subendocardium activate and repolarize later compared to endocardial activation of the ventricular wall (Fig. 7). The additional conduction delay encountered between epicardial and M regions during epicardial stimulation may further amplify of the transmural dispersion of repolarization, which could create the substrate for the development of reentry.

A potential proarrhythmic effect of CRT in a subgroup of patients is an issue of considerable importance in view of the current controversy regarding the need of ICD backup in the patients receiving CRT (103, 104). The controversy is fueled in part by some of the limitations associated with interpretation of the results of the two famous CRT trials, the COMPANION Trial (105) and CARE-HF Trial (106). Although the COMPANION trial included both a CRT-pacemaker group and a CRT-defibrillator group, the two groups were compared against a control group and not against each other. This left the unanswered question of whether a CRT-defibrillator is superior to a CRT-pacemaker in all candidates for CRT, in the majority of CRT candidates, or only in a specific subgroup of CRT patients. The CARE-HF trial showed significant long-term benefits of CRT alone with respect to survival as a single endpoint. Whether or not inclusion of defibrillation therapy in the study would have resulted in better survival in this group of patients is not clear. Obviously, further *in vivo* studies for evaluation of the proarrhythmic effect of CRT may help us settle this controversy (107, 108).

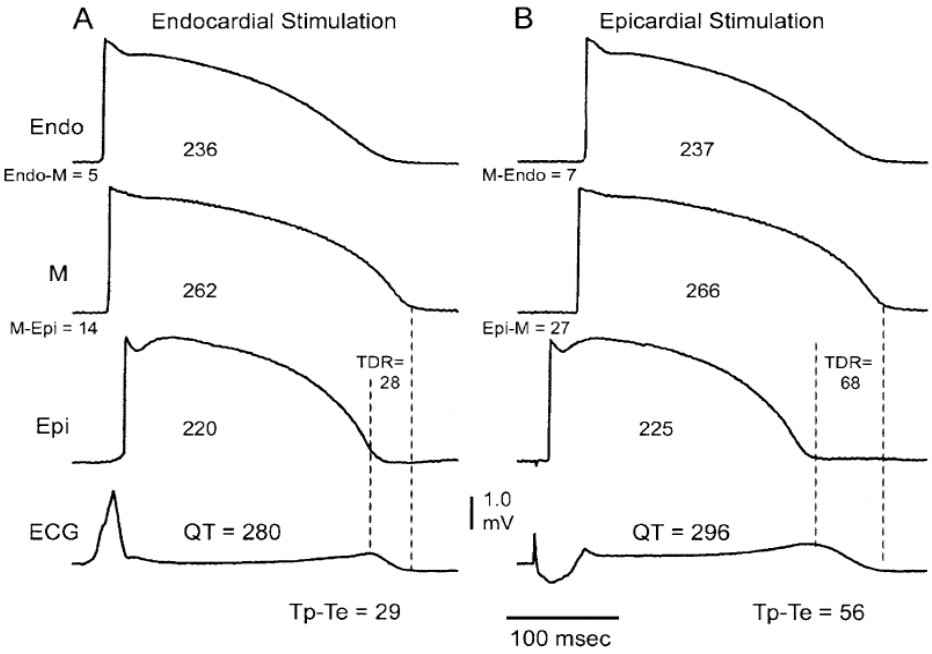

Fig. 7: Effect of reversal of transmural sequence of activation in canine LV wedge preparation. Epicardial (Epi), endocardial (Endo), and M-cell action potentials and a transmural electrocardiogram were simultaneously recorded during endocardial (A) and epicardial (B) pacing at a basic cycle length of 2,000 ms. All numbers are in milliseconds. Reproduced with permission from Fish JM, *et al*. (96).

4. Sequence of ventricular replorization

Controversial findings on sequence of ventricular repolarization

The ECG finding that the polarities of the T wave are concordant with those of the QRS complex has been interpreted using the conventional concept that the repolarization sequence is in a direction opposite to that of the activation sequence (109). The main experimental findings used to support this concept were the existence of transmural gradients, with the inner wall being more negative than the outer wall (35), or as reported recently, two opposite gradients between the endocardium and the M region and between the epicardium and the M region (9, 50). Repolarization gradients in the global dimension, i.e. from the apex to the base (apico-basal gradients) and from the anterior to the posterior aspects of the ventricles (ventricular gradients) are relatively unclear (110-112). Findings that MAP duration was longer at the apex than at the base and longer in the anterior

than in the posterior aspects were interpreted as evidence of a reversed repolarization sequence (39, 111, 113).

Much of the data available in the literature does not, however, support the concept of reverse ventricular repolarization sequence. Toyoshima *et al*. recorded epicardial MAPs from 32-43 sites in open-chest dogs and found that the repolarization sequences were similar to the activation sequences across the anterior epicardium of the canine ventricles (114). Lux *et al*. recorded high-resolution arrays of unipolar electrograms from the canine right ventricular epicardium and measured the activation-repolarization interval for assessment of the repolarization sequence (110). They found that the repolarization 'waves' propagated away from the pacing site, regardless of its location, and replicated 'collision' when multiple sites were simultaneously paced, which clearly indicated that repolarization followed the same sequence as activation. Gepstein *et al*. recorded unipolar electrograms from 50–70 sites in the left ventricular endocardium in pigs using the CARTO electroanatomic mapping system (Biosense Webster, Waterloo, Belgium) (115). By measuring the activation recovery intervals and reconstructing three-dimensional maps of activation and repolarization, they also found that the repolarization sequence resembles that of activation in most of the maps.

On the other hand, Efimov *et al*. recorded optical action potentials from epicardium in Langendorff-perfused guinea pig hearts and studied the propagating feature of the repolarization process (116). When their pacing electrode was progressively from epicardium to endocardium, the epicardial repolarization sequence remained being from the apex to the base. Based on these findings, the authors concluded that the repolarization was independent of the activation sequence (117, 118) and was mainly guided by the spatial differences in the AP duration between apex and base.

Thus, the available data suggest that a repolarization sequence may exist over the canine, swine, and guinea pig ventricular epi- and endocardium. Whether the sequence of repolarization follows that of activation is still controversial.

Ventricular repolarization sequence by MAP mapping

Recently, a MAP mapping technique that combines the MAP recording and the CARTO mapping techniques has been developed in Lund and used for global mapping of the repolarization sequence over the ventricular endocardium in healthy pigs and in humans (37). MAPs were recorded from around 50 left and/or

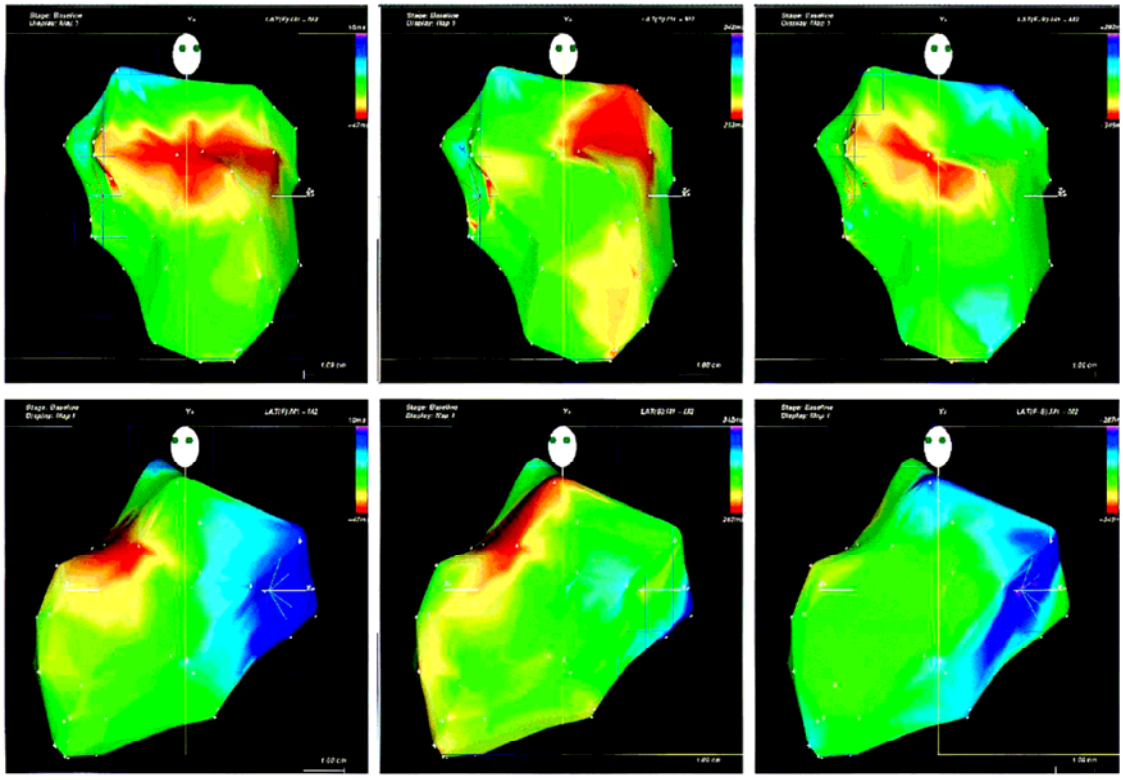

Fig. 8: Left ventricular maps from a pig during sinus rhythm: right anterior oblique (upper panel) and left anterior oblique views (lower panel). (Left) Activation started from the upper midseptum (red area), proceeded eccentrically towards the superior septum, antero- and posteroparaseptal and apical areas, and then passed through the free walls (yellow and green areas) to end in the posterolateral basal (blue and purple) area. (Middle) The end of repolarization sequence is similar to the activation sequence. (Right) The longest monophasic action potentials (MAPs) (red area) were recorded in the area activated earliest, and the shortest (blue and purple) near the area activated latest. Note that the MAP duration map was reconstructed using the negative values of the MAP durations in this figure, so that the red area represents the longest MAPs and the purple one the shortest. Reproduced with permission from Yuan S, *et al*. (37).

right ventricular sites in healthy pigs and in patients, using the CARTO system. Local AT, EOR time, and MAP duration were calculated and 3-dimensional global maps of AT and EOR were constructed. It was found that an EOR sequence was recognizable, and it followed the activation sequence in the majority of pigs and patients (Fig. 8). These findings do not support the existence of reverse repolarization gradients across the ventricular endocardium (39, 113), but are in accordance with the aforementioned experimental data in dogs (110, 114) and pigs (115). The concordant sequences of EOR and activation in this study were not only observed in maps during sinus rhythm and normal ventricular activation, but also in maps associated with secondary ST-T changes due to bundle branch block or ectopic activities, where the activation sequence was apparently abnormal.

In addition, the correlation and regression analyses in this study provide further evidence that the sequence of repolarization is dictated by that of activation (110) and by the spatial distribution of MAP duration (116). The magnitude of the progressive shortening of MAP duration with progressive later activation, relative to the magnitude of local AT, is a critical factor governing the direction and pattern of repolarization. That is, repolarization follows the same sequence as activation when the shortening of the MAP duration is globally less than the local AT, while a reverse sequence of repolarization may result when the shortening is globally greater than the local AT.

Due to the fact that the data in this study were from the endocardium alone, and the number of observations made was limited, further studies are warranted to validate this novel finding.

5. Dispersion of ventricular repolarization and its relationship with ventricular tachyarrhythmias

DVR has been widely used to describe nonhomogeneous recovery of excitability or heterogeneity of ventricular repolarization. Increased DVR was

found to be highly associated with the development of ventricular tachyarrhythmias as has been suggested by previous experimental studies (12, 25, 27, 32, 34, 63, 119-134), and is therefore considered to be an important arrhythmogenic mechanism. DVR is usually defined as the maximum difference in repolarization time in the area concerned, e.g. DVR in the left ventricle, DVR on the epicardium, etc. (63, 127). An increased DVR can be a consequence of disturbances in conduction, heterogeneity of AP duration, or a combination of both. These disturbances may exist between the right and left ventricle, between the endocardium, midmyocardium and epicardium, and/or between the apex and base, and are influenced by a variety of physiological, pharmacological and pathologic factors such as temperature, drugs, electrolyte imbalance, and ischemia etc (26-37, 43, 56, 63, 123, 124, 133, 135).

During the past two decades, transmural dispersion of repolarization has been highlighted by studies using ventricular wedge preparations (9, 44, 63, 85, 95, 123, 136). In these studies, the transmural dispersion of ventricular repolarization, the differences in AP duration between the epicardial, endocardial and M cells, have been addressed in great detail - exploring molecular mechanisms behind the development of ventricular arrhythmias, and providing a unique model for the study of diseases associated with repolarization disturbances such as the Long QT syndrome and the Brugada syndrome (7, 10, 63). However, arrhythmias resulting primarily from conduction disturbances such as VT postmyocardial infarction or different types of cardiomyopathies, where reentry confined to an anatomical substrate often constitutes the mechanism of arrhythmias, account for a large proportion of clinically important arrhythmias. In these cases, trans-epicardial or trans-endocardial DVR may be more relevant to the underlying mechanism (119, 120, 129, 137, 138), where delay in conduction is the dominant factor for increased DVR (91, 115, 137).

Background

Many studies on trans-epicardial and trans-endocardial DVR have adopted the MAP recording technique. About a decade ago, Yuan *et al*. recorded MAPs simultaneously from the right ventricular apex and outflow tract and found that DVR between these 2 sites was more pronounced in patients with polymorphic ventricular tachycardia/fibrillation than in patients with monomorphic ventricular tachycardia (121, 122), which suggested that different magnitudes of the DVR are even associated with different types of ventricular tachyarrhythmias. In addition, DVR measurements between 2 contiguous sites have also been used and correlated to ventricular arrhythmias in patients with cardiomyopathies (128, 139, 140). Besides measurements from simultaneous MAP recordings, DVR was also measured from sequential MAP recordings at 8-10 epicardial sites (113) or 5-11 endocardial sites (39) in patients, and increased DVR was consistently found to be correlated with ventricular tachyarrhythmias. In most of these studies, however, DVR has been estimated from MAP recordings at a limited number of epicardial or endocardial sites due to the difficulties in extensive MAP mapping (39, 113, 121, 122, 128, 139, 140).

Using the CARTO mapping system, Kongstad *et al*. recorded MAPs from 61±18 left or right ventricular sites in 10 pigs and 44±16 left, or right ventricular sites in 8 patients and compared the global DVR with the DVR at adjacent sites (120). They found that in both pigs and humans DVR values at 3-7 adjacent sites were significantly smaller than the global DVRs, as was the DVR between 2 remote sites. These findings suggested that global DVR is poorly estimated from MAP recordings at a few adjacent or remote sites, and they emphasize the importance of obtaining global information on repolarization.

To further explore the global DVR in great detail, we recently recorded MAPs from 211±54 left and right ventricular epi- and endocardial sites in healthy pigs using the CARTO system and found that the DVR on the epicardium of both the right and left ventricles were significantly greater than that of each ventricle alone

and the total DVR on both the epi- and endocardium was significantly greater than that on the epi- and endocardium alone (119). Thus, the DVR was significantly greater in biventricular maps than in single ones, and greater in a global context than in local areas. At sites with longer differences in conduction time, DVR tended to be greater in both pigs and humans. These findings suggest that the magnitude of DVR may be related to the size of the area involved, i.e. relatively greater DVR would be expected in relatively larger areas, while a limited number of recordings would tend to underestimate the DVR.

In summary, there is evidence that increased DVR may be proarrhythmic, since it facilitates reentry. However, the global DVR from *in vivo* models - and especially from patients with arrhythmias - are far from clear. Further experimentation in these areas is certainly warranted. It is worth mentioning that a markedly increased DVR is not always followed by proarrhythmic consequences, when it is due to gradual repolarization gradients between distant sites. On the other hand, a relatively smaller increase in DVR can be highly proarrhythmic when reentry can occur (34, 127, 128).

6. Electrocardiological index for ventricular repolarization

Although abnormalities in DVR are influential in determining the susceptibility to ventricular tachyarrhythmia and sudden cardiac death, few reliable clinical tools exist to identify such presence of ventricular repolarization abnormalities. In clinical and epidemiological practice, the temporal aspect of ventricular repolarization is measured by several interval-based indices. The QT interval is the most widely used index, despite the controversies regarding the appropriate corrections for its dependence on heart rate (141-153). Attempts have been made to capture the spatial aspect of repolarization by means of QT dispersion (30, 149, 154-160), and the transmural aspect by means of T_{peak}-T_{end} interval (95, 107, 108, 161, 162). However, as currently defined and measured on

the 12-lead ECG, these parameters have lacked *in vivo* validation and still have conceptual limitations that raise concerns about its validity as a measure of ventricular repolarization.

Genesis of T wave and T_{peak}-T_{end} interval

Deflections in the ECG result from voltage differences in the heart, which can be recorded on the body surface. The QRS complex reflects the electrical activation of the ventricles whereas the T wave reflects the process of repolarization. The duration of the T wave is much longer than the duration of the QRS complex. The short duration of the QRS complex is the result of the fast upstroke of the ventricular AP, and also of its fast conduction over the specialized conduction system with a velocity of around 60 cm/s in the longitudinal direction and about 20 cm/s in the transverse direction (163). The duration of the T-wave is much longer than that of the QRS, because the repolarization process is much slower, and it is not propagated along any existing pathway. Thus, the repolarization process is not a matter of propagation, but of synchronization with the tendency to a progressively shorter AP in later activated sites, as mentioned above in the section of 'ventricular repolarization sequence'.

The genesis of the T wave has been a matter of debate for several decades (9, 13, 30, 61, 65, 132, 164-169). In the early days, it was hypothesized that the T wave vector is generated by different levels of local repolarization in the heart (164, 167), so that the T wave emerges from inhomogeneous recovery throughout the heart. Based on this theory, the width of the T wave represents the time interval during which the repolarization process occurs in the heart, and is postulated to be highly correlated with the DVR. Thus, the T_{peak}-T_{end} interval was chosen as a measurement of half the T wave width due to difficulties in determining the onset of the T wave, and was shown to be highly correlated with dispersion of AP duration and recovery time in isolated rabbit heart model (30).

In recent years, studies using the arterially perfused canine ventricular wedge preparation have sought to define the transmural voltage gradients responsible for the T wave patterns under normal conditions, as well as in patients with a variety of arrhythmogenic cardiomyopathies (9, 165). Transmural differences in the time course of repolarization of the three predominant myocardial cell types, epicardial, endocardial and M cells, have been shown to be largely responsible for the inscription of the T wave (Fig. 9).

Voltage gradients developing as a result of the different time courses of repolarization of phases 2 and 3 in the three cell types give rise to opposing voltage gradients on either side of the M region, which are in large part responsible for the inscription of the T wave (Fig. 9) (9). When the T wave is upright, the epicardial AP is the earliest to repolarize and the M cell AP is the last. Full repolarization of the epicardium coincides with the peak of the T wave and repolarization of the M region is coincident with the end of the T wave. In this

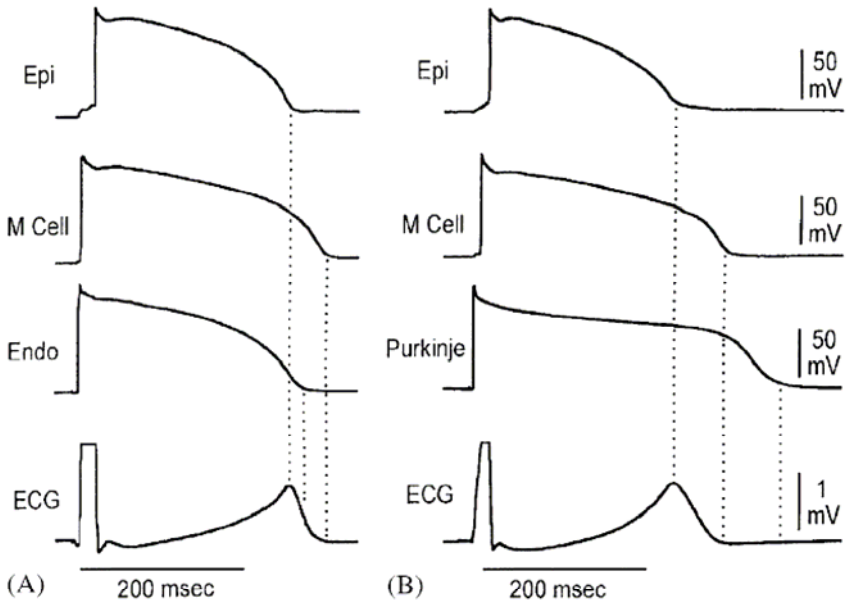

Fig. 9: Simultaneous transmembrane potentials and transmural pseudo-ECG recorded in a canine transmural wedge preparation. “Epi” denotes subepicardial, “M-cell” midmyocardial and “Endo” subendocardial action potential recording. Panel A shows that the peak of the T-wave on the pseudo-ECG coincides with epicardial repolarization. M cell repolarization coincides with the end of the T-wave in this registration. Panel B shows that the repolarization moment in Purkinje fibers occurs after inscription of the T-wave and is not reflected in the transmural ECG. Reproduced with permission Yan GX, *et al*. (9)

model the AP duration of the M cells determines the QT interval, whereas the AP duration of the epicardium determines the QT_{peak} interval. Thus, the T_{peak}–T_{end} interval was suggested to be an index of transmural DVR under baseline and long QT conditions (9) (Fig. 10). Based on these findings, they suggested that the transmural gradients were largely responsible for the inscription of the T wave, whereas the apico-basal voltage gradient contributes little to the genesis of the T wave (9) (Fig. 11). Several clinical studies have been attempted and have suggested that the T_{peak}-T_{end} interval may be a useful index of transmural dispersion. They may thus be prognostic of arrhythmic risk under a variety of conditions (95, 107, 108, 162).

However, it is questionable that to which extent the transmural voltage differences in such a preparation may explain the genesis of the T-wave *in vivo*. In addition, the functional relevance of M-cells under *in vivo* conditions is under

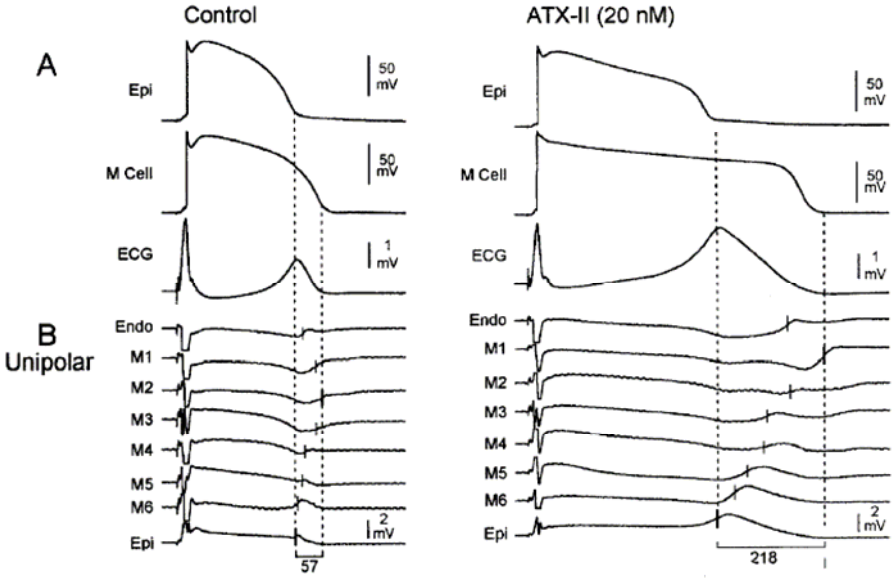

Fig. 10: T_{peak}-T_{end} interval provides a measure of transmural DVR and correspondence among transmembrane, unipolar, and ECG in the absence (left) and the presence (right) of ATX-II (20 nmol/L). A: Transmembrane APs recorded from and epicardial sites of a canine ventricular wedge preparation together with a transmural ECG recorded across the bath (BCL of 2000 ms); B Eight intramural unipolar electrograms recorded from endocardial (Endo), M (6 sites) and epicardial (Epi) regions. Dashed vertical lines in the unipolar electrograms denote the time maximum of the first derivative of the T wave. Close correspondence between the repolarization time of the cells deep within the wedge and those at the cut surface indicate a high level of uniformity of electrical activity in the respective transmural layers. Reproduced with permission from Shimizu W, *et al*.(10).

debate (31, 36, 64, 170) - even in dogs (135), as mentioned above. In a study on the dispersion of repolarization in the normal human heart, a comparison of the mean of the latest repolarization time in seven patients with endocardial MAP measurements and three with epicardial MAP measurements showed that the earliest repolarization on the epicardium was similar to the latest repolarization on the endocardium (39). Further *in vivo* studies are required to clarify whether it is transmural or global (apical-basal) DVR that mainly contributes to the genesis of the T wave.

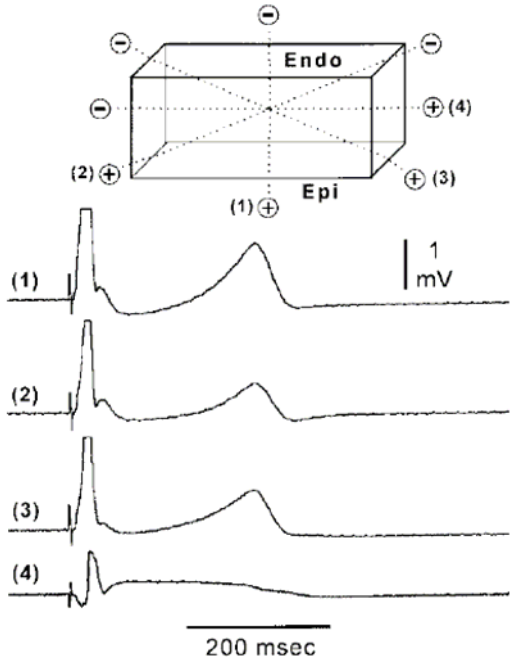

Fig. 11: Contribution of transmural gradients (as compared to apico-basal and anterior-posterior gradients) to the registration of the T wave. The 4 ECG traces were simultaneously recorded at 0°, 45°, 245°, and 90° angles relative to the transmural axis. Inscription of the T wave is largely the result of voltage gradients along the transmural axis. Reproduced with permission from Yan GX, *et al*. (9).

QT interval and QTc

The QT interval is a summation of the ventricular depolarization and repolarization recordable on the surface. The QT interval was first measured in the frog heart by Burdo-Sanderson and Page in 1880 (144), and Einthoven first introduced the term “QT interval” (171). Rate-dependence of the QT interval was recognized over 80 years ago by Bazett (141), with subsequent development of the commonly adopted heart rate correction (QTc) (143, 146, 172, 173). In the past 15

years, a resurgence of application of the QTc for risk stratification has been seen, in part fueled by an evolving understanding of the genetic bases of the congenital long QT syndromes. Also, prolongation of the QTc interval has been associated with an increased risk of sudden death in the congenital long QT syndromes (174) and with an increased risk of cardiovascular and all-cause mortality in a broad range of clinical populations (142, 149, 153, 173). However, the clinical usefulness of the QT interval remained clouded by questions regarding the accuracy of QT interval measurement (156, 175, 176) and the validity of the Bazett formula for correcting the QT over a wide-range of RR intervals (143, 151, 152, 177, 178).

The best way of measuring the QT interval has long been a major issue, with questions of how to identify the T wave offset, which leads to measurement of the QT interval, and whether to use manual or computer-based measurements. Accurate manual identification of the T wave offset is sometimes difficult, particularly in the presence of low-amplitude T waves, T-U fusion, and at high heart rates when the P wave may become superimposed on the T wave (156, 175, 176). As a consequence, both intra- and interobserver variability in manual QT interval measurements have been high, limiting the applicability of this approach (178). On the other hand, the accuracy and reproducibility of computerized identification of T wave offset has also been an issue (150, 179), though some computerized approaches to QT interval measurement have been shown to have superior reproducibility (151). Computer determination of the QT interval frequently involves measurement from the earliest onset of the QRS in any of the 12 leads to the latest offset in any of the 12 leads (152), which will result in longer QT intervals than when manual measurements of the longest QT interval in any ECG lead are used. Recent studies, comparing careful manual measurements made in 3 leads with computerized measurements in all 12 leads, have found a high degree of correlation between manual and computer-measured QT intervals (173). Importantly, they have found only minor differences in the predictive value of

careful manual measurements and computer QT measurements, and that these differences were negated by further adjustment for heart rate - which suggests that with careful QT measurement and adjustment of normal limits for the method used, either manual or computer-based QT interval measurements may be used for risk stratification (173).

The most commonly used formula for heart rate correction of the QT interval is that of Bazett ($QT_c = QT/\sqrt{RR}$) (141). This nonlinear power correction has been widely examined and found to undercorrect the QT interval at low heart rates and to overcorrect at high rates. As a consequence, numerous QT rate-correction formulae have been developed using linear regression and other nonlinear power functions (143, 151, 173, 177). However, many of these methods are computationally more complex, also have residual correlations with heart rate, and have not been adequately tested for clinical use. Thus, despite the limitations, the Bazett equation remains in widespread clinical use today. In a recent study, Dekker *et al*. examined three different equations for rate correction of the QT interval: Bazett, Hodges linear-regression equation, and the nonlinear QT. They found high degrees of correlation between the three methods and, importantly, there were only minor differences in the risk stratification provided by all three, with the Bazett correction appearing to provide slightly better separation - thus supporting the continued clinical use of this imperfect approach (173).

QT dispersion

The measurement of QT dispersion has been proposed as a simple noninvasive measurement of DVR available from 12 lead surface ECG since the 1990s (154, 159). An increased QT dispersion on the ECG is related to propensity for arrhythmias during treatment for the long QT syndrome, for example (159).

Several factors may contribute to an increased QT dispersion, however. Firstly,

the determination of the end of the T wave is often difficult, as mentioned above in the section of QT interval. Secondly, at each time instant, the vector of repolarization has different spatial coefficients and a different voltage. During the time period of repolarization, these vectors constitute a loop, which is projected on the body surface. The T wave, observed in any precordial lead, is a registration of the projection of this T loop at that particular site on the body surface. Abnormalities in repolarization will affect the projection of this T loop. An increased dispersion at the end of the T wave is related to a more complex T loop (155). Regional dispersion in repolarization time may lead to QT dispersion through a more complex T loop, and an unusual projection of this loop (157, 158). The opposite, however, does not necessarily hold true. QT dispersion resulting from a more complex T loop does not necessarily reflect either a large local (157) or a huge global DVR (160). Despite the limitations mentioned above, QT dispersion can discriminate groups, and if not a direct measure of dispersion in repolarization, it is at least a measure of T wave abnormalities.

Late potentials on the signal-averaged ECG

Signal-averaged ECG is a noninvasive means of determining the presence of electrical late potentials in the ventricle. Signal averaging uses filtering and noise-reduction techniques to detect low-amplitude electrical potentials (180). Signal-averaged ECG records myocardial activation that occurs after the QRS complex. These very low-amplitude delayed signals are not detected by a routine ECG and correspond to delayed and fragmented areas of slow conduction in the ventricle, which predispose to the reentry and development of VT (181, 182). Signal-averaged ECG has an excellent negative predictive value of around 95% of future arrhythmic events; however, the positive predictive value is 14% to 29%. Thus, a positive signal-averaged ECG is not helpful in indicating which therapy is required. Consequently, the signal-averaged ECG alone has not been established

as an accurate predictor of ventricular tachyarrhythmias, but has been used as an adjunct to other invasive or noninvasive diagnostic modalities in the evaluation of mortality of ventricular tachyarrhythmias (180).

Microvolt T wave alternans

Microvolt T wave alternans is a beat-to-beat measurement of the amplitude and morphology of the ECG measurement of repolarization in the ST segment and T wave (183). ECG leads are placed in the standard positions with 3 leads placed in an orthogonal position to perform a T wave alternans testing. Patients are asked to exercise to a target heart rate ranging from 105 to 115 beats per minute for approximately 5 minutes. The amplitude of QRS alterations is measured in microvolts using spectral analysis. Compared to invasive electrical programmed stimulation, recent studies have estimated the sensitivity and specificity of the T wave alternans to be 77-86% and 72-75%, respectively, and the negative and positive predictive powers to be 92% and 42%, respectively, for prediction of the risk of ventricular tachyarrhythmias (183, 184).

Currently, the hypothesis regarding the arrhythmogenic mechanisms associated with T wave alternans is based on the concept that increased dispersion of repolarization produces reentrant ventricular tachyarrhythmias (133, 138, 185-187). The heterogeneity in dispersion of repolarization results in a 2:1 appearance on the surface ECG and provides a conduction block in the areas with prolongation of repolarization, which fractionates the wavefront and facilitates reentry. Shimizu *et al*. studied an experimental model of long QT syndrome using an arterially perfused wedge of canine left ventricular wall (7). When the preparation was paced at a critical fast rate, there was a pronounced alternation in AP duration of M cells, resulting in a reversal of the transmural repolarization sequence and leading to T wave alternans in the unipolar ECG. The alternation in AP duration for M cells observed under long QT conditions may exaggerate

transmural dispersion of repolarization and develop Torsades de Pointes. The changes in ionic currents during T wave alternans are not so clear. There is some evidence that the T wave alternans is linked to alternations in calcium homeostasis, which can significantly influence the AP duration (188). In addition, potassium channels may also play an important role in ischemia-induced T wave alternans. The different sensitivity of K_{ATP} channel activation during ischemia between epicardium and endocardium has been shown to be linked to T wave alternans at the cellular level (189-191).

Compared with signal-averaged ECG, T wave alternans had a higher sensitivity and more accurate negative and positive predictive values when both tests were compared with electrical programmed stimulation alone in determining which patients would have inducible or spontaneous ventricular arrhythmias (183). Most importantly, T wave alternans has been established as an independent predictor of VT, VF, and sudden death. On the other hand, the combination of T wave alternans and signal-averaged ECG is superior to either modality alone in predicting the risk of sudden cardiac death from VT/VF (184).

7. Methods used for assessment of ventricular repolarization

Transmembrane action potential

In evaluation of repolarization, transmembrane recordings of the AP are the reference method to which all other methods are compared. The system consists of a glass micropipette with a sharpened tip of a few microns, filled with a high-impedance KCl solution. The micropipette is coupled to one of the inputs of a high-impedance input amplifier, and a reference electrode is coupled to the other input channel. With the use of a micromanipulator，the tip is advanced through the cell membrane. This method can usually only be used in cell preparations or myocardial slices.

Sequential measurement of the effective refractory period

Sequential measurement of the myocardial effective refractory period from several myocardial sites is another way of evaluating the dispersion of cardiac repolarization, and has been widely used. Studies measuring effective refractory periods from one or several atrial sites have demonstrated more dispersion in patients with paroxysmal or chronic atrial fibrillation (shortly after cardioversion) than in patients without spontaneous atrial fibrillation (192). Similarly, the dispersion of the effective refractory period was found to be significantly different in patients with different kinds of ventricular arrhythmias (193). However, this method is very time consuming and therefore global data from sufficient number of sites were difficult to obtain. Besides, the refractoriness is not always parallel to the repolarization (194).

Optical mapping

A high-resolution optical mapping technique with use of imaging techniques based on voltage-sensitive dyes could accurately determine the local repolarization times and evaluate the sequence and dispersion of cardiac repolarization among hundreds of simultaneously recorded APs in the same cardiac cycle (8). Thus, optical mapping was considered to be the only technique capable of recording high-resolution maps of cardiac repolarization, and the only method to allow uninterrupted and artifact-free recordings of the transmembrane potentials during pacing (195) and defibrillation shocks (196, 197). This technique has been used for investigation of the time course and spread of endo- and/or epicardial repolarization, mainly in *in vitro* studies.

A major limitation of the optical mapping technique is the lack of absolute calibration (198). Unlike many ratio-metric fluorescent probes for calcium

imaging, voltage-sensitive dyes can only provide relative information about changes in transmembrane voltage. In addition, whether or not this system can be used to study myocardial electrophysiology *in vivo* remains to be determined. Furthermore, optical mapping is only applicable to visible areas, i.e., exposure of the heart is a prerequisite and the lateral aspects - and more especially the posterior aspects - of the heart are not accessible using this method.

Activation recovery interval from unipoar recordings

The activation recovery intervals, or "QT" intervals, on the intracardiac unipolar electrogram have also been used to evaluate the dispersion of ventricular repolarization (110, 115, 199). Gepstein *et al* recorded unipolar electrograms from 50-70 left ventricular endocardial sites in pigs using the CARTO system, and evaluated the dispersion of the activation recovery intervals (115). Our previous studies also suggested the usefulness of the activation recovery time measurement in evaluation of ventricular repolarization. Similar to the measurement of QT dispersion, however, the accuracy of this unipolar electrogram technique was found to be limited by the low-amplitude, multiphasic, and/or distorted pattern of the local "T waves" (195, 200).

8. Monophasic action potential recording and its global mapping

Monophasic action potential

Since the 1990s there has been a surge in the use of MAP recordings, in both clinical and experimental settings. This is because MAPs reproduce not only the local time course of myocardial repolarization with high accuracy, but also provide an accurate measure of the local activation (201-204). Several studies have examined the accuracy of MAP by simultaneously recording the MAP and transmembrane AP in close proximity. The MAP faithfully reflects both the

duration and the configuration of repolarization phases 1 through 3 of the transmembrane AP (Fig. 12) (201-203). Even during interventions that influence the AP configuration and duration, changes in the shape and duration were found to be almost identical in the transmembrane AP and MAP recordings (201). Thus, MAP recording has become an integral part of electrophysiological studies that are concerned with our understanding of basic electrophysiology and arrhythmia mechanisms in the intact heart.

Compared with the gold standard, transmembrane AP, the main advantage of MAP recordings is their *in vivo* applicability. Transmembrane AP recordings require the impalement of an individual cardiac cell by a glass-microelectrode and are therefore limited to *in vitro* preparations, while MAPs can be recorded from the endo- and epicardium of the beating heart *in situ*, including the human heart. With this advantage, the MAP recording technique is now considered the method of choice for studying characteristics of local myocardial repolarization both in

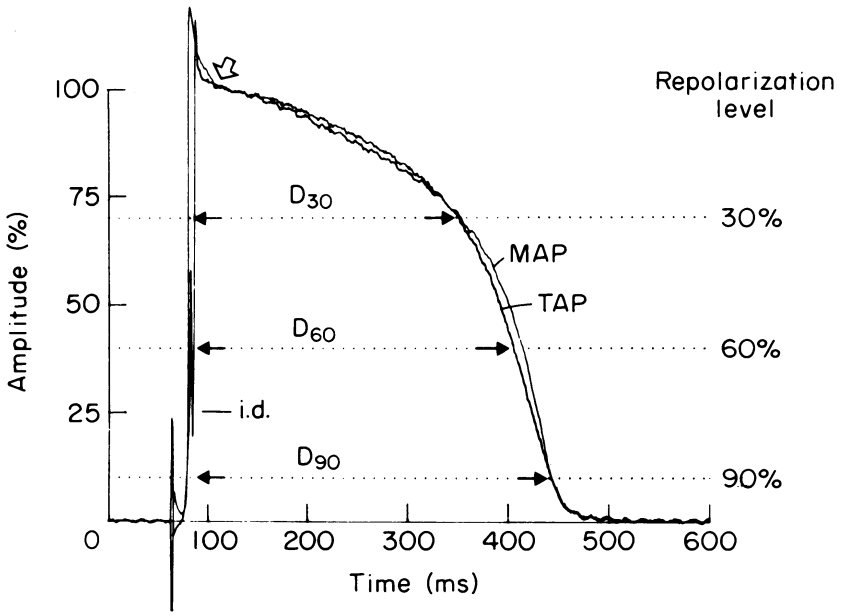

Fig. 12. Comparison of MAP and TAP recorded simultaneously from closely adjacent sites in a rabbit isolated perfused interventricular septum preparation. After being rescaled to match in amplitude, the MAP signal was superimposed onto the TAP signal. MAP = monophasic action potential; TAP = transmembrane action potential. Reproduced with permission from Franz MR, *et al*. (201).

experimental (205-208) and in clinical (30, 37, 39, 119-122, 128, 209) settings.

However, the MAP recording technique also has its limitations. The main limitation is its inability to provide information on absolute voltage of resting potential and AP amplitudes, or on absolute upstroke velocity. Another limitation is the decline of MAP amplitude during long-term recording. Although long-term recording of MAPs for up to 3 hours from the same endocardial site without further manipulation of the catheter has been reported (210), a decrease in the MAP amplitude is often seen in practice when the recording time at the same site is longer than 30 minutes.

Genesis of MAP

MAPs reflect the local time course of transmembrane potentials of a group of cells underlying the catheter tip during normal rhythms and during arrhythmias. The exact reason why this extracellular electrode in contact with myocardium closely reflects the time course of the transmembrane AP of the cells underlying the electrode is still not clearly known. The classic explanation is that, the MAP is generated underneath the distal electrode of the contact catheter: the catheter tip partially depolarizes the tissue subjacent to the tip. Thus, ionic current is flowing periodically at the interface between the depolarized tissue and the adjacent normal myocardium. As the depolarized tissue is electrically inactive, this sink current and its driving voltage gradient are proportional to the changes in membrane potential on the myocardium in the interface area, as demonstrated by a computer simulation model (202, 211).

However, there have been findings challenged this concept, claiming that the indifferent electrode should be the exploring electrode, i.e. that the recorded signal is not from the cells immediately beneath the tip electrode but rather from cells surrounding the tip at a distance of 2-3 mm (212, 213). Contrast to these findings, Knollmann *et al*. found that similar MAPs could be recorded between the tip and

the proximal electrode of the MAP catheter as well as between the tip and a remote indifferent electrode, but not between the proximal electrode on the MAP catheter and the remote indifferent electrode in isolated, perfused mouse hearts (214, 215), which is in agreement with the classic understanding. In a very recent study, Coronel *et al*. further demonstrated that MAPs are recorded from the depolarizing electrode (216).

The most available data support the classic concept of MAP genesis, and MAP recordings using close bipolar electrodes in larger hearts, as in humans and pigs, in the present PhD project reflect local activation and repolarization of the myocardium (204, 214-218). Consequently, detailed MAP mapping of the heart in situ will nevertheless yield global information about repolarization.

MAP recordings using an ablation catheter

Traditionally, silver-silver chloride (Ag-AgCl) electrodes have been used for

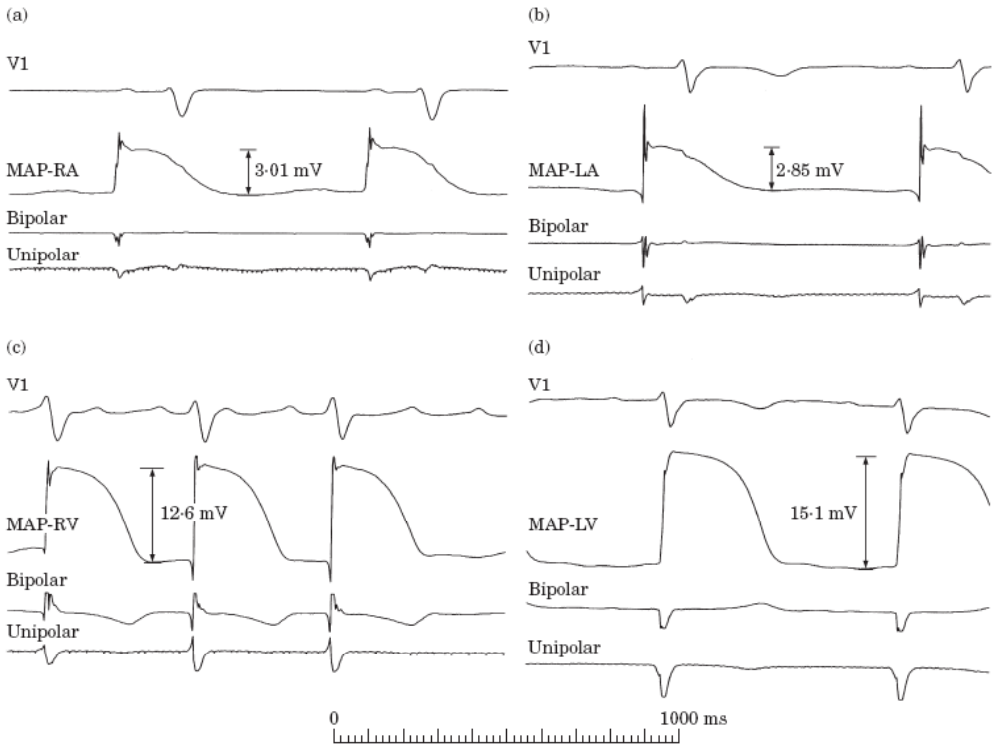

Fig. 13. Monophasic action potentials (MAPs) recorded using platinum-electrode ablation catheters from the right atrium (a), left atrium (b), right ventricle (c) and left ventricle (d) had characteristics consistent with those recorded using Ag-AgCl electrode catheters. Reproduced with permission from Yuan S, *et al*. (219).

MAP recordings. Recently, it has been verified that an ordinary ablation catheter with electrodes of platinum-iridium can be used for MAP recordings (Fig. 13). In a study of 40 patients undergoing electrical programmed stimulation and/or catheter ablation (219), 142 MAP recordings were obtained from the endocardium using the ordinary ablation catheter. During sinus rhythm and pacing, 90% of the ventricular MAPs and 100% of the atrial MAPs had a stable baseline. During these MAP recordings, an additional MAP was simultaneously recorded via an Ag-AgCl electrode catheter in the immediate vicinity of the ablation catheter. The MAPs via the ablation catheter were of somewhat lower amplitude, but otherwise had characteristics consistent with those via the Ag-AgCl catheter and revealed the same measurements regarding MAP duration, which verified that a platinum electrode catheter can be used for prompt recording of MAPs of acceptable quality (219). To further improve the quality of the MAP signals obtained with conventional ablation catheters, we developed a modified tip-electrode, i.e. by adding a contact ball 1.0 mm in diameter and 0.5 mm in length to the end surface of the tip-electrode (Fig. 14) in order to reduce the contact area of the Navi-Star mapping/ablation catheter. This modified-tip catheter was evaluated in another study and we found that MAPs recorded using this catheter were associated with more stable baselines and higher amplitudes than those recorded using the ordinary Navi-Star catheter (220). The method was both safe and feasible for *in vivo* MAP mapping, and provided us with the possibility of using the CARTO mapping system to perform detailed MAP mapping of myocardial repolarization.

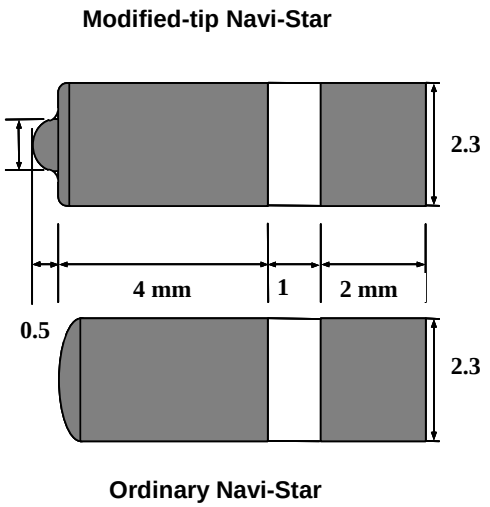

Fig. 14: Schematic comparison of the modified-tip electrode (upper) and the normal-tip electrode (lower) of the Navi-Star catheter. Reproduced with permission Liu S, *et al*. (220)

Electroanatomic CARTO mapping system

In order to evaluate global sequence and dispersion of repolarization, one needs 1) sufficient number of recordings reflecting local repolarization time and

AP/MAPd, and 2) accurate correlation of the recordings with the anatomical locations of the recording sites. The MAP recordings can meet the former requirement, and the electroanatomical mapping (CARTO) system can meet the latter.

The CARTO system is a sequential mapping system with a sophisticated display (221). During mapping, the torso of the subject is covered by three magnetic fields of different frequencies. A location reference (Ref-Star) is fixed on the back of the subject, while a mapping catheter (Navi-Star) navigates within the cardiac chambers or on the surface of the heart. The magnetic sensors equipped in the tip of the mapping catheter and the location reference continuously compare the intensities of the three magnetic fields, ensuring that the location of the mapping catheter can be accurately determined and displayed in real-time. Three-dimensional maps of endocardial or epicardial activation can be constructed from accurately localized electrograms recorded using the mapping catheter. The accuracy of spatial localization has been verified to be 0.7 mm *in vivo* (221).

The introduction of the CARTO system provided the possibility of rapid cardiac activation assessment with high spatial accuracy. It is not necessary to follow any anatomical scheme since the system accurately memorizes the recording sites and the acquired signals. However, the CARTO system is designed for evaluation of cardiac activation. Information of cardiac repolarization is not available by using this system in previous studies. A prerequisite for use of the CARTO system to evaluate repolarization is that the MAP recording catheter must be locatable by the system. We first validated the possibility of recording MAPs using a conventional platinum electrode ablation catheter (219) and then verified the feasibility of recording MAPs using a CARTO sensor equipped catheter. Using the special Navi-star catheter with a modified tip as mentioned above, the MAP recording technique has been successfully integrated with the CARTO electroanatomical mapping technique, and a series of experimental and clinical studies have verified the feasibility of this novel technique (37). In this Ph.D. project, the MAP mapping technique is used as a key technique in all 5 papers.

The quality of MAP recordings

The criteria for quality of MAP recording have not been well established, due to difficulties in getting MAPs from large series of healthy subjects. Generally speaking, the MAP should have a stable baseline so that the MAP duration could be correctly measured and reach an amplitude so that it faithfully reproduce the time course of intracellular AP. Olsson *et al*.(203) proposed that the atrial MAP should exceed 3 mV, the ventricular MAP should exceed 15 mV and baseline disturbance should not exceed 10% of the MAP amplitude. The ventricular MAPs recorded using the suction electrode (222) or the Ag-AgCl electrode (223) are at about 20 to 40 mV, while those recorded using conventional electrode catheters are of lower amplitude, at an average amplitude of 13.8 mV (219). Importantly, the repolarization times measured from the MAPs recorded using the conventional electrode are well consistent with those from the simultaneously recorded MAPs in close vicinity using an AG-AgCl electrode (219)

MAP measurements

The MAP analysis can be performed off-line using the feature of double annotations of the CARTO system. The first annotation line is set at the onset of the MAP upstroke, representing the local activation, the second at the intersection between the baseline and the tangent to the steepest slope on phase 3 of the MAP, representing the local EOR (37, 119, 120). The two annotation lines are both manually set and can be carefully checked under a time scale of 200 mm/s and 100 mm/s, respectively.

During analysis, the AT is defined as the time interval between the earliest recorded ventricular activation and the local activation, the MAP duration as the time interval between local activation and the local EOR, and the EOR time as the interval between the earliest ventricular activation and the local EOR. Taking the peak of the QRS complex on the upright ECG lead as the time reference, the AT, MAP duration, and EOR time can be calculated. Based on these values, three-dimensional maps of the activation sequence, EOR sequence and the spatial distribution of MAP durations are reconstructed (Fig. 8). The maximal differences in the AT, EOR time, and MAP duration, i.e. the total ranges of the scales of these maps, represent the total magnitude of the disparity between the measurement values, and are called the maximal dispersion of these parameters.

9. Some issues warranting further study

In summary, ventricular repolarization and its disturbances are of theoretical and clinical importance since they are linked to the occurrence of life-threatening ventricular tachyarrhythmias. However, our understanding of the mystic process is far from clear. The development of the MAP mapping technique provides us with the possibility of evaluation of the global sequence and dispersion of ventricular repolarization in healthy animals and in patients with and without ventricular arrhythmias. The MAP mapping technique is therefore a unique tool, and the data obtained by this method are a reliable standard for validation of the wide-spreadly adopted noninvasive methods. Consequently, the following issues form the basis of the current PhD project.

Recording of MAPs using the modified-tip catheter and the CARTO system provides the possibility of detailed global mapping of ventricular repolarization. On the other hand, the activation recovery interval from unipolar electrograms is a good estimate of local repolarization, and is much easier to obtain compared to MAP recording and optical mapping, etc. It is therefore of interest to test whether global activation recovery interval from unipolar electrogram and CARTO system could be used for evaluation of global sequence and dispersion of ventricular repolarization.

In arterially perfused ventricular wedge preparations, the full repolarization of the epicardium coincides with the peak of the T wave (T_{peak}), and that of the M cells coincides with the end of the T wave (T_{end}) on the pseudo-ECG. The apico-basal voltage gradient was suggested to contribute little to the genesis of the T wave. However, many *in vivo* studies have failed to verify the existence of marked transmural DVR. The coincidence of the T_{peak} and full repolarization of the epicardium, and T_{end} and full repolarization of endocardium has never been validated *in vivo*. In addition, the relationship between the QT interval/QT dispersion, T_{peak}-T_{end} interval, and the global ventricular repolarization needs to be clarified.

Ventricular pacing has been widely used in patients with bradycardia, and recent studies have highlighted the benefits of resynchronization therapy of biventricular pacing in patients with congestive heart failure. In contrast to the

extensive *in vivo* explorations of ventricular repolarization during sinus rhythm, however, the characteristics of repolarization during ventricular pacing are poorly understood. Our recent studies have suggested that, contrary to the conventional concept that the repolarization sequence is in the direction opposite to that of the activation, the global sequence of repolarization follows that of activation during sinus rhythm. Moreover, previous data from *in vitro* ventricular preparations have suggested that the altered activation sequence could lead to changes in ventricular repolarization. How the global ventricular repolarization sequence is changed by altered ventricular activation sequence, however, has never been evaluated *in vivo*.

Importantly, recent experimental studies have shown that the altered ventricular activation sequence during epicardial pacing may increase transmural heterogeneity of repolarization of the ventricular myocardium, which may be linked to the development of Torsades de Pointes in patients with biventricular pacing. Thus, assessment of the global DVR under epicardial pacing is of important clinical applications.

AIMS

1. To validate whether the global sequence and dispersion of ventricular repolarization measured from MAP recordings can be estimated by the ART measurements on unipolar electrograms using the CARTO mapping system in patients with arrhythmias (Study I).

2. To determine whether the full repolarization of the epicardium is consistent with the T_{peak}, and that of the endocardium is consistent with the T_{end}, by simultaneous recordings of MAPs from both the epicardium and endocardium and 12-lead ECG using the CARTO mapping system in swine (Study II).

3. To verify the T_{peak}-T_{end} interval and QT dispersions as an index of global DVR using MAP mapping over both the epicardium and endocardium and simultaneously recorded 12-lead ECG in swine, and to validate the measurement methods for the T_{peak}-T_{end} interval (Study III).

4. To explore the global sequence of ventricular repolarization *in vivo* under ventricular pacing at two of the most commonly used pacing sites, endocardial pacing at the RV apex, and epicardial pacing at the lateral LV, and to examine whether altered activation sequence governs the ventricular repolarization sequence under these pacing protocols (Study IV).

5. To evaluate the global DVR *in vivo* during altered activation sequences under endocardial pacing at the RV apex and epicardial pacing at the lateral of the LV, and to determine whether LV epicardial pacing could lead to augmentation of the global DVR (Study V).

SUBJECTS AND ANESTHESIA

1. Patients (Study I)

Twelve patients (10 men and 2 women, mean age 57.6±13.7 years) referred for electrophysiological study and/or radiofrequency catheter ablation were recruited: 7 patients were diagnosed with ventricular tachycardia, 2 patients with ventricular fibrillation, and 3 patients with supraventricular tachycardias. None of the patients had had amiodarone treatment within the previous 3 months. All other antiarrhythmic drugs had been withdrawn for a period equivalent to at least 5 half-lives before the study. The patients received local anesthesia and sedation with Valium, but were conscious during the whole procedure. The local ethics committee approved the study, and informed consent was obtained from all patients. The electrophysiological procedures were performed in accordance with the guidelines of the local institution.

2. Animals (Studies II - V)

Twenty healthy pigs weighing 46-53 kg were included in this project. The pigs were raised on a special low-fat diet and on a regular exercise program for medical experiments in accordance with the "Guide for the Care and Use of Laboratory Animals" by the National Institutes of Health (NIH Publication 85-23, revised 1985). The local ethics committee of Lund University, Sweden, approved the animal studies.

All 20 pigs were premedicated with pancuronium bromide (0.1mg/kg), thiopental (5mg/kg) and atropine (0.015mg/kg). Anesthesia was maintained with an infusion of 10 mL/hour of a mixture of 1 mg fentanyl and 20 mg pancuronium bromide. Intubation and artificial ventilation of the pigs were performed during the study. Volume-controlled ventilation of 8L/min, 20 breaths/min, positive end-expiration pressure of 5cm H_2O and FiO_2 of 0.5 was used. In the first series of the 10 pigs, thoracotomy and pericardectomy were performed to expose the heart for the purpose of epicardial MAP mapping (the 10 open-chest pigs). In the second series of 10 pigs, only endocardial MAP mapping was performed and therefore no thoractomy was performed (the 10 close-chest pigs).

METHODS

1. MAP recording using the CARTO system (Studies I-V)

Recording procedure

The magnetic pad of the CARTO system (Biosense Webster, Waterloo, Belgium) was fixed under the examination bed, in relation to the position of the heart. A Navi-Star catheter with (in pigs) or without (in patients) a modified tip (Biosense Webster) was introduced and navigated over the endocardium and/or epicardium of the left and/or right ventricles to record MAP signals.

The MAPs were recorded sequentially at a filter band of 0.05-400 Hz. In the real-time monitor window of the CARTO system, one lead ECG, the MAP (Fig. 15), and a unipolar electrogram from the indifferent electrode were displayed. Caution was taken to place the mapping catheter perpendicularly against the endocardium with gentle contact pressure to obtain satisfactory MAP recording. When the amplitude and morphology of the MAP appeared satisfactory (204), the signals were captured into a sampling window for further inspection. In order to estimate global information accurately, effort was made to record at least one MAP in an area of 2 cm^2 (Fig. 16). To avoid the influence of variations in heart rate, the cycle length stability monitor function of the CARTO system was used and MAP sampling was performed when the cycle length was within ± 5% of the

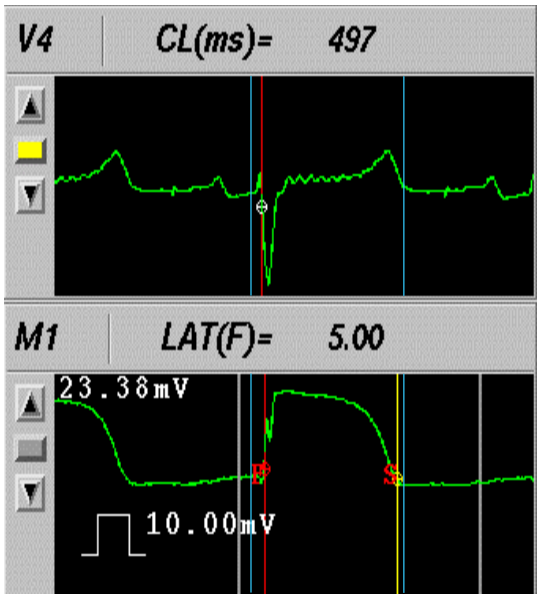

Fig. 15: Ventricular monophasic action potential (MAP) recorded during right atrial pacing in the sampling window of the CARTO system. On the ECG (upper tracing), the time reference line is set on the maximum slope of the QRS complex (second line). On the MAP (lower tracing), MAP duration is measured as the interval between the two annotation lines, the 3rd and 4th lines. The second line in the lower tracing denotes the earliest activation time; thus, the interval between this 2nd line and the 4th line represents the local end of repolarization time.

baseline cycle length in Study I, whereas in Studies II-V the MAP mapping was performed under stable atrial or ventricular pacing in the pigs. Accepted MAP signals, together with 12-lead ECG, were stored on the hard disc using a sampling frequency of 1 kHz for off-line measurement.

Definitions of MAP measurements

AT: activation time, the time interval from the earliest recorded ventricular activation to the local activation.

MAPd: MAP duration, the time interval from the local activation to the local end of repolarization (EOR) time.

EOR: end of repolarization time, the time interval from the earliest ventricular activation to the local repolarization point, which is equal to the sum of AT and MAPd at that recording site. EOR_{epi} refers to the EOR times calculated over the epicardium, EOR_{endo} over the endocardium, and EOR_{total} over both.

Dispersion of AT and EOR: the greatest differences in the parameters among all the recordings of the area concerned.

"Global" was added to the parameter to represent that obtained from all the

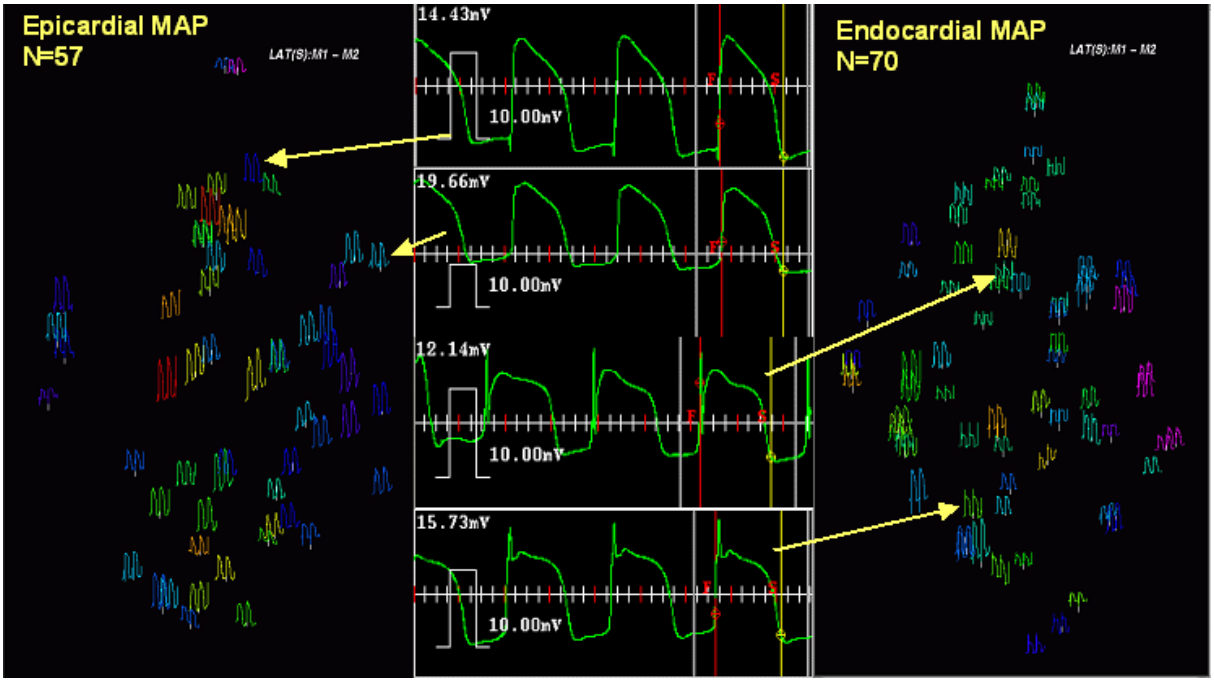

Fig. 16: Selected monophasic action potential recordings from the 2-dimentional views of all the MAPs from the epicardium (left) and endocardium (right) in an open-chest pig. Recording sites over both epicardium (n = 57) and endocardium (n = 70) are displayed, with at least one MAP in an area of 2 cm^2.

recordings of the whole ventricle.

Off-line MAP analysis using the CARTO system

MAP analysis was performed off-line using the double-annotation feature of the CARTO system. The first annotation was defined as the onset of the rapid phase of the MAP upstroke, representing local activation. The second was defined as the intersection between the baseline and the tangent to the maximal slope on phase 3 of the MAP, representing the local EOR (Fig. 15). When there was a baseline disturbance and/or distortion of MAP morphology, the MAP signal of the previous beat was also measured for necessary corrections. The two annotation lines were both manually set and carefully checked with display time scales of 200 mm/s and 100 mm/s, respectively. Taking the maximum/minimum value, or maximum slope of an QRS complex on the simultaneously recorded ECG as the time reference, the relative values of AT and EOR were obtained according to the above-mentioned definitions (Fig. 15). Based on these values, 3-dimensional maps of the sequences of activation and repolarization over the endocardium and/or the epicardium in the left and/or right ventricles were constructed using the CARTO system.

2. Recording of unipolar electrograms and measurement of ART using the CARTO system (Study I)

Recording procedure

In Study I, unipolar electrograms were recorded simultaneously using the same tip-electrode as that for MAP recording at a filter bandwidth of 0.1-120Hz. Unipolar electrograms with low amplitude and distorted pattern, where the end of "T" wave was difficult to define, were excluded along with the MAP from the same site. Thus, unipolar electrogram was also recorded, with at least one recording in an area of 2 cm^2.

Definitions of ART, and its analysis

On the unipolar electrograms, the ART was defined as the time interval from the earliest recorded ventricular activation to the intersection between the baseline and the tangent to the maximal slope on the terminal phase of the "T" wave in each individual recording. Taking the same time reference as that for the MAP analysis from the surface ECG, the relative values of ART were obtained at each site (Fig. 17; Study I).

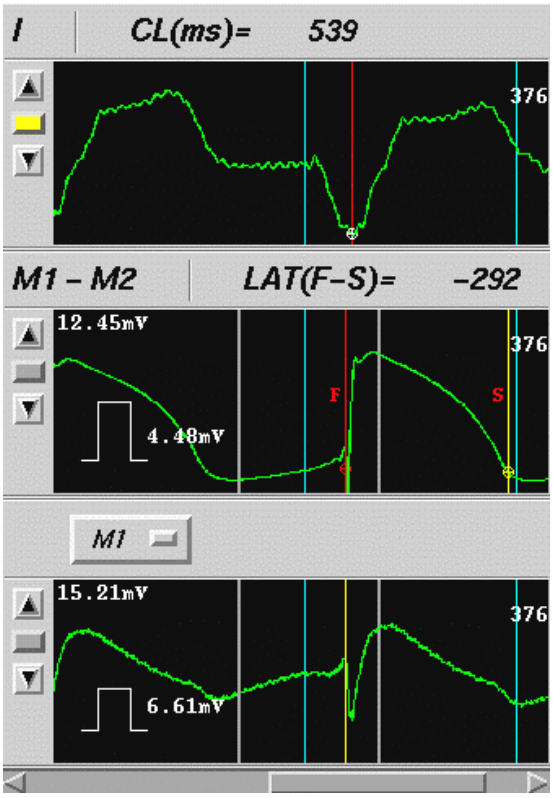

Fig. 17: Recordings of MAP and unipolar electrogram from the left ventricle during ventricular tachycardia in the sampling window of the CARTO system. On the ECG (upper tracing), the time reference line is set on the peak of the QRS complex (2nd line). On the MAP (middle tracing), MAPd is measured as the interval between the two annotation lines, the 3rd and 5th lines. The 2nd line denotes the earliest recorded activation and thus the interval between this 2nd line and the 5th line represents the local end of repolarization time. On the unipolar electrogram (lower tracing), the 2nd line represents the earliest recorded activation and the 5th line is on the intersection between the baseline and the tangent to the maximal slope on the terminal phase of the "T" wave. Between the 2nd and 5th lines is the activation recovery time. Time scale: 100 mm/s.

Two investigators measured the EOR times and ARTs independently and the means of their measurements were used for data analysis. Based on these values, three-dimensional maps of the EOR and ART were constructed. The global dispersion in ART was calculated as the maximum difference in ART over the left or right ventricular endocardium.

3. Pacing protocols (Studies II - V)

In the 10 open-chest pigs, to avoid the influence of variations in heart rate, the MAP mapping was performed during constant pacing at the high lateral right atrium at 130 beats/min, with the temporal pacing 6F leads introduced through the right femoral vein.

In the 10 close-chest pigs for studies IV and V, three kinds of pacing protocols were performed, which was right atrial (RA) pacing, endocardial pacing at the RV apex (RV_{endo}), and epicardial pacing at the LV lateral-basal wall (LV_{epi}). For RA and RV_{endo} pacing, a temporary myocardial active fixation pacing lead (Model 646, Medtronic) was introduced through the right jugular vein and attached to the endocardium of the high lateral RA or the RV apex. For LV_{epi} pacing, a 4F pacing electrode was used. The electrode was relatively difficult to deliver due to the anatomy of the porcine coronary venous system, in which the great cardiac vein joins with a prominent left azygous vein at the posterolateral atrioventricular groove - where it becomes the coronary sinus (10) (Fig. 18). During the studies, a 6F lumen catheter was introduced into the coronary sinus, through which the 4F pacing lead was delivered, avoiding going up to the left azygous vein, into the great cardiac vein, as far as possible until it stopped to allow a stable LV epicardial pacing. Thus, the pacing leads were located on the epicardial side at the laterobasal part of the LV (Fig. 18). The pacing leads were connected to an external pacemaker (Model 30-77; St. Jude Medical) with the output at twice diastolic threshold and 0.4 ms pulse width.

These 10 close-chest pigs were divided into two groups. In 5 pigs (Group I),

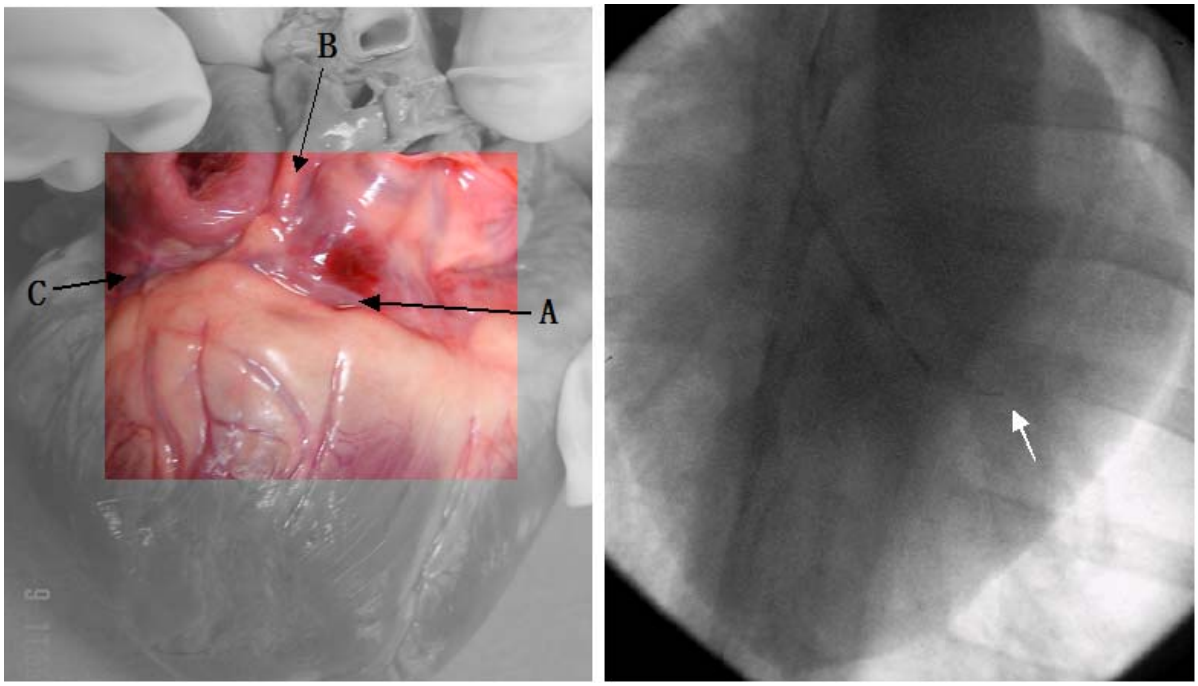

Fig. 18: The anatomy of the coronary sinus in pigs. Left: photo of coronary sinus. A: coronary sinus; B: left azygous vein; C: great cardiac vein. Right: left ventricular epicardial pacing lead located at the lateral free wall of left ventricle in anterio-posterior view under X-ray (white arrow).

endocardial MAPs were recorded from both the right and left ventricles during RA pacing, and then during RV_{Endo} pacing. In the remaining 5 pigs (Group II), endocardial MAPs were recorded from both ventricles during LV_{Epi} pacing, and then during RV_{Endo} pacing. A period of sinus rhythm for more than 30 min was kept between the two pacing protocols. MAPs were always recorded after 30 min of atrial/ventricular pacing to reach the steady state. To avoid potential time-dependent changes, the mapping procedure of each pacing protocol was limited to 3 hours or less. In addition, to avoid the influence of variations in heart rate and thereby the capture of sinus beats, the pacing rate was set at 130 beats/min, - i.e. 20-30 beats/min faster than the baseline rate - during the mapping.

4. Endocardial and/or epicardial mapping and MAP analysis

Endocardial mapping in patients (Study I)

MAP recording was performed using a 7F Navi-Star catheter (Biosense-Webster, Waterloo, Belgium) before or after clinical electrophysiology and/or radiofrequency catheter ablation procedure. The catheter was introduced into the left ventricle via the femoral artery (n = 3) or into the right ventricle via the femoral vein (n = 9), depending on the location of the arrhythmogenic substrate. Care was taken to place the mapping catheter perpendicularly against the endocardium with gentle contact pressure to obtain satisfactory MAP recording. Unipolar electrograms were recorded simultaneously using the same tip-electrode as that for MAP recordings.

Endocardial mapping and epicardial mapping in 10 open-chest pigs (Studies II and III)

In the series of 10 open-chest pigs, both endocardial and epicardial mapping were performed after thoracotomy and pericardectomy. In 2 pigs both of the right and left ventricles were mapped, and in the remaining 8 pigs only the left ventricle was mapped. A modified-tip, 7F Navi-Star catheter (Biosense Webster) was used, which has a contact ball 0.5 mm in length and 1 mm in diameter at the end of the tip-electrode (220).

For endocardial mapping, the catheter was introduced into the left ventricle via the right femoral artery, and/or into the right ventricle via the right femoral vein. For epicardial mapping, the epicardial surface was first exposed by way of a medial sternotomy with the pericardium opened along the median line from apex to aortic arch. The mapping catheter was mounted on an elastic handle of an epicardial-mapping probe (EP Technologies, Sunnyvale, CA). The probe was held with the electrode tip perpendicular to the myocardial surface with a gentle pressure. Two saline lines were hung over the left and right ventricles, with warm saline drip to keep the myocardial temperature constant and thus to facilitate electrical contact of the electrodes with the epicardium. A thermometer (myocardial needle temperature probe) was inserted into the myocardium of the right ventricular outflow tract for monitoring of myocardial temperature during the whole experiment (Fig. 19). If necessary, the temperature and speed of the saline drop were adjusted.

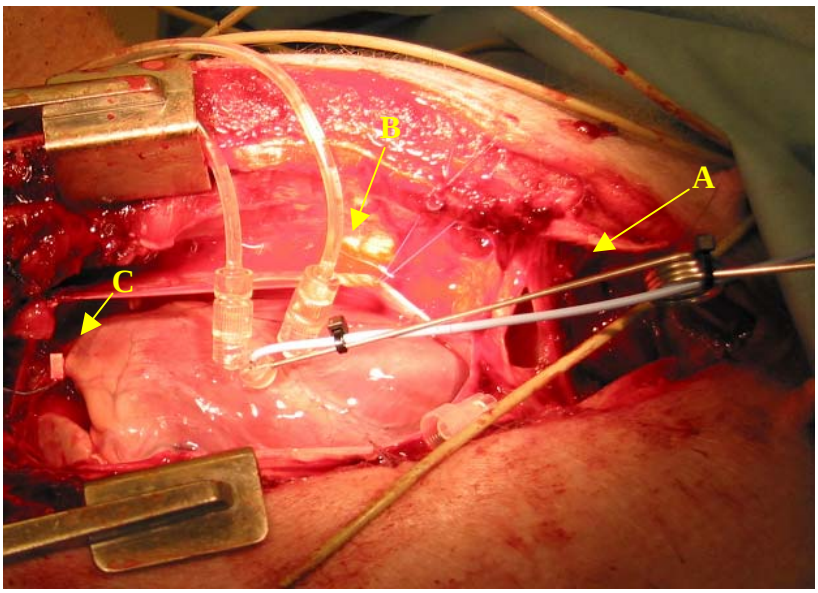

Fig. 19: Epicardial mapping with a modified-tip NaviStar catheter mounted on an elastic handle (A). Myocardial temperature was kept constant by drips of warm saline (B) controlled by a temperature monitor (C).

Endocardial mapping under ventricular pacing in 10 close-chest pigs (studies IV and V)

A modified-tip Navi-Star catheter (7F, Biosense Webster) was used in this series of 10 close-chest pigs (220). For left ventricular mapping, the catheter was introduced into the left ventricle via the right carotid artery and/or the right femoral artery. For right ventricular mapping, the catheter was introduced via the right jugular vein and/or the right femoral vein. A 7F long sheath (St. Jude

Medical) was used to facilitate catheterization in some areas of the right or left ventricle whenever required.

In Group I, endocardial MAPs were recorded from both right and left ventricles during RA pacing, and then during RV_{Endo} pacing. In Group II, endocardial MAPs were recorded from both ventricles during LV_{Epi} pacing, and then during RV_{Endo} pacing (Fig. 20).

5. Recording and analysis of the 12-lead ECG (studies II - V)

In all the pigs, twelve-lead ECG was recorded simultaneously with the MAP recordings at a filter setting of 0.5-120 Hz using the CARTO system, with the recording electrodes being placed referencing to the electrode placement in humans.

Measurement of the QT_{peak} and QT_{end} intervals

QT_{peak} and QT_{end} intervals were measured as the time intervals from the earliest QRS onset to the peak and end of the T wave, respectively, in each of the 12 leads. T_{peak} was defined as the time point at which the T wave had the maximum amplitude. T_{end} was defined using the slope method, i.e. the intersection of the tangent to the point of maximum slope of the terminal T wave with the isoelectric

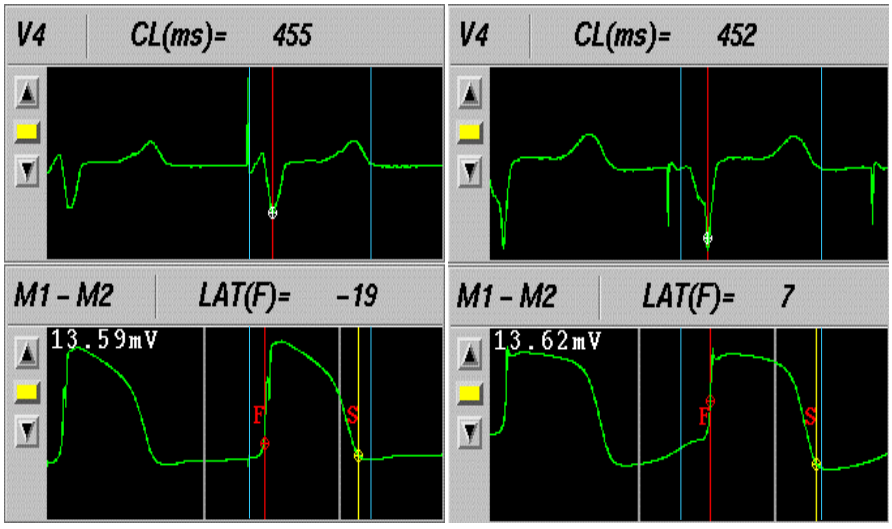

Fig. 20: Ventricular MAP recorded during RV_{endo} pacing (left) and LV_{epi} pacing (right). On the ECG (upper tracing), the time reference line is set on the minimum value of the QRS complex (2^{nd} line). On the MAP (lower tracing), the measurements of AT, MAPd and EOR are the same as shown in Fig. 15.

level defined by the T-P segment. The measurement was conducted on-screen at a sweep speed of 50 mm/s. Leads with high noise levels were discarded from analysis, as were flat or distorted T waves that made the identification of T_{peak} and/or T_{end} impossible (Fig. 21).

In the 10 open-chest pigs (Studies II and III), the ECGs were recorded after the thoractomy. The QT_{peak} and QT_{end} intervals in each of the 12 leads were measured manually three times at the beginning, middle, and end of the MAP mapping procedure using an on-screen electronic caliper. Each time, the above parameters were measured from 2 consecutive beats and the mean was obtained. The mean values of the above-mentioned 3 measurements were again averaged and the mean was used for final analysis. Due to the variations of the T_{peak} and T_{end} time points between the 12 leads, the maximal, mean, and minimal QT_{peak} and QT_{end} intervals were calculated for each pig.

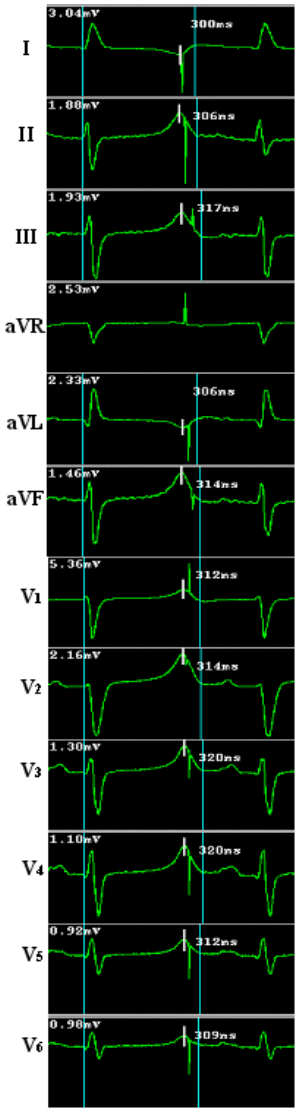

Fig. 21: ECG measurements from an open-chest pig. In each ECG lead, the first vertical line denotes the earliest activation time, and the second vertical line denotes the end of the T wave. The short white line marks the peak of the T wave. The values on the second line in each lead are QT_{end} intervals.

In the 10 close-chest pigs (Studies IV and V), the ECG parameters were measured 30 min after the onset of the pacing under each pacing protocol. QT intervals were calculated as the time intervals from the earliest QRS onset to the latest end of the T wave in the 12 leads. The terms of T_{peak} and T_{end} were defined in the same way as described above in the open-chest pigs.

Measurement of QT dispersions and T_{peak}-T_{end} intervals

In the 10 open-chest pigs, QT_{peak} dispersion was defined as the difference between the maximum and minimum QT_{peak} intervals, and QT_{end} dispersion was defined as that between the maximum and minimum QT_{end} intervals. Due to

the variation in the peaks and ends of the T wave, T_{peak}-T_{end} intervals were calculated as maximal, minimal and mean values in the 12 leads, which was from the earliest T_{peak} to the latest T_{end}, from the latest T_{peak} to the earliest T_{end}, and the average of all the T_{peak}-T_{end} intervals of the 12 leads, respectively.

In the 10 close-chest pigs under ventricular pacing, only QT dispersion, and average and maximum T_{peak}-T_{end} interval were calculated. QT dispersion was defined as the difference between the maximal and minimal QT intervals in the 12 leads. The T_{peak}-T_{end} interval was also measured in each lead and the average T_{peak}-T_{end} interval and the maximum T_{peak}-T_{end} interval, the difference between the earliest recorded T_{peak} to the latest recorded T_{end}, were obtained

6. Statistical analysis

All data are presented as mean ± 1 SD. A p value < 0.05 was considered statistically significant.

In Study I, the ART on the unipolar electrograms was compared with the EOR time on simultaneously recorded MAP recordings. The difference between EOR time and ART at each site was calculated and the summarized data in each map and in all the 473 recordings were acquired. Student's t-test was performed to analyze these differences and their dispersions. Correlation analyses were used to study the relations between the EOR time and ART. Agreement analyses were also performed to test whether the ART measurements agreed with the EOR times; the limits of agreement were set as the mean difference ± 2 standard deviations (SD) (224, 225). The difference between the ART and EOR time at each site was plotted against the average of these two measurements. If the differences between these two measurements fall in the range of the mean difference ± 2 SD of the mean, this suggests that the two measurement methods agree well with each other. The 95% confidence intervals for the lower and upper limits were also calculated.

In the series of 10 open-chest pigs, paired, two-tail Student's t-test was used to study the differences between QT_{peak}/QT_{end} intervals and the EOR times (Study II), and between the dispersion of EOR-epi/endo and dispersion of EOR-total (Study III). In addition, the QT_{peak} dispersion, QT_{end} dispersion and T_{peak}-T_{end} intervals were compared with the dispersion of EOR-total, respectively (Study III). Moreover, correlation analyses was also used to study the relationships between

the ECG parameters and EOR times (Study II), and between the DVR parameters and the relevant ECG repolarization variables (Study III).

In the series of 10 close-chest pigs, differences of AT, MAPd, EOR time, and the relative dispersion parameters between the two groups and among the 3 pacing protocols were all analyzed using Mann-Whitney test (Studies IV and V). Linear correlation and regression analyses were used to study the relationship between the MAPd and AT and between the EOR time and AT. Thus, all MAPds and the EOR times in a map were plotted against AT, regardless of recording sites (Study IV).

MAIN RESULTS

1. General data on MAP recordings in patients (Study I)

Right ventricular mapping was performed during sinus rhythm in 8 patients and during sustained ventricular tachycardia in 1 patient. In the remaining 3 patients, the left ventricle was mapped twice: in patient #1 during ventricular premature beat and during sustained ventricular tachycardia, in patient #2 during sustained ventricular tachycardia and during sinus rhythm, and in patient #6 before and after radiofrequency catheter ablation of left-sided accessory pathway. In total, MAPs were recorded at 473 sites in the 12 patients with 9 sets of right ventricular and 6 sets of left ventricular maps constructed. During the mapping procedure, cycle length variation was $\leqslant$5% during sinus rhythm and $\leqslant$1% during ventricular premature beat or sustained ventricular tachycardia.

In these patients, the MAP plateau amplitude was 10.2±4.0 mV for the left ventricular MAPs and 10.4±5.8 mV for the right ventricular MAPs during sinus rhythm. During ventricular tachycardia or ventricular premature beat, the amplitude of the left ventricular MAPs was 9.1±5.0 mV, and that of right ventricular MAPs was 8.8±4.9 mV. The baseline disturbance was less than 10% of the plateau amplitude in 80% of the recordings and less than 15% of the plateau amplitude in all of the 473 recordings.

2. General data on unipolar elecrtrogram in patients (Study I)

In these patients, the unipolar electrocardiograms were somewhat different in morphology from the patterns of conventional recording methods (Fig. 18). Slight “ST” elevation was observed in most of the recordings, probably due to the contact pressure applied for simultaneous recording of the MAPs using the same electrode. However, the elevation of “ST” segment did not affect the determination of the end of ART. The local “T” wave could be classified as having a positive, negative, or biphasic morphology. In about 20% of the unipolar electrograms, the end of “T” wave was difficult to define and they were discarded along with the MAP from the same site, even if the MAPs were of acceptable in quality. In the remaining recordings, the intersection between the baseline and the

tangent to the steepest slope on the terminal phase of the "T" wave could be clearly defined.

3. General data on MAP recordings in pigs (Studies II - V)

Epi- and Endocardial MAP recordings in the 10 open-chest pigs (Studies II and III)

In the 10 open-chest pigs, MAPs were recorded from 51±10 epicardial sites and 64±9 endocardial sites of the left ventricle in all 10 pigs, and from 41±4 epicardial sites and 53±2 endocardial sites of the right ventricle in 2 of the 10 pigs. Based on these data, 12 sets of endo- and epicardial maps were constructed. The MAP plateau amplitude was 13.6±5.0 mV for the epicardial MAPs and 13.6±5.6 mV for the endocardial MAPs from the left ventricles, and 12.8±4.6 mV for the epicardial MAPs and 13.0±5.0 mV for the endocardial MAPs from the right ventricles. The baseline disturbance was less than 10% of the plateau amplitude in 80%, and less than 15% of the plateau amplitude in all the 591 epi- and 746 endocardial MAP recordings.

Twelve-lead ECG was recorded before and after the thoracotomy. No motion artefact from heartbeat was observed on the ECG during the MAP recording procedure. The baseline appeared stable without 50-Hz disturbances. During the QT interval analysis, 1±1 leads were discarded because of flat or distorted T waves. No U wave was documented in any of the 10 pigs. The minimal, mean and maximal QT_{peak}/QT_{end} intervals are presented in Table 1.

For EOR time and QT interval measurement, the onset of the earliest QRS was used as the earliest recorded ventricular activation in the MAP analysis in all 10 pigs. Thus, the QT intervals and the EOR times were calculated from the same starting point. In addition, the local activation times measured from the MAP recordings were found to cover the whole duration of the QRS complex in all the pigs.

Thus, 3-dimensional maps of the repolarization sequences of EOR time over both the epi- and endocardium were constructed in the 10 open-chest pigs.

Endocardial MAP recordings in the 10 close-chest pigs (Studies IV and V)

In the 10 close-chest pigs, MAPs were recorded from 112±16 endocardial sites of both ventricles during RA pacing in 5 pigs (Group I), from 122±23 sites during RV_{Endo} pacing in all 10 pigs (Groups I and II), and from 126±26 sites during LV_{Epi} pacing in 5 pigs (Group II). The endocardial AT and MAPd of the right and left ventricles were measured in each group during RA pacing, RV_{Endo} pacing and LV_{Epi} pacing, respectively (Table 2). Based on these data, the EOR times were calculated and three-dimensional maps of activation and repolarization under each pacing protocol were reconstructed in each pig. Thus, in total 20 sets of ventricular maps were constructed. The MAP plateau amplitude was 13.8±5.7 mV during RA pacing, 13.2±5.3 mV during RV_{Endo} pacing, and 13.7±5.6 mV during LV_{Epi} pacing for the ventricular endocardial MAPs. The baseline disturbance was less than 10% of the plateau amplitude in 80% of endocardial MAP recordings, and less than 15% of the plateau amplitude in all 2416 endocardial MAP recordings.

Table 1: Comparison between the QT intervals and the end of repolarization times from the monophasic action potential recordings in the left ventricles of the 10 open-chest pigs

	Endocardium			Epicardium			Min EOR_{-total}	Max EOR_{-total}	Min QT_{peak}	Mean QT_{peak}	Max QT_{peak}	Min QT_{end}	Mean QT_{end}	Max QT_{end}
	Sites	Min EOR	Max EOR	Sites	Min EOR	Max EOR								
Pig 1	56	287	350	67	291	330	287	350	286	291	300	333	339	352
Pig 2	59	272	349	67	289	328	272	349	254	261	269	287	305	310
Pig 3	57	318	379	32	312	341	312	379	309	315	321	354	362	369
Pig 4	75	251	306	49	255	281	251	306	250	258	267	286	302	307
Pig 5	72	299	331	47	301	349	299	349	294	300	305	321	340	343
Pig 6	49	264	328	50	279	310	264	328	286	297	306	334	345	350
Pig 7	66	282	314	47	276	303	276	314	266	275	281	285	310	314
Pig 8	59	329	372	45	309	354	309	372	340	348	354	373	389	395
Pig 9	77	280	320	48	268	306	268	320	254	261	266	284	297	300
Pig10	70	292	338	57	285	318	285	338	287	291	294	318	331	341
	64±9	287±24	*339±24	51±10	287±18	†322±23	‡282±20	#341±24	283±28	290±28	296±28	318±32	333±29	338±30

Data are presented in ms. * $p > 0.05$ compared with the maximal QT_{end} interval; † $p < 0.05$ compared with the minimal, mean, and maximal QT_{peak} intervals; ‡ $p > 0.05$ compared with the minimal QT_{peak} interval; # $p > 0.05$ compared with the maximal QT_{end} interval. Min and Max: minimal and maximal; EOR: end of repolarization time; EOR_{-total}: EOR times on both the epicardium and endocardium.

Table 2: The activation times and MAP durations of right and left ventricles during RA, RV_{Endo} and LV_{Epi} pacing in the 10 close-chest pigs

	n =	Activation time (ms)			MAP duration (ms)		
		RV + LV	RV	LV	RV + LV	RV	LV
RA pacing (I)	5	28 ± 6	22 ± 6	25 ± 8	217 ± 12	213 ± 9	222 ± 10
RV_{Endo} Pacing (I)	5	34 ± 8	23 ± 9	27 ± 10	223 ± 14	220 ± 11	228 ± 11
LV_{Epi} Pacing (II)	5	43 ± 11	39 ± 11	30 ± 11	*235 ± 16	229 ± 13	247 ± 15
RV_{Endo} Pacing (II)	5	35 ± 9	24 ± 9	27 ± 10	220 ± 14	217 ± 13	223 ± 8
RV_{Endo} Pacing (I + II)	10	34 ± 9	23 ± 9	27 ± 10	221 ± 13	219 ± 11	225 ± 11

Data are presented as mean ± 1SD in ms. *: MAP duration during LV_{Epi} pacing was significantly greater than that during RV_{Endo} and RA pacing ($p < 0.05$). MAP: monophasic action potential; RA: right atrial; RV_{Endo}: right ventricular endocardial; LV_{Epi}: left ventricular epicardial. I and II: Group I and Group II.

In Group I, MAPd during RV_{Endo} pacing, which was 228±11 ms in LV and 220±11 ms in RV, was similar to that during RA pacing, which was 222±10 ms in LV and 213±9 ms in RV (both $p > 0.05$). In Group II, however, MAPd during LV_{Epi} pacing was 247±12 ms in LV and 229±10 ms in RV, which was significantly greater than that during RV_{Endo} pacing (223±8 ms in LV and 217±13 ms in RV; both $p < 0.05$). During RV_{Endo} pacing, no significant difference in MAPd was found between the 2 groups ($p > 0.05$), suggesting that in Group II the earlier LV_{Epi} pacing did not have a significant effect on MAPd recorded during RV_{Endo} pacing.

4. Relationship between ART and EOR times in patients (Study I)

Comparison of the ART and EOR time and their dispersions

To quantify the difference between the ART and EOR times acquired from the patients, their values were compared (Table 3). For the total of 473 paired measurements in the 15 maps, the difference between the ART and the EOR time was 2±22 ms ($p > 0.05$). The differences between ART and EOR times were also compared as paired measurements in each map, and in all right and left ventricular maps. No statistical significance was found for these comparisons. Furthermore, the maximum dispersion of ART and that of EOR time were not either statistically different from each other (Table 3).

Table 3: Measurement values and maximum dispersion of the activation recovery time (ART) and end of repolarization (EOR) time in patients

	N	Sites	ART		EOR time	
			Values	Max. disp.	Values	Max. disp.
LV	6	28±10	346±27	75±28	342±24	82±39
RV	9	38±13	352±37	83±44	350±33	75±33
Total	15	34±12	350±35	79±35	348±29	78±35

Mean ± 1 SD in ms. Max. disp: maximum dispersion; LV and RV: left and right ventricles. $P > 0.05$ for all comparisons between the ART and EOR time measurements.

Correlation and agreement analyses

Correlation analysis revealed a significant positive correlation between the ART and EOR time for all the 473 recordings, with r = 0.77 and $p < 0.05$ (Fig. 22), and for all 15 maps, with r = 0.58±0.22 and $p < 0.05$. Agreement analyses showed that the differences between these two measurements were almost all within the range of the mean difference ± 2 SD for each individual map (Fig. 23) and for all 473 recordings in the 15 maps (Fig. 22). For all 473 recordings, the mean difference in the ART and EOR measurements was –2 ms and the lower and upper limits of agreement were -47 and 43 ms, i.e. the ARTs were at most 47 ms shorter and 43 ms longer than the EOR times in this study. The differences between the ART and EOR time were within the range of mean difference ± 2 SD in 459 of the 473 paired recordings (97%). The 95% confidence limits for the lower limit were between -50 and -43 ms, and that for the upper limit between 39 and 46 ms (Fig. 22).

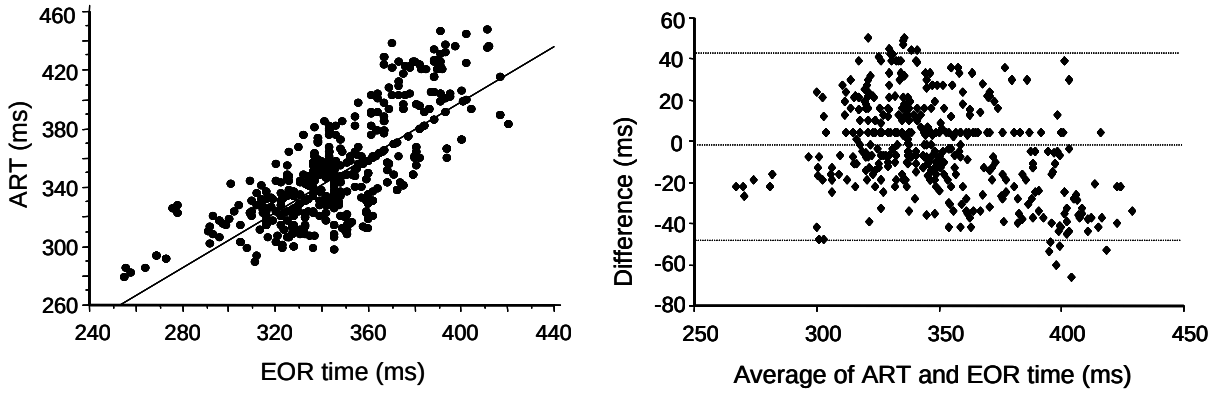

Fig. 22: Correlation (left) and agreement analysis (right) between the ART and EOR times for all 473 recordings. A statistically significant positive correlation between the ART and EOR time was found, with r = 0.77 and $P < 0.05$. The mean difference in the ART and EOR measurements is –2 ms and the lower and upper limits of agreement were -47 and 43 ms, respectively. The 95% confidence limits for the lower limit were between -50 and -43 ms, and those for the upper limit were between 39 and 46 ms. Note that the differences between the ART and EOR time were within the range of mean difference ± 2 SD in 459 of the 473 paired recordings (97%).

5. The sequence of ventricular repolarization (Studies I-V)

Comparison of the EOR and ART sequence in patients (Study I)

In all patients, the earliest recorded ventricular activation was identical on the ART and as on the EOR times measurements. Thus, the construction of the EOR and ART maps was made from the same reference time point. During MAP and ART mapping, due to technical difficulties and/or clinical limitations, there were small incomplete areas in the septum, outflow tract, or basal areas on the EOR and ART maps, 11 areas in total in the 15 maps. However, evaluation of the ventricular repolarization sequence was possible in all maps, since the earliest and latest activation areas were recorded in all cases and the incomplete areas were all smaller than 3 cm^2.

Three-dimensional maps of the repolarization sequences of EOR time and those of ART were compared. ART sequences were recognizable in 8 of the 9

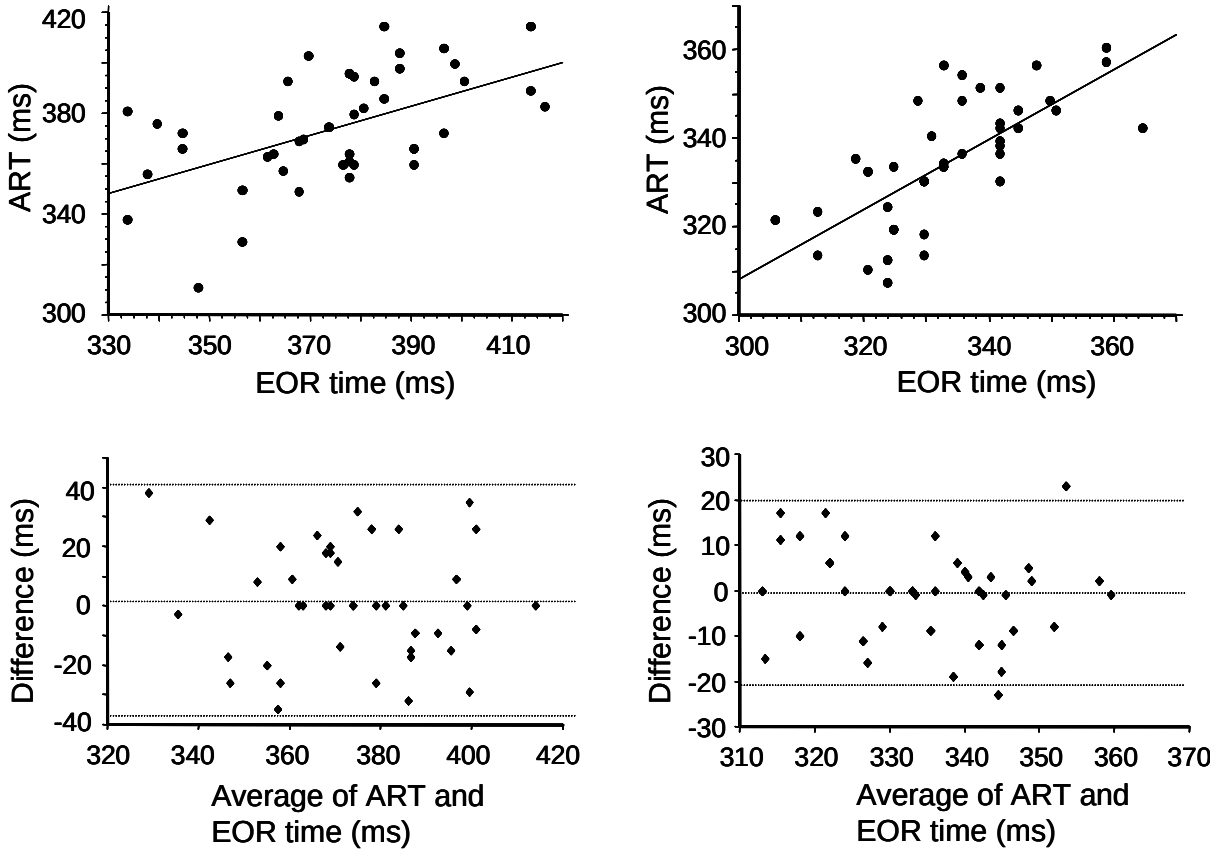

Fig. 23: Linear correlation analyses (upper panel) and limits of agreement analyses (lower panel) between the ARTs and EOR times. Left and right are data from 2 different patients. A positive correlation is shown during sinus rhythm (upper left, r = 0.54, $P < 0.01$) and ventricular premature beats (upper right, r = 0.71, $P < 0.01$). Agreement analysis in the patient during sinus rhythm (lower left) shows that the mean difference between the ART and EOR times is 1 ms and the limits of agreement are from -38 to 41 ms, the 95% confidence limits for the lower limit being -50 to -30 ms, and those for the upper limit being 28 to 48 ms. In the patient with ventricular premature beats (lower right), the mean difference is -1 ms and the limits of agreement are from -21 ms to 20 ms, with 95% confidence limits for the lower limit being -27 to -16 ms, and those for the upper limit being 14 to 25 ms.

right ventricular maps. Of these 8 maps, in the 7 recorded during sinus rhythm, the end of ART started from the anteroseptal area and ended in the lateral or posterolateral basal area. These ART sequences were generally the same as those of the EOR times (Fig. 24), although 3 of them had left or right bundle branch block and secondary ST-T changes on ECG. In the 8th right ventricular map, recorded during sustained right ventricular tachycardia, the ART sequence was from the right outflow tract area, where the focus of the tachycardia was located, to the posterolateral basal area, and the sequence was also similar to that of the EOR times. The ART sequence was unrecognizable on a map during sinus rhythm in a patient with ventricular tachycardia, whereas the EOR sequence was discernible on this map.

The left ventricular ART sequences were identifiable in all 6 maps, and they followed the same sequences of the EOR in all of these maps. In patient #1, mapped during left ventricular premature beats, the end of ART started from the anterolateral basal area and ended in the posteroseptal area. In patient #2, the ART started from the left anteroseptal area and ended in the laterobasal area during sinus rhythm. In the two maps during sustained ventricular tachycardia, the ART started from the left laterobasal area to the posteroparaseptal area (patient #1) (Fig. 25), and from the left anteroseptal area to the laterobasal area (patient #2). In patient #6 with Wolff-Parkinson-White syndrome, the ART followed similar sequences before and after catheter ablation of the accessory pathway, starting from the posteroseptal area and ending in the laterobasal area, with the basal areas being a long, late ART zone.

In total, repolarization sequences were recognizable in 14 of 15 ART maps as compared to the EOR sequence, which was recognizable in all 15 maps. The ART sequence was consistent with the EOR sequence in these 14 maps (Study I).

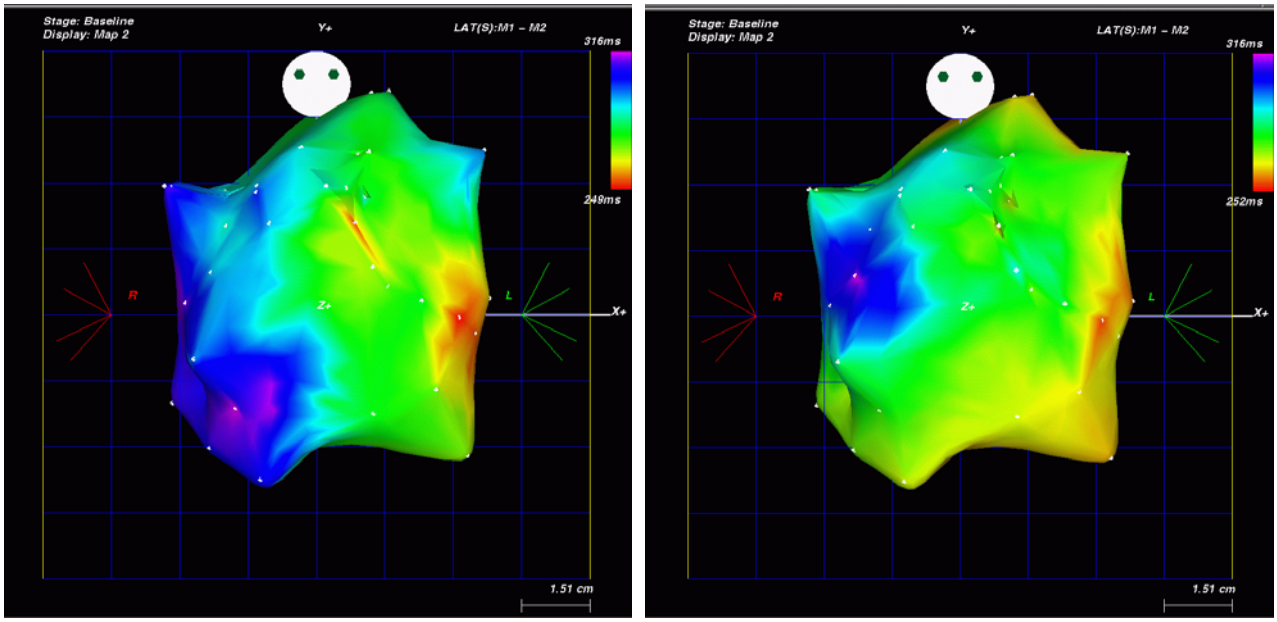

Fig. 24: Posterior-anterior views of the EOR (left) and ART (right) maps of the right ventricle during sinus rhythm from a patient with monomorphic ventricular tachycardia. The EOR starts from anteromidseptal area (red area), proceeds eccentrically towards the basal, lateral, posteroseptal and the outflow tract areas and ends in the posterolateral basal areas (blue and purple areas). The maximum dispersion of EOR is 67 ms. The ART sequence is consistent with the EOR sequence and the maximum dispersion of ART is 64 ms.

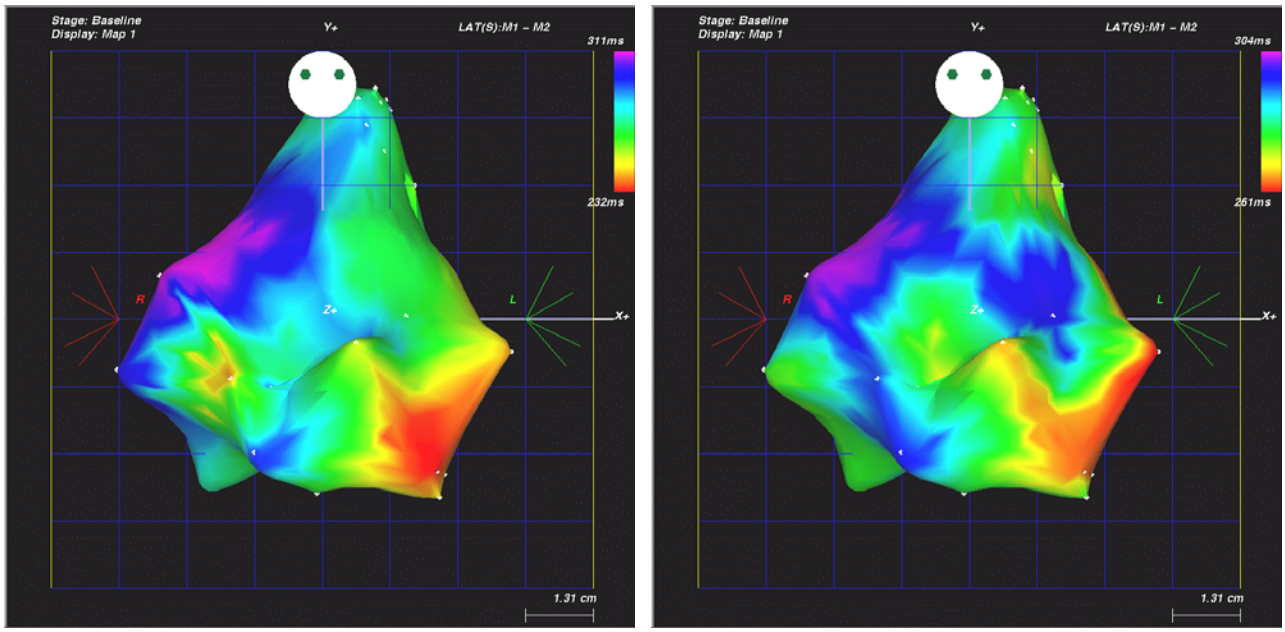

Fig. 25: Posterior-anterior views of the EOR (left) and ART (right) maps of the left ventricle during sustained ventricular tachycardia from a patient with ventricular tachycardia. The EOR starts from the left laterobasal area (red area) to the posteroparaseptal area (purple area) with the maximum EOR time dispersion 79 ms. The ART sequence is consistent with the EOR sequence and the maximum dispersion of ART is 43 ms.

EOR times, EOR sequence and QT intervals in 10 open-chest pigs (Studies II and III)

Three-dimensional maps of the repolarization sequences of EOR time over both the epi- and endocardium were constructed in the 10 open-chest pigs during right atrial pacing. Of these maps, the EOR commonly started from the anteroseptal/apical area and ended in the lateral or posterolateral basal area (Fig. 26). The minimal and maximal EOR times, i. e. the earliest and latest EORs, over the epi- and endocardium among all the MAP recordings in the 10 pigs were presented in Table 1, as well as the minimal, mean, and maximal QT_{peak} and QT_{end} intervals. In addition, the 5 longest EOR_{epi}, EOR_{endo} and EOR_{total}, as well as the 5 shortest EOR_{epi}, EOR_{end} and EOR_{total} were also observed in each pig (Table 4, see *Page 93*). The minimal and maximal EOR_{total} were observed in the left ventricle in all the 10 pigs, including the 2 pigs in which the right ventricle was also mapped. The minimal EOR_{total} was on the epicardium in 5 pigs and on the endocardium in the other 5 pigs. The maximal EOR_{total} was on the endocardium in 9 pigs and on the epicardium in the remaining pig. In all these 10 pigs, the sequence of the EOR was the same as that of activation both on the epicardium and the endocardium, but this is beyond the scope of Studies II and III.

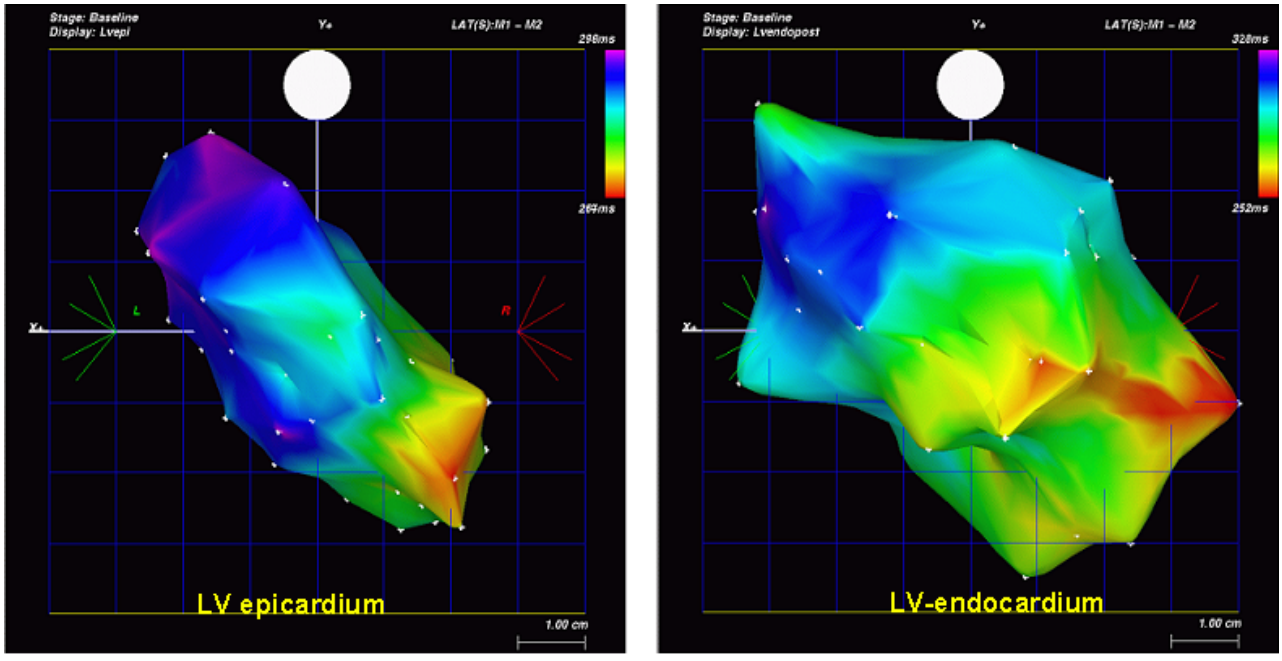

Fig. 26: CARTO maps of the end of repolarization sequences (EOR) of the epi- (left) and endocardium (right) from pig 6. The end of repolarization started from the apical area and ended in the posterolateral basal area. The recorded minimum EOR time is 264 ms, and the recorded maximum EOR time is 328 ms.

The activation sequence in pigs under ventricular pacing (Studies IV and V)

Three-dimensional maps of the activation and repolarization sequences from both the right and left ventricles were constructed in the 10 pigs during different pacing protocols. During RAP, the activation started from the anterioseptum (n = 3) or midseptum (n = 2) of the LV, propagated to the RV septum and continued eccentrically towards the apex and the anterior and posterior parts of both ventricles, finally ending in the left posterolateral (n = 2) or right lateral basal areas (n = 3).

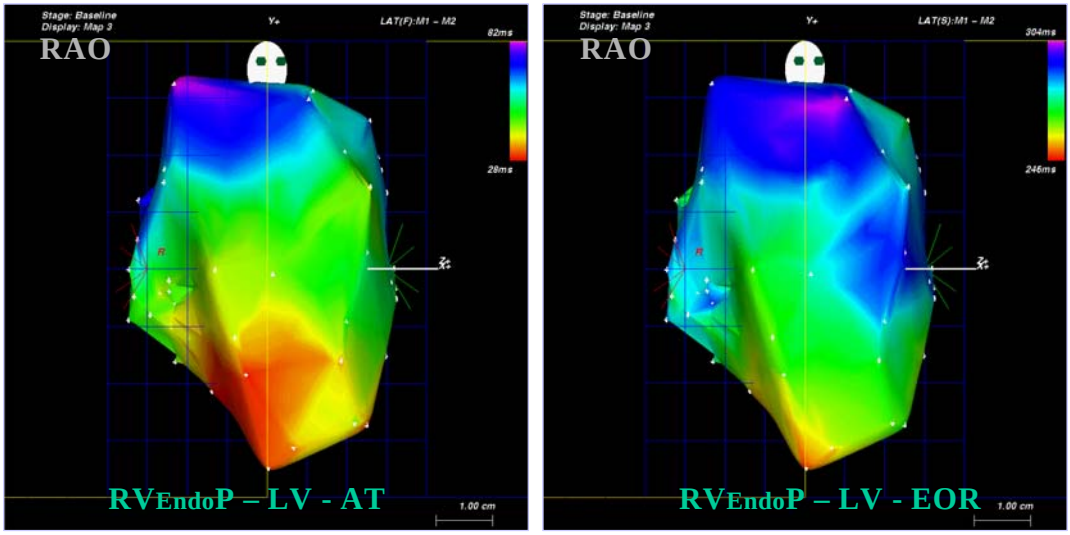

Fig. 27: Right anterior oblique views of AT (left) and EOR (right) sequences of the left ventricle (LV) during endocardial pacing at the right ventricular apex ($RV_{Endo}P$) in a pig. The LV breakthrough site is at the apicoseptal area. The EOR sequence is very similar to that of the AT, including a similar breakthrough point at the apical septum.

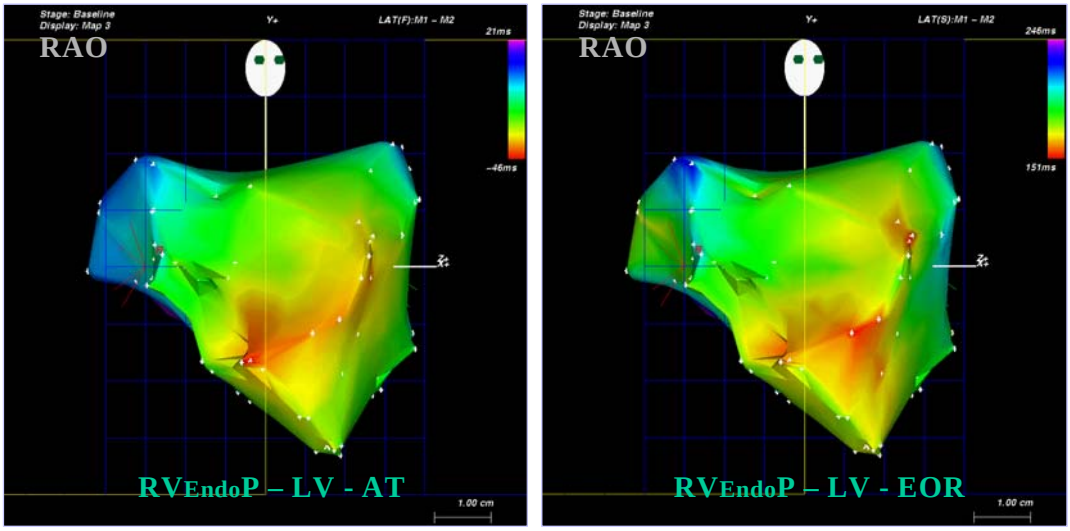

Fig. 28: Right anterior oblique views of AT (left) and EOR (right) sequences of the left ventricle (LV) during endocardial pacing at the right ventricular apex ($RV_{Endo}P$) in a pig. The LV breakthrough sites are seen at both apicoseptal and midseptal regions. In the LV, the EOR sequence also follows that of the AT, with similar breakthrough points at the midseptum and apical septum.

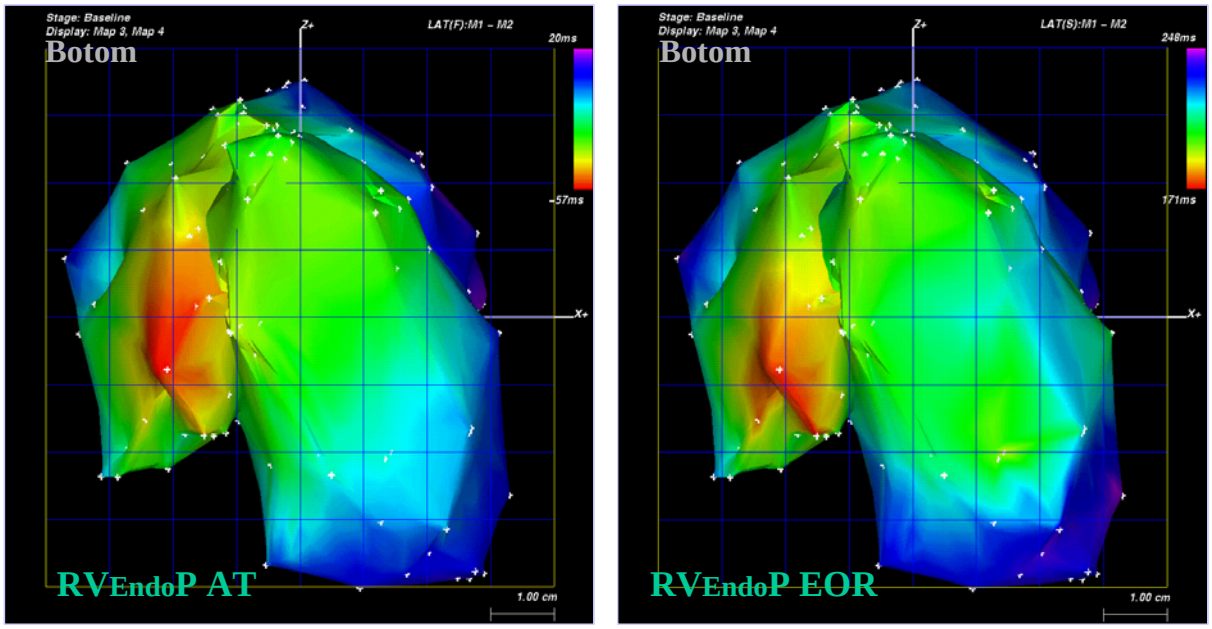

Fig. 29: Bottom views of AT (left) and EOR (right) sequences of both right and left ventricles (RV and LV) during endocardial pacing at the RV apex ($RV_{Endo}P$) in pig 8. The activation starts from the pacing site at the RV apex, and propagates eccentrically toward the septum and the RV free wall. In the LV, the activation spread eccentrically toward the apex, anterior, and lateral wall. The latest activation is located at the posterolateral basal area of the LV. The EOR sequence follows that of the AT.

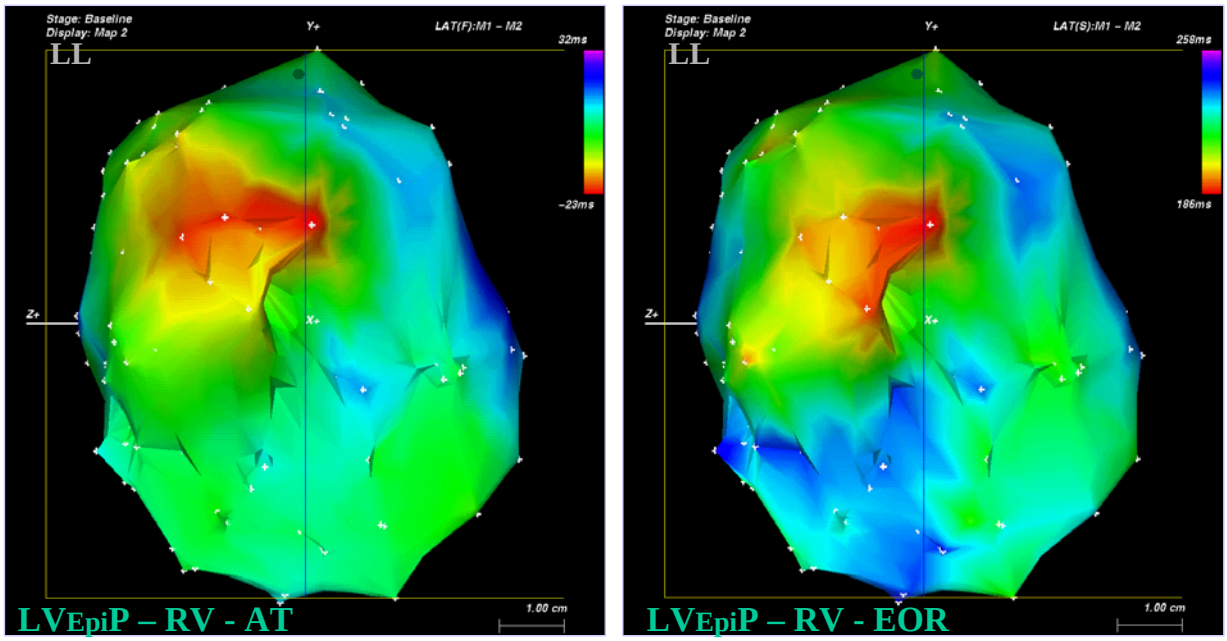

Fig. 30: Left lateral views of AT (left) and EOR (right) sequences of the right ventricle (RV) during epicardial pacing at a laterobasal site of the left ventricle ($LV_{Epi}P$) in pig 9. The RV breakthrough site of the AT is located at the posterior septum, and the activation then propagates eccentrically from the septum to the apex and the anterior and lateral wall, finally ending at the right laterobasal areas. The EOR breaks into the RV also at the posterior septum, and follows a sequence similar to that of the AT.

During RV_{Endo} pacing, in both groups the activation started from the pacing site at the right ventricular apex and propagated eccentrically towards the septum and the RV free wall. The LV breakthrough was observed at the apicoseptal area in 5 pigs (Fig. 27, left), at the midseptal area in 3 pigs, and both areas in 2 pigs (Fig. 28, left), respectively. After entering the LV, the activation spreads eccentrically toward the apex, anterior and lateral wall of the LV. The latest activation was located at the lateral (n = 2) or posterolateral (n = 4) basal areas of the RV, and the posterolateral basal area of the LV (n = 4), respectively (Fig. 29, left).

During LV_{Epi} pacing, the earliest activation started at the pacing site in the laterobasal area of the LV, and propagated eccentrically towards the left anterior wall, apex and septum. The activation broke into the RV at the midseptal (n = 1) or posteroseptal regions (n = 4) (Fig. 30, left), and propagated eccentrically from the septum to the apex, anterior and lateral wall, finally ending at the posterobasal (n = 1) or laterobasal (n = 4) areas of the RV (Fig. 31, left).

The repolarization sequence in pigs under ventricular pacing (Studies IV and V)

During RA pacing, the EOR sequence was recognizable on all 5 maps and it was similar to the AT sequence. The EOR started from the superior- (n = 3) or mid-septum (n = 2) of the LV, proceeded towards the RV septum, continued eccentrically to both ventricles, and ended in the posterolateral LV (n = 2) or the lateral basal RV (n = 3). In these 5 maps, the longest MAPds were all recorded in or near the earliest activation areas, i.e. the septal/apical areas, while the shortest MAPds were recorded in or near the latest activation areas.

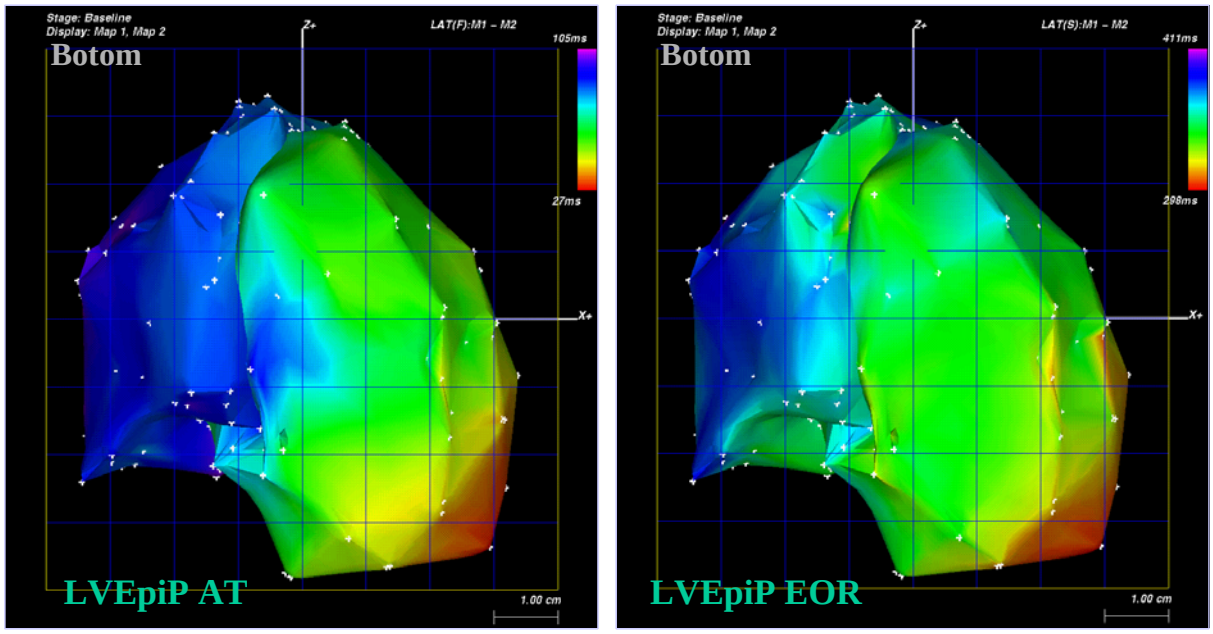

Fig. 31: Bottom views of AT (left) and EOR (right) sequences of both right (RV) and left ventricles (LV) during epicardial pacing at a laterobasal site of the LV ($LV_{Epi}P$) in pig 9. The earliest activation starts at the left laterobasal pacing area, propagates eccentrically towards the left anterior wall, apex and septum. In the RV, the activation propagates eccentrically from the septum to the apex and the anterior and lateral wall, finally ending at the right laterobasal area. The EOR follows a similar sequence to that of the activation.

During RV_{Endo} pacing, the EOR sequence was recognizable in all 5 pigs from group I and in 4 of the 5 pigs from group II. In these 9 pigs, the EOR followed sequences similar to those of the activation (Fig. 29, right). The earliest EOR started from the pacing site at the RV apex and proceeded eccentrically towards the septum and the RV free wall. Interestingly, in the LV the earliest EORs were observed in similar regions around the activation breakthrough sites, which were at the apicoseptal area in 6 pigs (Fig. 27, right), at the midseptal area in 2 pigs, and at both areas in 1 pig (Fig. 28, right). In the LV, the EOR spread eccentrically toward the apex and the anterior and lateral LV wall. The latest EOR ended at the lateral (n = 2) or posterolateral (n = 2) basal areas in the RV, or at the posterolateral basal area of the LV (n = 5). On these 9 maps, the longest MAPds were recorded in or near the earliest activation areas, while the shortest MAPds were recorded in or near the latest activation areas. The EOR pattern of the remaining pig was so complex on the LV map that no clear EOR sequence was recognizable.

During LV_{Epi} pacing, the EOR sequence was recognizable in all 5 pigs of Group II, and the sequence of EOR followed that of activation. The earliest EOR

started at the lateral pacing area and proceeded eccentrically towards the anterior wall, apex and septum of the LV. Similar to what was observed during RV_{Endo} pacing, the earliest EOR in the RV was located at the activation breakthrough areas, which were in the midseptal (n = 1) and posteroseptal regions (n = 4) (Fig. 30, right). The EOR then proceeded eccentrically from the septum to the apex and the anterior and lateral wall, and finally ended at the laterobasal areas (n = 5) of the RV (Fig. 31, right). The longest MAPs were recorded in or near the LV laterobasal pacing area in 4 of the 5 pigs. In 2 pigs, some of the longest MAPs were also observed around the septal/apical areas, though these MAPs did not affect the global repolarization sequence. The shortest MAPs were recorded in or near the latest activation areas, the laterobasal areas in the RV, in all 5 pigs.

Table 5: Linear regression analysis of MAPd vs. AT, and of EOR vs. AT during altered pacing protocols in the 10 close-chest pigs

	n=	sites	MAPd vs. AT		EOR vs. AT	
			slope	r	slope	r
RAP	5	112 ± 16	-0.46 ± 0.13	-0.43 ± 0.18	0.47 ± 0.11	0.45 ± 0.14
$RV_{Endo}P$	10	122 ± 23	-0.32 ± 0.11	-0.42 ± 0.08	0.51 ± 0.10	0.53 ± 0.16
$LV_{Epi}P$	5	126 ± 26	-0.25 ± 0.09	-0.33 ± 0.16	0.54 ± 0.10	0.59 ± 0.19

MAPd: monophasic action potential duration; AT: activation time; EOR: end of repolarization time; RAP: right atrial pacing; $RV_{Endo}P$: right ventricular endocardial pacing; $LV_{Epi}P$: left ventricular epicardial pacing.

Correlation and regression analysis during altered pacing protocol (Study IV)

A negative correlation between MAPd and AT and a positive correlation between the EOR and AT were found in all maps, regardless of whether during RA, RV_{Endo}, or LV_{Epi} pacing. The correlation was statistically significant in all of the maps (p < 0.05-0.001, Table 5). For the linear regression between MAPd and AT, the slope during LV_{Epi} pacing (-0.25±0.09) tended to be less steep than that during RA pacing and RV_{Endo} pacing (-0.46±0.13 and -0.32±0.11, Fig. 32), though the differences were not statistically significant (p > 0.05). For the linear regression between the EOR time and AT, the slope during LV_{Epi} pacing (0.54±0.10) was similar to that during RA pacing and RV_{Endo} pacing (0.47±0.11 and 0.51±0.10, p > 0.05) (Fig. 32, Table 5).

6. The dispersion of ventricular activation and repolarization (Studies II, III and V)

The dispersion of EOR times over both epicardium and endocardium (Studies II and III)

In the 10 open-chest pigs, the EOR times over the endocardium and epicardium were obtained as shown in Table 6. Three-dimensional maps of the repolarization sequences over both the epicardium and endocardium were constructed in the 10 pigs. Of these maps, the EOR commonly started from the anteroseptal/apical area and ended in the lateral or posterolateral basal area, i.e. the minimal EOR times were all recorded around the anteroseptal /apical area, and the maximal EOR times around the lateral or posterolateral basal area (Fig. 26).

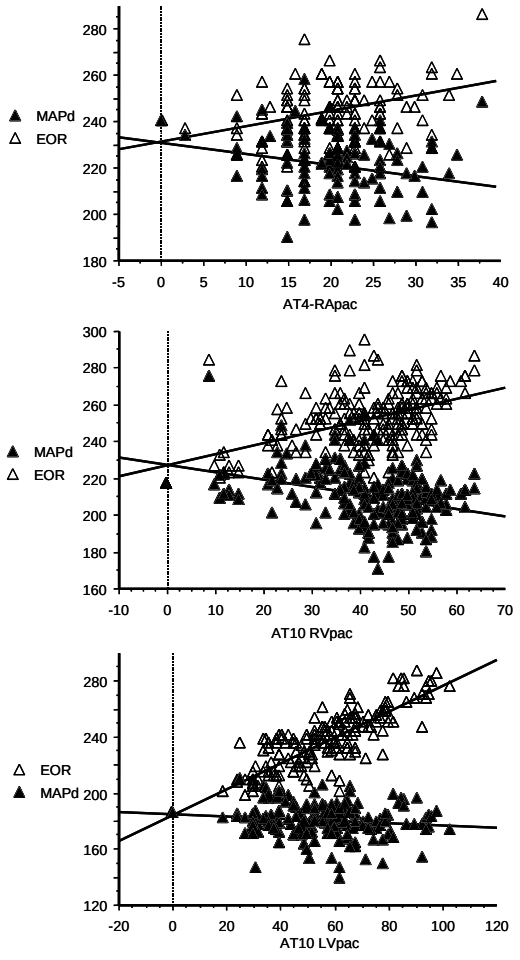

Fig. 32: Linear correlation analysis for one of the pigs between MAPd and AT, and between EOR and AT during RA pacing (upper), RV_{Endo} pacing (middle) and LV_{Epi} pacing (lower), respectively. Under these different pacing protocols, negative correlations were found between MAPd and AT whereas positive correlations were found between EOR and AT.

The dispersions of EOR-epi, EOR-endo, and EOR-total were 36±8, 51±15 and 58±11 ms, respectively. The dispersion of EOR-total was significantly greater than the dispersion of EOR-epi and dispersion of EOR-endo ($p < 0.001$ and $p < 0.05$, respectively) (Table 6). In addition, in the 2 pigs in which both left and right ventricles were mapped, the maximal and minimal EOR times were all found in the left ventricle recordings. Thus, the

measurements from the right ventricle did not affect the maximal dispersion of EOR times in these 2 pigs (Study III).

Table 6: The end of repolarization time and its dispersion over the epicardium and endocardium during right atrial pacing at 130 bpm in 10 open-chest pigs

Pigs	Epicardium of LV			Endocardium of LV			DVR-total
	Site	EOR	DVR	Site	EOR	DVR	
1	67	313±10	39	56	322±14	63	63
2	67	311±10	39	59	313±19	77	77
3	32	328±6	29	57	353±15	61	67
4	49	272±7	26	75	281±12	55	55
5	47	323±11	48	72	315±9	32	50
6	50	299±8	31	49	295±15	64	64
7	47	294±7	27	66	302±8	32	38
8	45	340±11	45	59	352±11	43	63
9	48	282±8	38	77	303±10	40	52
10	57	303±9	33	70	315±12	46	53
Total	51±10	306±21	36±8*	64±9	312±25	51±15†	58±11

EOR data are presented as mean ± 1 standard deviation in milliseconds. EOR: end of repolarization time; LV: left ventricle; DVR: dispersion of the end of repolarization times. * $p < 0.001$ and † $p < 0.05$ compared with the DVR-total.

The dispersion of activation under ventricular pacing (Study V)

In the series of the 10 close-chest pigs, the earliest recorded endocardial AT was consistent with the earliest onset of QRS complex during RA (3±1 ms difference), and with the endocardial pacing artifacts of the surface ECG during RV_{Endo} pacing (4±1 ms difference). During LV_{Epi} pacing, however, the earliest recorded endocardial AT was 28±8 ms later than the epicardial pacing artifacts, representing the local transmural conduction from the epicardial pacing site to the endocardium (Fig. 20).

In Group I, the dispersion of AT during RV_{Endo} pacing, which was 64±12 ms in the RV, 63±10 ms in the LV, and 68±13 ms in both, was significantly greater than that during RA pacing, which was 51±10 ms in the RV, 52±19 ms in the LV and 55±12 ms in both ($p < 0.05$), respectively. In Group II, during LV_{Epi} pacing, the dispersion of AT in the RV (60±12 ms) and in the LV (65±17 ms) were both similar to those during RV_{Endo} pacing, which was 59±9 ms in the RV and 67±15 ms in the LV ($p > 0.05$). However, the dispersion of AT in both ventricles during

LV_{Epi} pacing (87±15 ms) was significantly greater than that during RV_{Endo} pacing (70±16 ms) ($p < 0.05$) (Table 7).

During RV_{Endo} pacing, no significant difference in dispersion of AT was found between Groups I and II ($p > 0.05$). Thus, the dispersion of AT in both ventricles during LV_{Epi} pacing in the 5 pigs (87±15 ms) was also significantly greater than that during RV_{Endo} pacing in all 10 close-chest pigs (69±15 ms) ($p < 0.05$) (Fig. 33).

The dispersion of EOR times under ventricular pacing (Study V)

In the 10 colse-chest pigs, during RA pacing (Group I, n = 5), the earliest EOR was located at the superior (n = 3) or midseptum (n = 2) of the LV, and the latest EOR was located at the posterolateral LV (n = 2) or the lateral basal RV (n = 3). During RV_{Endo} pacing (Groups I and II, n = 10), the earliest EOR was found at the pacing area in the RV/LV apex in both groups, and the latest EOR was located at the lateral (n = 2) or posterolateral (n = 2) basal areas of the RV, or the posterolateral basal area of the LV (n = 6). During LV_{Epi} pacing (Group I, n = 5), the earliest EOR was found in the pacing area of the lateral LV, and the latest was found in the laterobasal areas of the RV (n = 5).

In Group I, the dispersion of EOR during RV_{Endo} pacing, which was 63±13 ms in the RV, 67±16 ms in the LV and 70±16 ms in both, appeared similar to that during RA pacing, which was 60±10 ms in the RV, 57±12 ms in the LV and 63±12 ms in both ($p > 0.05$). In Group II, during LV_{Epi} pacing, the dispersion of EOR in the RV (65±13 ms) and in the LV (61±10 ms) were both similar to those during RV_{Endo} pacing, which was 62±8 ms in the RV and 68±17 ms in the LV ($p > 0.05$). However, the dispersion of EOR in both ventricles during LV_{Epi} pacing (94±17 ms) was significantly greater than that during RV_{Endo} pacing (74±18 ms), ($p < 0.05$) (Table 7).

Table 4: The mean differences in the 5 longest and 5 shortest EOR times from the QT_{peak} and QT_{end} intervals in the 10 open-chest pigs

Pig	Epicardium		Endocardium		Both epicardium and endocardium			
	5 longest EOR	QT_p vs. 5 longest EOR	5 longest EOR	QT_e vs. 5 longest EOR	5 shortest EOR	QT_p vs. 5 shortest EOR	5 longest EOR	QT_e vs. 5 longest EOR
1	329	-40	344	7	292	-3	344	7
2	327	-40	342	10	278	9	342	10
3	336	-11	376	5	317	8	376	5
4	279	-18	301	8	253	8	301	8
5	344	-25	330	7	304	15	344	-7
6	310	-36	318	1	270	4	318	1
7	301	-32	312	15	280	-11	312	15
8	352	-43	369	1	318	-9	369	1
9	296	-33	318	7	273	-10	318	7
10	316	-27	338	6	288	1	338	6
	319±23	-31±10	335±24	7±4	287±21	1±9	336±24	5±6

Data are presented in ms and the differences are derived from the QT intervals minus end of repolarization times. EOR: end of repolarization times. QT_p and QT_e: QT_{peak} and QT_{end} intervals.

Table 7. The global dispersion of activation times and end of repolarization times of the right and left ventricles during RA, RV_{Endo} and LV_{Epi} pacing in the 10 close-chest pigs

	N	Sites	Dispersion of AT			Dispersion of EOR		
			RV + LV	RV	LV	RV + LV	RV	LV
RA pacing (I)	5	112 ± 16	55 ± 12	51 ± 10	52 ± 19	63 ± 12	60 ± 10	57 ± 12
RV_{Endo} Pacing (I)	5	118 ± 20	68 ± 13	64 ± 12	63 ± 10	70 ± 16	63 ± 13	67 ± 16
LV_{Epi} Pacing (II)	5	126 ± 26	#87 ± 15	60 ± 12	65 ± 17	#94 ± 17	65 ± 13	61 ± 10
RV_{Endo} Pacing (II)	5	126 ± 21	70 ± 16	59 ± 9	67 ± 15	74 ± 18	62 ± 8	68 ± 17
RV_{Endo} Pacing (I + II)	10	122 ± 23	*69 ± 15	62 ± 14	65 ± 17	72 ±18	62 ± 12	68 ± 18

Data presented as mean ± SD in ms. * $p < 0.05$ as compared to that during RA pacing; # $p < 0.05$ as compared to both during RA and RV_{Endo} pacing; AT: activation time; EOR: end of repolarization time; RA: right atrial; RV and LV: right and left ventricle; RV_{Endo}: right ventricular endocardial; LV_{Epi}: left ventricular epicardial; I: Group I; II: Group II.

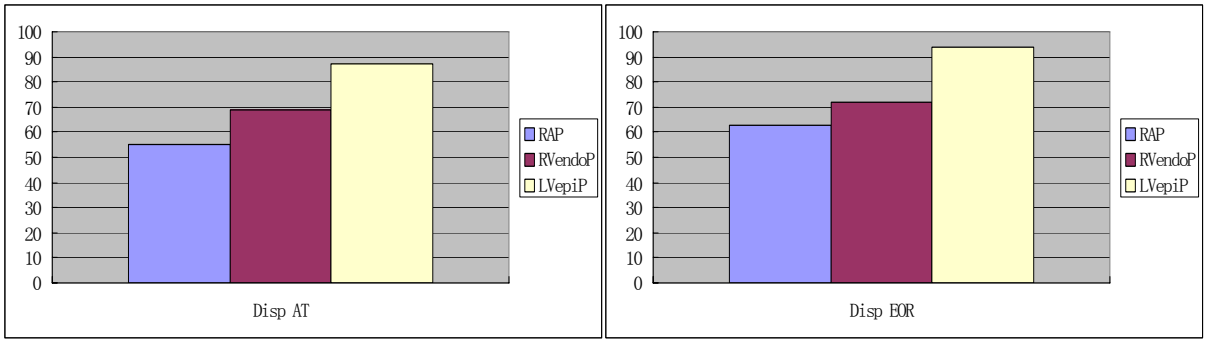

Fig. 33: Effect of different pacing protocols on dispersion of ventricular activation time (AT) and end of repolarization time (EOR) in 10 close-chest pigs. During left ventricular epicardial pacing ($LV_{Epi}P$), the dispersions of AT (left) and EOR (right) are significantly greater than those during right atrial pacing (RAP) and right ventricular endocardial pacing ($RV_{Endo}P$). Graphs are presented as mean value in ms.

During RV_{Endo} pacing, no significant difference in EOR dispersion was found between Groups I and II ($p > 0.05$). Consequently, the dispersion of EOR in both ventricles (94±17 ms) during LV_{Epi} pacing in the 5 pigs of Group II was significantly greater than that during RV_{Endo} pacing in all the 10 pigs (72±18 ms) ($p < 0.05$) (Fig. 33).

7. Repolarization parameters on the surface ECG (Studies II, III and V)

QT_{peak} and QT_{end} intervals

In the 10 open-chest pigs, the minimal, mean and maximal QT_{peak} and QT_{end} intervals were aquired as shown in Table 1 (*See page 77*).

In the 10 close-chest pigs, QT interval during LV_{Epi} pacing (328±24 ms) was

Table 8. Dispersion of ECG parameters on ventricular repolarization during different pacing protocols in 10 close-chest pigs

	n	QT interval	QT dispersion	T_{peak}-T_{end} interval	
				Average	Maximum
RA pacing	5	285 ± 13	17 ± 3	49 ± 6	58 ± 8
RV_{Endo} pacing	10	304 ± 17	18 ± 3	49 ± 8	60 ± 8
LV_{Epi} pacing	5	328 ± 24*	33 ± 6*	63 ± 7*	71 ± 8*

Data are presented as mean ± SD in ms. * $p < 0.05$ as compared to those during RA and RV_{Endo} pacing. RA: right atrial; RV_{Endo}: right ventricular endocardial; LV_{Epi}: left ventricular epicardial.

significantly greater than that during RA pacing (295±13 ms) ($p < 0.05$) and RV_{Endo} pacing (304±17 ms) ($p < 0.05$), whereas no significant difference was found between that during RA and that during RV_{Endo} pacing (Fig. 34; Table 8).

QT dispersion and T_{peak}-T_{end} intervals

For the 10 open-chest pigs (Studies II and III), the QT dispersion parameters are presented in Table 9. QT_{peak} dispersion was significantly smaller than QT_{end} dispersion in the 10 pigs (15±2 vs. 21±4 ms, $p < 0.01$). The minimal, mean and maximal T_{peak}-T_{end} intervals were 20±9, 44±5 and 57±7 ms, respectively. The maximal T_{peak}-T_{end} intervals were significantly greater than the minimal and mean T_{peak}-T_{end} intervals ($p < 0.0001$ and $p < 0.0001$, respectively). The maximal and mean T_{peak}-T_{end} intervals were also greater than the QT_{peak} dispersion and QT_{end} dispersion ($p < 0.0001$ vs. $p < 0.0001$). In addition, T_{peak}-T_{end} intervals from lead II and V_5 were also compared with each other, but no significant difference was found between them (41±6 vs. 43±5 ms, $p > 0.05$). However, the T_{peak}-T_{end} intervals from these two leads were significantly smaller than the maximal T_{peak}-T_{end} intervals ($p < 0.0001$) (Table 9).

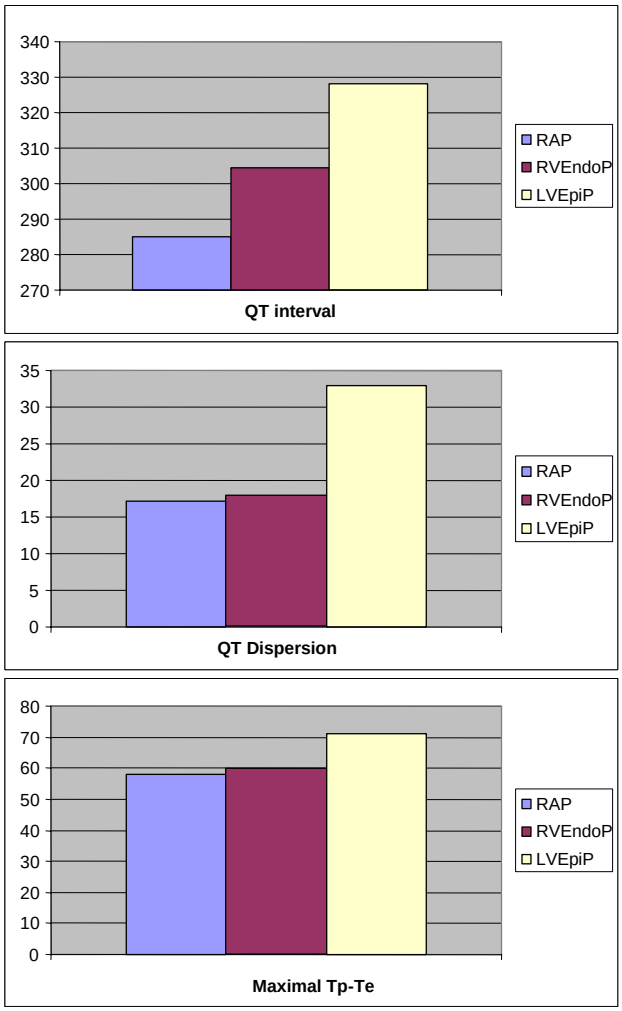

Fig. 34: Effect of different pacing protocols on ECG parameters of ventricular repolarization. During left ventricular epicardial pacing ($LV_{Epi}P$), QT intervals (upper panel), QT dispersion (middle panel) and maximal T_{peak}-T_{end} intervals (lower panel) are all significantly greater than those during right atrial pacing (RAP) and right ventricular endocardial pacing ($RV_{Endo}P$).

In the 10 close-chest pigs, QT dispersion during LV_{Epi} pacing (33±6 ms) was significantly greater than that during RA (17±3 ms, $p < 0.05$) and RV_{Endo} pacing (18±3 ms, $p < 0.05$). No significant difference in QT dispersion was found during RA pacing and RV_{Endo} pacing ($p > 0.05$) (Fig. 34). In

addition, during RA pacing, the average and maximum T_{peak}-T_{end} intervals were 49±6 ms and 58 ± 8 ms, which were similar to those during RV_{Endo} pacing (49±8 ms and 60±8 ms, both $p > 0.05$). However, during LV_{Epi} pacing, the average and maximum T_{peak}-T_{end} intervals increased significantly to 63±7 ms and 71±8 ms (both $p < 0.05$) (Fig. 34).

Table 9: ECG dispersion parameters in the 10 open-chest pigs

Pigs	Min T_p-T_e	Mean T_p-T_e	Max T_p-T_e	T_p-T_e V_5	T_p-T_e II	QT_p Disp	QT_e Disp
1	33	48	66	48	49	14	19
2	18	44	56	44	37	15	23
3	33	47	60	44	46	12	15
4	19	44	57	44	41	17	21
5	16	40	49	43	49	11	22
6	30	48	64	51	46	18	16
7	4	41	48	43	34	15	29
8	19	41	55	39	40	14	22
9	18	36	46	37	34	12	16
10	14	40	54	35	37	17	23
Total	20±9	*44±5	57±7	*43±5	*41±6	15±2	†21±4

Data are presented as mean ± 1 SD in ms. Min, Mean and Max T_p-T_e: minimal, mean and maximal T_{peak} to T_{end} interval. II and V_5: ECG leads II and V_5. QT_p and QT_e Disp: dispersion in QT_{peak} and QT_{end} intervals, respectively. * $p < 0.0001$ compared with Max T_p-T_e. † $p < 0.01$ compared to QT_p Disp.

8. Relationship between dispersion of EOR times and ECG dispersion parameters in the 10 open-chest pigs (Studies II and III)

Comparison of the EOR times and the ECG parameters (Study II)

In the 10 open-chest pigs, the EOR times and the related ECG parameters were compared (Study II). The minimal, mean and maximal QT_{peak} intervals were all significantly smaller than the maximal EOR_{epi} (322±23 ms) ($p < 0.01$, Table 1). No significant differences were found either between the mean QT_{end} intervals (333±29 ms) and the maximal EOR_{endo} (339±24 ms) ($p = 0.34$), or between the maximal QT_{end} intervals (338±30 ms) and the maximal EOR_{endo} ($p = 0.92$), with the differences being 6±19 ms and 1±19 ms, respectively (Table 10). The minimal QT_{end} interval (318±32 ms) was significantly smaller than the maximal EOR_{endo} ($p < 0.05$), with the difference being 21±19 ms (Table 10).

Table 10: Differences between the maximal, mean, and minimal QT_{peak} and QT_{end} intervals and the maximal and minimal end of repolarization times over the epi- and endocardium in the 10 open-chest pigs.

Pig	Min QT_p	Mean QT_p	Max QT_p	Min QT_e	Mean QT_e	Max QT_e	Min QT_p	Max QT_e
	Max EOR_{-epi}			Max EOR_{-endo}			Min EOR_{-total}	Max EOR_{-total}
1	-44	-39	-30	-17	-11	2	-1	2
2	-74	-67	-59	-62	-44	-39	-18	-39
3	-32	-26	-20	-25	-17	-10	-3	-10
4	-31	-23	-14	-20	-4	1	-1	1
5	-55	-49	-44	-10	9	12	-5	-6
6	-24	-13	-4	6	17	22	22	22
7	-37	-28	-22	-29	2	0	-10	0
8	-14	-6	0	1	17	23	31	23
9	-52	-45	-40	-36	-23	-20	-14	-20
10	-31	-27	-24	-20	-7	3	2	3
	-39±17*	-32±18*	-26±18*	-21±19†	-6±19#	-1±19#	0±15‡	-2±18‡

The data presented are time interval differences in ms, which are derived from the QT intervals minus the end of repolarization times. Min and Max: minimal and maximal; EOR_{-epi}, EOR_{-endo} and EOR_{-total}: end of repolarization times over the epicardium, endocardium, and over both. QT_p and QT_e: QT_{peak} and QT_{end} intervals. *: significantly smaller than the Max EOR_{-endo} ($p < 0.05$); #: No significant difference from the Max EOR_{-endo} ($p < 0.05$); †: Significantly smaller than the Max EOR_{-endo} ($p < 0.05$); ‡: No significant difference from the Min EOR-total and the Max EOR_{-total}, respectively ($p > 0.05$)

No significant difference was found bewteen the minimal QT_{peak} intervals (283±28 ms) and the minimal EOR_{total} (282±20 ms, $p = 0.95$), with the difference being 0±15 ms. The minimal EOR_{total} sites were all recorded around the anteroseptal/apical area. Likewise, no significant difference was found between the maximal QT_{end} intervals and the maximal EOR_{total} (341±24 ms, $p = 0.69$), with the difference being 2±18 ms (Table 10) (Fig. 35). The maximal EOR_{total} values were all recorded around the lateral or posterolateral basal area. Furthermore, a significant positive correlation was found between the minimal QT_{peak} and the minimal EOR_{total} ($r = 0.85$, $p < 0.005$), and also between the maximal QT_{end} and the maximal EOR_{total} ($r = 0.80$, $p < 0.01$) (Fig. 36).

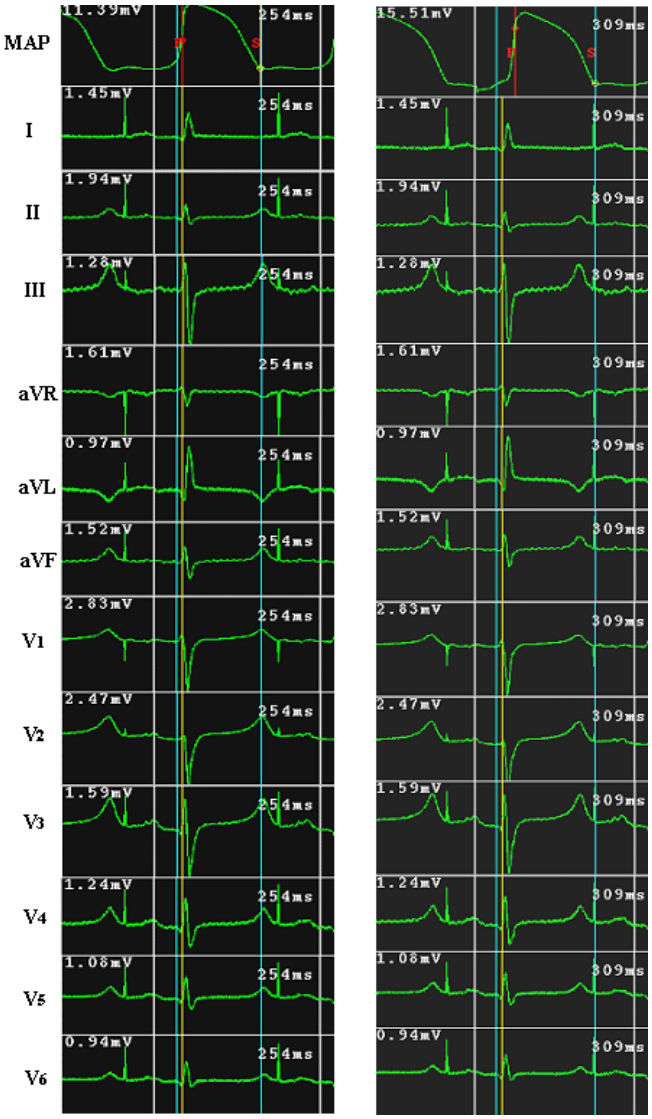

Fig. 35: Comparison of the earliest and latest end of repolarization times on the monophasic action potential recordings with the T_{peak} and T_{end} time points on the 12-lead ECGs in pig 2. Left panel: the T_{peak} coincides well with the earliest EOR time (first tracing) recorded at the left anteroseptal area on the endocardium (forth line). Right panel: the T_{end} is consistent with the latest EOR (first tracing) recorded at the laterobasal area on the endocardium (forth line). Lead I was discarded from analysis due to the flat T wave.

During online analysis within the sampling window, the minimal QT_{peak} and maximal QT_{end} intervals were compared with each of the 5 shortest and 5 longest EOR times over the epicardium, the endocardium, and over both in each pig. The mean of the 5 differences was calculated and is shown in Table 4. Similarly to the above results, the minimal QT_{peak} intervals were significantly smaller than the 5 longest EOR_{epi} values (319±23 ms) ($p < 0.05$), with the difference being –31±10 ms, whereas no significant difference was found between the maximal QT_{end} intervals and the 5 longest EOR_{endo} values (335±24 ms) ($p >$

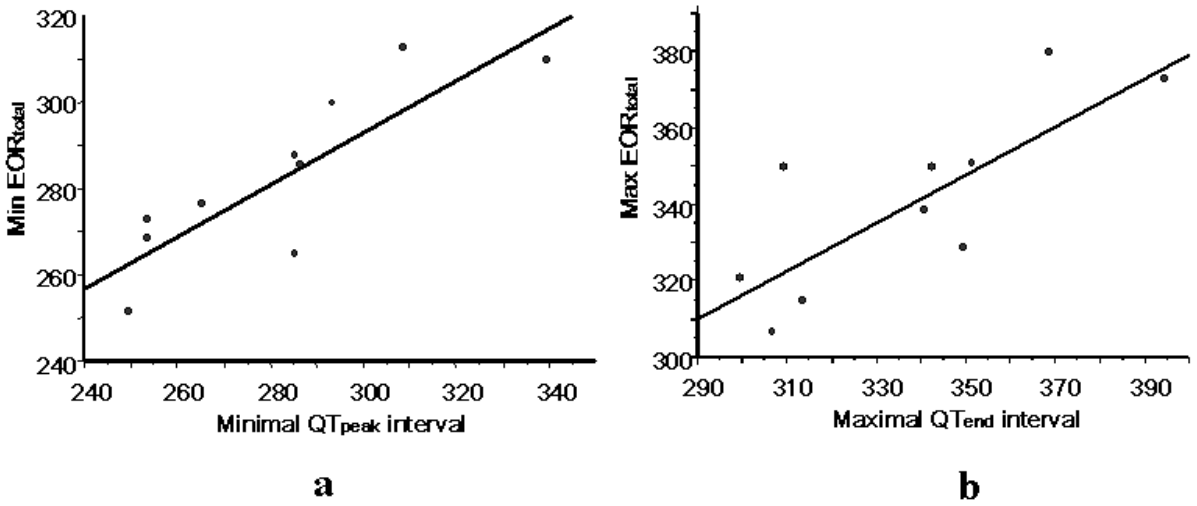

Fig. 36: A significant positive correlation could be found between the minimal QT_{peak} and the minimal EOR_{total} (a), as well as between the maximal QT_{end} and the maximal EOR_{total} (b). Data are from the 10 open-chest pigs, and presented in ms.

0.05), with the difference being 7±4 ms. Likewise, no significant difference was found between the minimal QT_{peak} intervals and the 5 shortest EOR_{-total} (287±21 ms) ($p > 0.05$) (Fig. 37), the difference being 1±9 ms, or between the maximal QT_{end} intervals and the 5 longest EOR_{total} (336±24 ms) ($p > 0.05$), the difference being 5±6 ms (Table 4).

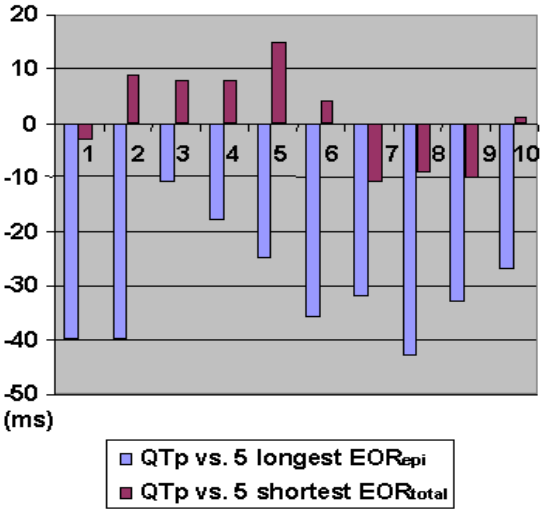

Fig. 37: The differences between the QT_{peak} intervals and the 5 longest and shortest end of repolarization times, showing that the QT_{peak} intervals were much shorter than the 5 longest EOR times on the epicardium (QT_p vs. 5 longest EOR_{epi}, gray bars), but quite close to the 5 shortest end of repolarization on both the epicardium and endocardium (QT_p vs. 5 shortest EOR_{total}, black bars). Data from the 10 open-chest pigs.

Corelation between T_{peak}-T_{end} interval and the dispersion of EOR times (Study III)

Also in the 10 open-chest pigs, no significant difference was found between the maximal T_{peak}-T_{end} interval and the dispersion of EOR-total ($p = 0.33$), whereas

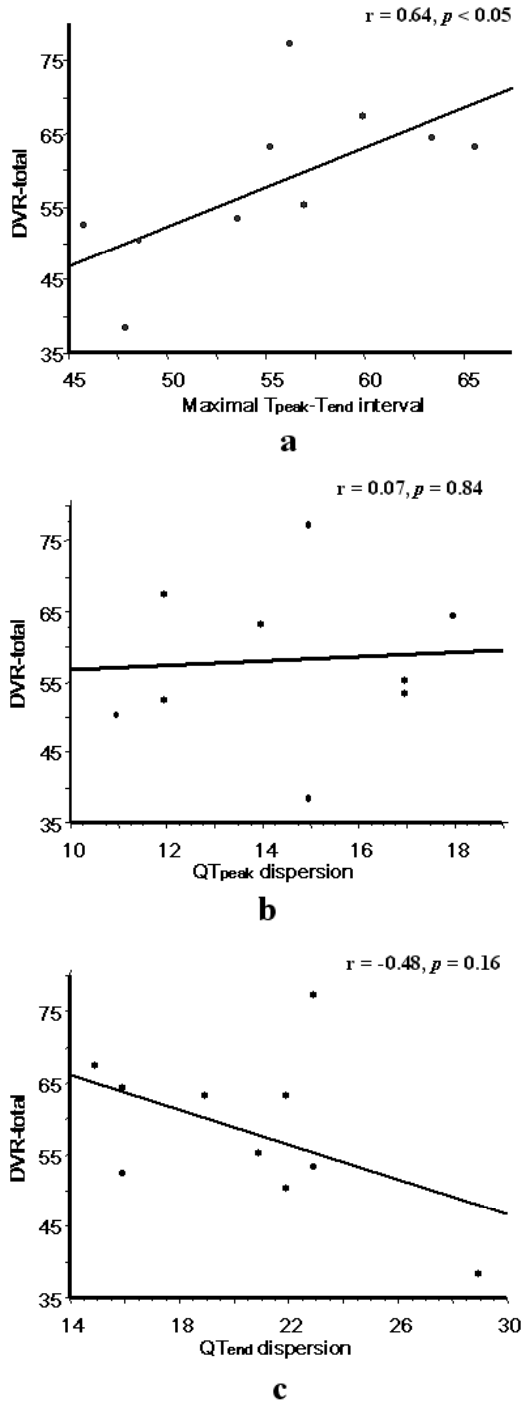

Fig. 38: Correlation analysis between the maximal T_{peak}-T_{end} interval and the global dispersion of EOR from all the MAP recordings (DVR-total) (upper panel (a)), between QT_{peak} dispersion and the DVR-total (center panel (b)), and also between QT_{end} dispersion and the DVR-total (lower panel (c)). There is high correlation between maximal T_{peak}-T_{end} interval and the DVR-total (a), whereas the QT_{peak} dispersion and QT_{end} dispersion correlate poorly with the DVR-total (b and c).

the mean and minimal T_{peak}-T_{end} intervals were both significantly less than the dispersion of EOR-total ($p < 0.01$ and $p < 0.0001$, respectively). The T_{peak}-T_{end} intervals from lead II and V_5 were also significantly less than the dispersion of EOR-total ($p < 0.001$ and $p < 0.01$, respectively).

Correlation analysis showed that there was a high correlation between the maximal T_{peak}-T_{end} interval and the dispersion of EOR-total (r = 0.64, $p < 0.05$) (Fig. 38, panel a), whereas correlation analysis between the mean T_{peak}-T_{end} interval and the dispersion of EOR-total gave an r value of 0.56 ($p = 0.09$). There was no correlation between T_{peak}-T_{end} intervals from lead II and V_5 and the dispersion of EOR-total (r = 0.30, $p = 0.40$ and r = 0.33, $p = 0.35$, respectively). In addition, no significant correlation was found when the dispersion of EOR-total was compared with the QT_{peak} dispersion and QT_{end} dispersion (r = 0.07, $p = 0.84$ and r = -0.48, $p = 0.16$, respectively) (Fig. 38, panels b and c).

GENERAL DISCUSSION

1. Methodological aspects of global MAP mapping and ART mapping (Study I)

In clinical electrophysiological studies, local refractoriness is usually assessed using programmed stimulation. However, programmed stimulation at multiple sites is time-consuming, which limits the usefulness of the method in evaluating global repolarization and its dispersion.

The activation recovery interval, measured from the local intrinsic deflection to the termination of the "T" wave on the unipolar electrograms, has been used to estimate the local refractoriness in epicardial, endocardial and intramural measurements in experimental studies (41), and has been shown to represent local effective refractory period of the human epicardium and endocardium (43, 199). Gepstein *et al.* measured this interval on unipolar electrograms of the left ventricle in pigs using the CARTO system to evaluate global ventricular refractoriness and explore the activation-repolarization coupling (115). Different from the activation recovery interval, the ART was often defined as the time from the onset of QRS complex to the termination of the T wave on the unipolar electrogram. Since the ART combines the local activation time and local activation recovery interval, it should be a better estimate of local EOR time. However, few studies on global ventricular ART sequence and ART dispersions have been reported, and most existing studies have calculated the ART from the body surface ECG. In the current PhD project in patients, we tried to measure the global ART and to evaluate its relationship with the global EOR time.

Previously, we have successfully used the MAP mapping technique, which integrates the MAP recording and CARTO mapping techniques, to study the global sequence of ventricular repolarization in pigs and humans (37). In the present thesis, we used the MAP mapping technique to test whether the ART measurements from the unipolar electrogram could estimate the EOR time from the MAPs, recorded simultaneously using the same electrode, and to verify if the ART sequence could reproduce that of the EOR. The results show that repolarization sequence was recognizable in almost all the ART maps, and the ART sequence was consistent with the EOR sequence. These findings suggest that

ART from unipolar electrograms is a reliable estimate of the EOR time obtained from MAP recordings.

The measurement of ART on the unipolar electrograms shares the same limitation as the measurement of QT interval in recordings with distorted and/or low amplitude "T" waves on the unipolar electrograms. In this project, we excluded all the unipolar electrograms where the end of the "T" wave was difficult to determine, along with the MAP recordings from the same site. In addition, we used the generally adopted intersection of the baseline with the tangent to the maximal slope on the terminal phase of the "T" wave to facilitate the determination of the end of the ART. Lastly, we recorded MAP and unipolar electrogram simultaneously using the CARTO mapping system, i.e. all the unipolar electrograms were recorded when an appropriate contact pressure was applied to the recording site. Thus, the morphologies of the unipolar electrograms were somewhat different from those of the conventional unipolar recordings, mostly with an "ST" segment elevation as seen in Fig. 17. As a result, the end of ART was much easier to define in comparison to conventional unipolar electrocardiogram recordings.

2. The agreement between the ART and EOR measurements (Study I)

The activation recovery interval on unipolar electrograms is approximately equal to the MAP duration, while the ART was approximately equal to EOR time on the MAP recordings. Thus, the global sequence of ART should reflect repolarization sequence, as does the EOR sequence on MAP recordings. In the patients of this project, the ART sequence was consistent with the EOR sequence in almost all of the maps (Figs. 24 and 25). The absolute measurement values of the ARTs were similar to the EOR times and close correlations between the ARTs and EOR times were found (Figs. 22 and 23). Furthermore, the global ART dispersion was very comparable to that of the EOR. More interestingly, our agreement analyses showed that the differences between these two measurements were almost all within the range of the mean difference ± 2 SD and the lower and upper limits of agreement were -47 and +43 ms for all the measurements (Fig. 22). Analysis of 95% confidence limits suggested that the ARTs could be at most 50 ms shorter or 46 ms longer than the EOR times, if the measurements were

repeated in another group of patients. Considering that the absolute measurement values are about 330-360 ms and the maximum possible differences are about 40-50 ms, i.e. 12-14% of the measurement values, the two measurements can be judged to agree well with each other.

These results suggest that the ART measured from unipolar electrograms is a good estimate of the EOR time from the MAP recordings, and thus the global recording of unipolar electrograms might be a useful alternative for analysis of the global sequence and dispersion of ventricular repolarization.

3. MAP mapping over both epi- and endocardium as a method for evaluation of global repolarization (Studies II and III)

As stated above, the MAP mapping technique, which integrates the MAP recording and CARTO mapping techniques, has been found to be reliable in studying the endocardial repolarization sequences of the atrium and ventricle in pigs and humans (37, 226). In this Ph.D. project, MAP was recorded over both the epicardium and endocardium in 10 open-chest pigs using the CARTO system, in order to evaluate the global ventricular repolarization, and its relationship with the ECG parameters of repolarization.

Intramural MAP recording was not available in these pigs. As a result, the repolarization of the M cells may be missing, which might lead to inadequate interpretation of global repolarization. However, the distribution of M cells in the porcine ventricle appears to be different from those in dogs (45, 51, 227). The major difference is that the cells with typical M cell features are not confined to the midmyocardial layers, but are also present in the epicardium (51). In addition, in contrast to humans and dogs, the pig has a transmural Purkinje system, so that in both right and left ventricular walls there is no spread of the activation from the endocardium to the epicardium, but rather a more or less simultaneous activation of the whole ventricular wall, in an apex to base direction (228). Furthermore, the significantly longer AP duration of M cells in isolated canine ventricle was mostly recorded at a cycle length of about 2000 ms (47, 50), whereas the transmural gradient would remarkably decrease at shorter cycle length. Thus, under the heart rate of 130 bpm in intact porcine ventricle, the AP duration of M cells may decrease and could be close to those of epicardial and endocardial myocytes. On

the other hand, MAP records the voltage gradients between cells depolarized by contact pressure of the recording electrode and the surrounding normal cells that periodically depolarize and repolarize (214, 215). Thus, it is not only the superficial layer of cells that is involved in the genesis of MAP potentials, although it is not clear exactly how deep the MAP records and whether the M cells contribute to the genesis of the MAP. Moreover, the range of local activation times on the MAPs we recorded was found to cover the whole duration of the QRS complex in all the pigs, which suggests that our MAP mapping was relatively complete. Thus, MAP mapping in these pigs over both the epicardium and endocardium provided the most detailed *in vivo* data available for evaluation of the global repolarization and the genesis of the T wave.

4. The T wave and global repolarization of the ventricle

Relationship of the peak and end of the T wave with the full repolarization of the epi- and endocardium

In contrast to previous studies (50, 169, 229), it was found in this Ph.D. work using 10 open-chest pigs that the T_{peak} was about 30-40 ms before the full repolarization of the epicardium. Interestingly T_{peak} coincided well with the earliest EOR as shown in Fig. 37, and a significant positive correlation was found between them. The data of maximal and minimal EOR_{epi}, EOR_{endo}, and EOR_{total} were all obtained by the measurement from a single site in each pig. Therefore the values of minimal and/or maximal EOR times may have been subject to measurement errors and may thus have affected our results analysis. To avoid this possibility, the 5 earliest and latest EOR time points were also selected and compared with the T_{peak} and T_{end} time points in the sampling window of the CARTO system. Consistently, the T_{peak} coincided with the 5 earliest EORs, which was different from the finding in the above-mentioned *in vitro* studies (50, 229). On the other hand, the T_{end} coincided well with the latest EOR in the *in vivo* models (Fig. 37), which agrees with previous observations (50, 229).

One possible reason for the different findings may be that the distribution of M cells and the Purkinje system in the porcine ventricle differ from those in dogs (45, 51, 227), which could make the repolarization pattern different from that of the

canine ventricle. However, the complex *in vivo* 3-dimensional pattern of the global repolarization gradients was more likely to be the reason for the different findings between the porcine model and the canine ventricular wedge preparations. As discussed above, the ventricular wedge preparations used in previous studies were too small and simple to reflect the complex 3-dimensional repolarization pattern. In such a small wedge, especially when paced in the middle at a very long cycle length of 2000 ms, the transmural repolarization gradient could be exaggerated while the gradient vertical to the transmural axis would be minimized. In the intact heart, at a much shorter cycle length, e.g. < 500 ms in our Studies II and III, the transmural repolarization gradient would be much smaller and the apico-basal repolarization gradients appeared to be much more important, which may be the reason why many *in vivo* and clinical studies have failed to demonstrate a significant transmural repolarization gradient (31, 32, 41, 135).

Our data presented here do not allow one to clarify the electrophysiological background for the coincidence between the T_{peak} and the earliest EOR in our model. One hypothesis would be that the global sequential EOR, starting within the septum, reaches the apex and/or the paraseptal areas near the apex, and then turns over towards the basal areas that make the apico-basal gradients predominant. As a result, the T vector would be seen to change sharply due to this gradient change, which would lead to the inscription of the T_{peak}. The earlier findings that the global repolarization sequence in principle follows the activation sequence in pigs and in humans (37) also lend support to this hypothesis. In other words, the *in vivo* ventricular repolarization is a complex process and besides transmural repolarization gradients, apico-basal repolarization gradients should also be involved in the genesis of the T waves. Further experiments are clearly needed to address this issue.

T_{peak}-T_{end} interval as an index of the global DVR

It has been hypothesized that the T wave vector is generated by different local levels of repolarization in the heart (164, 167), so that the T wave emerges from inhomogeneous recovery throughout the heart. Based on this theory, the T wave width, which represents the repolarization time differences in the heart, was postulated to correlate highly with the dispersion of repolarization. Thus, the

T_{peak}-T_{end} interval was chosen as a measurement of half the T wave width due to the difficulties in determination of the T wave onset, and reported to be highly correlated with the dispersion of AP duration and recovery time in isolated rabbit heart model (30).

As mentioned above, *in vitro* studies in the dog have suggested that full repolarization of the epicardium coincides with the peak of the T wave and that of the subendocardially located M cells coincides with the end of the T wave (161, 169). The T_{peak}-T_{end} interval was therefore proposed and used as an index of transmural DVR. Several clinical studies have demonstrated the potential usefulness of this variable as a predictor of ventricular arrhythmias (95, 162). However, *in vivo* evaluation of the relationship between T_{peak}-T_{end} interval and the global DVR is still lacking.

In the Studies II and III, data from about 100 MAP recordings over both the epicardium and endocardium in each of the 10 pigs were analyzed using the electroanatomic mapping technique. We found that the maximal T_{peak}-T_{end} interval appeared to be similar to, and positively associated with the DVR-total. These results are not completely consistent with those of previous studies (161, 169). Since the dispersion of EOR-total, the maximal EOR time differences over both the epicardium and endocardium, reflects not only the transmural gradients, but also the apico-basal gradients, our results suggest that the maximal T_{peak}-T_{end} interval may be a good estimation of global DVR. To our knowledge, this is the first *in vivo* validation of the T_{peak}-T_{end} interval as an index of the global DVR. Certainly, the relationship between T_{peak}-T_{end} intervals and global dispersion of EOR times was validated here in normal heart, not in a model of heart disease. In addition, due to the missing information on repolarization of the midmyocardial cells, our data did not allow us to clarify the relationship between the global dispersion of repolarization and transmural gradients in greater depth.

The method for T_{peak}-T_{end} interval measurement must also be established. T_{peak}-T_{end} interval measured from the earliest T_{peak} to the latest T_{end} on the 12 lead ECG, i.e. the maximal T_{peak}-T_{end} interval, may be a better index of the global dispersion of EOR times. As we know, time points of the T_{peak} and T_{end} vary from lead to lead, which results in the T_{peak}-T_{end} intervals showing a discrepancy on different leads of the ECG. Some studies have selected special leads such as II, V_5, an average of all leads, or ambulatory ECG to analyze the T_{peak}-T_{end} interval (162,

230, 231). However, our results have shown that the T_{peak}-T_{end} interval from lead II, V_5, or the average T_{peak}-T_{end} interval of all 12 leads, does not correlate with the DVR-total as well as it might, but the maximal T_{peak}-T_{end} interval does. This suggests that the T_{peak}-T_{end} interval measurement from a single lead or an average value from the 12 lead ECG was not reliable as an index of the global dispersion of repolarization. Certainly, the placement of leads in pigs in Studies II and III, especially the precordial ones, did not correspond exactly to the placement of leads in humans - since the vector summation should be different due to the difference in anatomy and the changes from open-chest surgery. However, our data still suggest that the measurement of T_{peak}-T_{end} interval should not be obtained arbitrarily from any lead of the surface ECG. Further investigation is clearly required in order to define the measurement of this ECG interval in humans.

QT dispersion failed to reflect global DVR

Since the 1990s, the measurement of QT dispersion has been proposed as a simple noninvasive measurement of DVR from 12-lead surface ECG (154). Increased QT dispersion was considered to reflect an increased DVR, and was thereby used as a prognostic tool in detection of future malignant ventricular arrhythmias or sudden death in patients with various heart diseases (154, 159). However, numerous prognostic studies have reported contradictory results, and the interpretation of QT dispersion seems to be contradictory to the vector loop theory of ECG wave forms (155, 157, 158, 160).

In Study III, the QT_{peak} and QT_{end} dispersion were both poorly correlated with the dispersion of EOR-total, suggesting that these variables do not reflect the global DVR. This is inconsistent with the findings of previous studies (30, 232). However, these previous studies were limited by the number of MAP recordings from the ventricle. The global DVR may be poorly estimated from a few adjacent or remote ventricular sites, as shown in a recent study (120), which may explain the inconsistency between our results and those of others. In Study III, both the epicardial and endocardial dispersion of EOR times were significantly smaller than the dispersion of EOR-total. This further emphasizes the importance of number of recording sites for evaluation of the global dispersion of repolarization. Hence, the increased QT dispersion more likely indicates a significantly disturbed

T vector loop. Although this may be a risk factor of malignant ventricular arrhythmias, QT_{peak} or QT_{end} dispersion were not reliable indexes of the global DVR.

5. Relationship between activation and repolarization sequence (Study IV)

Repolarization sequence follows that of activation under ventricular pacing

The conventional view is that the repolarization sequence is in the direction opposite to that of the activation, which has been supported mainly by the ECG finding that the polarities of the T wave are concordant with those of the QRS complex (109). Experimental findings supporting the above concept were mainly based on evidence of transmural gradients, with the inner wall being more negative than the outer wall (35). Earlier clinical studies found a negative correlation between MAPd and AT in MAP recordings from 5-11 sites, and this was used to support the concept of opposite directions of activation and repolarization (39, 113). In later *in vitro* studies using the optical mapping technique (116-118), the repolarization sequence was considered to be independent of activation sequence. This was based on the phenomenon that repolarization shows a relatively uniform pattern associated with ventricular fiber orientation when the pacing is altered from the epicardium to the endocardium in ventricular sheet preparations (116). Obviously, the relationship between activation and repolarization sequence has not been investigated in sufficient depth.

Recently, in a series of experimental and clinical studies from our institution, around 50 MAPs from the endocardium of the LV were recorded during sinus rhythm using the CARTO system (37). In spite of a significant negative correlation between the MAP duration and AT, a positive correlation between the EOR time and AT was demonstrated, suggesting that the magnitude of the progressive shortening of MAP duration was not enough to compensate for the progressive delay in the AT. As a result, the sequence of repolarization was similar to that of activation during sinus rhythm, as has also been supported by other studies (114, 115). In Study IV, a negative correlation between the MAPd and AT and a positive correlation between the EOR time and AT were also found

during RA pacing. Interestingly, after changes in the activation sequence by RV_{Endo} and LV_{Epi} pacing, the repolarization sequence also changed to follow the activation sequence. These results are consistent with our previous findings of concordant sequences of the EOR and AT (37), and they strongly support the importance of the activation sequence in modulating the repolarization patterns. An earlier study by Lux *et al*. lends experimental support to our conclusion. These authors recorded high-resolution arrays of unipolar electrograms from the canine epicardium and found that the repolarization "waves" propagated away from the pacing site, irrespective of its location, and replicated "collision" when multiple sites were paced simultaneously (110).

Contribution of activation time to patterns of repolarization during ventricular pacing

Under normal ventricular activation, the repolarization follows the activation sequence – as shown in an the study of Yuan *et al* (37). In Study IV, the repolarization followed the activation sequence even under RV_{Endo} and LV_{Epi} pacing. The mechanisms of modulation of repolarization by the activation sequence are still unclear. One of the mechanisms that have been proposed to explain the effect of activation sequence on repolarization is electrotonic interaction (86, 233-235). Passive electrotonic coupling between cells can impose an electrical load on myocytes during propagation, and altered activation sequence may modulate AP duration by altering the electrotonic load during repolarization (235). AP duration would be shortened in the direction of propagation as repolarized upstream cells may abbreviate repolarization of the AP plateau of downstream cells. In addition, the significant and persistent change in AP duration demonstrated by other investigators has suggested that many currents, such as I_{to}, are also being changed under such conditions (236-238), which could also be involved in the mechanisms of the repolarization changes.

In addition to these possible mechanisms, our *in vivo* data suggest that the relatively slow ventricular activation time during ventricular pacing may make an essential contribution to the sequence and pattern of ventricular repolarization. During RA pacing, impulse conducts quickly in the ventricles through the Purkinje system at around 3-4 m/s (239). During ventricular stimulation from the

base of the LV and the apex of the RV, however, the activation does not spread along the Purkinje fibres, but goes slowly through the ordinary myocardial fibres at about 0.2-1 m/s (240, 241), as also indicated by the relatively greater global AT of ventricles during ventricular pacing in the 10 close-chest pigs. In addition, impulses conduct faster along the endocardial fibres and, as a result, the total activation time required for the activation is shorter under endocardial pacing than under epicardial pacing (239), which could explain the shorter total AT during RV_{Endo} pacing than during LV_{Epi} pacing in the study. Thus, the considerably delayed AT during ventricular pacing accounts more for the corresponding late EOR than does the progressive shortening of MAP with progressively later AT, which was evidenced by the less steep slope between the MAPd and AT during LV_{Epi} pacing in Study IV. Moreover, the concordant sequence between activation and repolarization during LV_{Epi} pacing in all pigs further supports the importance of slow impulse propagation in modulating the repolarization pattern during ventricular pacing.

Short-term electrical remodeling by altered activation sequence

In the 10 close-chest pigs under altered ventricular pacing, there was a negative correlation between MAPd and AT, despite the change of pacing site under different pacing protocols, and during LV_{Epi} pacing MAPd appeared significantly greater than during RV_{Endo} pacing. Interestingly, the inducement of this electrical remodeling was observed within only a few hours of altered activation sequences.

Previous reports on the influence of altered activation sequence on ventricular repolarization have mainly been studies on cardiac memory, and the available data were generally obtained after the cessation of a period of altered ventricular activation (79, 82, 238, 242). The repolarization changes that happen during alteration of activation sequence, especially those under abrupt sequence changes, were little known. In canine wedge preparations, Libbus *et al*. found that the transmural AP duration could be changed significantly a few minutes after the pacing site was altered from the endocardium to the epicardium (85, 238). In isolated rabbit heart preparations, Costard-Jackle *et al*. observed a negative

correlation between the AT and AP duration during either RA pacing or 60-120 min of RV pacing (86), which is consistent with our results.

One may argue that in these 10 close-chest pigs, the MAP sequentially recorded during the first few hours of ventricular pacing may have been influenced by the time-dependent changes, as observed in the isolated rabbit heart preparations: that continuous ventricular pacing could produce slow changes of AP duration (86). However, each corresponding set of AT, MAPd and EOR time used for correlation analysis in our study was measured on the same recording from the same site, which has cancelled the potential time-dependent effect. Moreover, the MAPs were randomly recorded over the right and left ventricular endocardium under each pacing protocol, which could also minimize the influence of the time-dependent changes, if any. In addition, previous studies have suggested that the AP duration should reach steady state after approximately 15 min of activation sequence changes (85, 238), which further supports the validity of our data acquired after at least 30 min of steady-state pacing for assessment of the modulation of the global repolarization under altered activation sequence. Importantly, the changes in repolarization during altered ventricular pacing protocols under *in vivo* conditions may be different from those during normal activation sequence, after the cessation of pacing in isolated heart preparations (86).

6. Increased global dispersion of ventricular repolarization during LV_{Epi} pacing (Study V)

Resynchronization therapy most commonly involves one endocardial pacing from the RV apex and one epicardial pacing from the LV free wall via a branch of the coronary sinus, which can obviously lead to a non-physiological activation sequence. Any pacing strategy that alters the normal activation sequence has the potential to alter the repolarization heterogeneity – either in a favorable or an unfavorable manner. Recent studies have suggested that the ventricular activation sequence during epicardial pacing may augment transmural DVR in the ventricular myocardium (95-97, 243), which might be associated with the malignant ventricular arrhythmia in patients under biventricular pacing. However, these studies have been focused mainly on changes in transmural repolarization;

little is known about the changes in global DVR induced by altered pacing strategy.

Increased DVR during epicardial pacing

Study V provides *in vivo* evidence that a pacing site-dependent change in activation sequence can lead to alterations in repolarization heterogeneities, and LV_{Epi} pacing may significantly increase the global DVR.

Several pacing site-dependent electrophysiological changes appear to be involved in the augmentation of DVR by LV_{Epi} pacing. Firstly, the repolarization gradients are significantly changed by the altered activation sequence. Either during LV_{Epi} or RV_{Endo} pacing, the changes in MAP duration and EOR time follow the same principle that the longest MAP and shortest EOR times are always located in the area closest to the pacing site, and the shortest MAP and longest EOR times close to the latest activated area, as has been described in the previous sections. Secondly, the altered conduction time under different pacing protocols has different roles in alteration of the DVR. In Study V, although the dispersion of AT during RV_{Endo} pacing was increased compared to that during RA pacing, the dispersion of EOR was not markedly augmented. During LV_{Epi} pacing, however, the increased dispersion of AT subsequently led to remarkable augmentation of the dispersion of EOR, i.e. the delayed conduction during LV_{Epi} pacing contributed more to the exaggeration of DVR. The expression “conduction is not a two-way street” is applicable not only to transmural activation *in vitro* (136), but also to global transmural depolarization *in vivo.* On the other hand, during LV_{Epi} pacing, the earliest recorded AT over the endocardium was around 30 ms later than the pacing artifact, i.e. a greater dispersion of AT could be observed if the mapping also included the epicardium. Consequently, an even greater DVR by LV_{Epi} pacing could be expected, which might constitute a further potential risk of malignant ventricular arrhythmias. Thirdly, MAP duration can be changed considerably by altered activation sequence. Compared to those during RA and RV_{Endo} pacing, the MAP durations were significantly increased during LV_{Epi} pacing, which also made a contribution to the augmentation of DVR. This seems inconsistent with findings from ventricular wedge preparations, in which an increase in DVR during LV_{Epi} pacing is the consequence of altered ventricular

activation sequence independently of intracellular AP duration (95, 96). One possible explanation is that our study was performed in pigs whereas the previous studies were performed in canine heart preparations. Even so, Libbus *et al*., using canine wedge preparations, also found prolonged AP duration after a period of alteration of activation sequence from endocardium to epicardium (85). Moreover, in a recent study, similar observations were found that LV_{Epi} pacing is associated with a prolongation of MAP duration in dogs (97), which lends *in vivo* support to our results.

Thus, in addition to the augmentation of transmural DVR during the LV_{Epi} pacing (95-97, 243), significant exaggeration of global DVR could also be observed, which may be linked to the development of ventricular tachyarrhythmias in a subgroup of patients with biventricular pacing therapy.

ECG parameters of dispersion of ventricular repolarization

In the series of close-chest pigs under ventricular pacing, several ECG parameters for DVR have been analyzed. QT intervals, QT dispersion and T_{peak}-T_{end} intervals during LV_{Epi} pacing were all significantly greater than those during RA and RV_{Endo} pacing, which is consistent with previous experimental studies (95-97, 243). However, a recent clinical study showed that in patients with congestive heart failure and left bundle branch block, the QT interval, QT dispersion and T_{peak}-T_{end} interval appeared similar during RV and LV pacing, although biventricular pacing could lead to a decrease in these parameters (244). The discrepancy between the findings of the latter study and the results presented in this thesis may be due to the fact that our data were from normal heart, whereas the other study involved failure heart with intraventricular conduction delay. Further studies in models mimicking the clinical situation are required.

T_{peak}-T_{end} interval has recently been proposed and used as an index of transmural DVR under both endocardial and epicardial pacing (161), and it was suggested to be a more reliable noninvasive parameter for assessment of DVR than QT interval and QT dispersion (244). On the other hand, in Study III we have suggested that T_{peak}-T_{end} interval also reflects the global repolarization gradients, which also supports the findings in Study V. The T_{peak}-T_{end} interval during LV_{Epi} pacing increased significantly in these 10 close-chest pigs as compared to that

during LA and RV_{Endo} pacing, but it did not show any precedence over the QT interval and QT dispersion for assessment of the global DVR. These data, however, were merely from the endocardium and thus do not allow us to access the transmural dispersion of repolarization. Although the prognostic value of these noninvasive parameters for repolarization heterogeneities remains controversial, the marked prolongations of the QT interval, QT dispersion and T_{peak}-T_{end} interval found in the pigs during LV_{Epi} pacing nevertheless suggest an increased DVR and a potential risk of ventricular tachyarrhythmias.

7. Clinical implications

ART mapping on evaluation of ventricular repolarization (Study I)

In the clinical setting, extensive MAP mapping is generally difficult. However, unipolar electrograms are readily obtainable using conventional electrode catheters. The ART obtained from the unipolar electrograms estimated the local repolarization parameters well, as shown in Study I. The global sequence and dispersion of ventricular repolarization evaluated using the MAP mapping technique could well be estimated from the ART measured from unipolar electrograms; thus the latter might serve as a method for studying the sequence and dispersion of ventricular repolarization in the clinical setting.

T_{peak}-T_{end} interval on assessment of DVR (Studies II and III)

Noninvasive detection of increased DVR bears important clinical implications. The T_{peak}-T_{end} interval is easily available from 12-lead ECG and has been demonstrated in Studies II and III to be a useful noninvasive index of the global DVR. Among the different measurement methods of this interval, the maximal T_{peak}-T_{end} interval - from the earliest T_{peak} to the latest T_{end} – appears from the present study to be suitable for estimation of the global DVR. On the other hand, based on our data, the QT_{peak} and QT_{end} dispersion were not favorable.

Increased DVR during ventricular epicardial pacing (Study V)

Although the clinical benefits of biventricular pacing therapy are well established, little is known about its influence on ventricular repolarization. In recent experimental studies, biventricular pacing has been suggested to have potentially detrimental effects on ventricular repolarization (95-97). Moreover, clinical documentations of tachyarrhythmias induced by biventricular pacing have been reported (95, 98-102), even though prospective, randomized studies have not found any evidence of excess mortality due to sudden death in these patients (105, 245, 246). In Study V, in addition to the augmentation of transmural DVR as observed in previous studies (95-97), increased global DVR during LV_{Epi} pacing was found - which may further expose a subset of patients to an increased risk of malignant ventricular arrhythmias. Further investigation is required to evaluate the value of DVR for risk stratification in patients with LV_{Epi} or biventricular pacing, and to assess whether the implantable cardioverter defibrillator backup might be necessary for a subgroup of patients with biventricular pacing therapy (92, 93, 98).

In addition, whether or not RV_{Endo} pacing, LV_{Epi} pacing, or biventricular pacing is the optimal strategy for managing patients with intraventricular conduction delays in the absence of significant ventricular dysfunction is still a controversial issue (247). Our *in vivo* findings suggest that LV_{Epi} or biventricular pacing should be selected with caution as an alternative strategy. Certainly, the increased DVR in our study is observed during LV_{Epi} pacing in normal porcine heart, and further studies are clearly needed to evaluate the changes of repolarization under different pacing protocols in models that mimic clinical situations.

8. Limitations of the present studies

Unipolar electrograms recorded via the same catheter as for MAP recordings (Study I)

In contrast to the conventional unipolar electrograms, the unipolar electrograms in Study I were recorded with the catheter perpendicular to and in contact with the endocardium and with a gentle contact pressure, as required by the simultaneous recordings of the MAPs. As a result, the morphology of the unipolar electrograms was different from that in conventional recordings.

Although the ART values and the sequence of the ART were consistent with those of EOR from MAP recordings in our results, the same result might not necessarily be obtained from conventional recordings of unipolar electrograms. Further studies are needed to verify whether the ARTs measured from conventional unipolar electrograms were also well correlated with the EOR times from MAP mapping.

No information on the intramural repolarization is available (Studies II and III)

Intramural MAP recording was not available in this project. As a result, the repolarization of the midmyocardially located M cells may be missing. However, It is not only the superficial layer of cells that is involved in the genesis of MAPs; the repolarization of deeper layers of cells could also be reflected by the MAP signals (214, 215), although exactly how deep the MAP records and whether or not the M cells contribute to the genesis of the MAP is not clear. In addition, in the porcine ventricle, M cells are not only confined to the midmyocardial layer; they are also present in the epicardial layer (45, 51, 227). Furthermore, in contrast to man and dog, the pig has a transmural Purkinje system, so that the activation does not spread from the endocardium to the epicardium, but rather goes more or less simultaneously through the different layers of the ventricular wall (228). Importantly, the significantly longer AP duration of M cells in isolated canine ventricle was mostly recorded at a cycle length of 2000 ms (9), whereas the transmural gradient would be markedly minimized at shorter cycle lengths, such as 130 bpm in the pigs of this project. These factors suggest that our findings from recordings over both epicardium and endocardium are nevertheless the most detailed *in vivo* data on global DVR available for validation of the related ECG variables.

Lack of recordings from the right ventricle (Studies II and III)

The MAP recordings were only performed in the left ventricle in most of the open-chest pigs, in which the repolarization of the right ventricle was missing. However, activation and repolarization in the two ventricles are synchronized and the left ventricular mass contributes predominantly to the genesis of the QRS

complex and the T waves. The range of local activation times on our recorded MAPs was found to cover the whole duration of the QRS complex in all 10 open-chest pigs, which indicates the relative completeness of our MAP mapping. Moreover, our observation in 2 of the 10 open-chest pigs that had both the left and right ventricles mapped showed that the minimal and maximal EOR times were located in the left ventricle in both, which further supports the validity of our data for the purpose of the Studies II and III.

Potential influence of time-dependent changes in ventricular repolarization (Studies I - V)

In all the 5 studies, MAPs were sequentially recorded during a procedure of 1-3 hours, whereas the ECG parameters were measured on 3 occasions during the mapping procedure of each ventricle. Time-dependent changes of MAP configuration might have influenced our EOR measurement, if existed (248). However, during on-line monitoring and off-line measurement of MAP and surface ECG, no alternans was observed. Importantly, the MAPs were recorded randomly from numerous sites and systematic findings were observed on the sequence and dispersion of repolarization, which suggest the results were not influenced by time-dependant changes. In addition, in Studies II and III, the ECG parameters were measured three times at the beginning, middle, and end of the MAP mapping procedure, and each time 2 consecutive beats were measured. Thus, the QT interval measurements were from 6 sets of measurement results, which may further minimize the influence of the potentially time-dependent changes on our analysis.

Potential influence of short-term remodeling by altered ventricular pacing (Studies IV and V)

Short-term cardiac memory studies have suggested that several hours of ventricular pacing could persistently modulate the ventricular repolarization (86, 249). Thus, in the 10 pigs with altered ventricular pacing site the MAPs were recorded sequentially over a few hours of ventricular pacing and the data from the latter pacing protocol may have been influenced by the former. However, previous studies have demonstrated that the AP duration would reach relatively steady state

after approximately 15 min of activation sequence changes (85), which supports the validity of our data acquired after 30 min of sinus rhythm and then at least 30 min of steady-state pacing under altered activation sequence. In addition, the MAPs were randomly recorded over the right and left ventricular endocardium under each pacing protocol, which could further minimize the influence of the time-dependent changes, if any. Moreover, in these close-chest pigs, the LV_{Epi} pacing did not show any significant influence on the MAP during the subsequent RV_{Endo} pacing in Group II, and no difference in the dispersion of AT and EOR was found between the two groups during RV_{Endo} pacing. These findings suggest that the short-term cardiac memory did not have any critical influence in Studies IV and V.

SUMMARY AND CONCLUSION

- The ARTs from unipolar electrograms and the EOR times from MAP recordings were globally mapped over the left or right ventricular endocardium using the CARTO system in 12 patients with cardiac arrhythmias.

  The differences between the two measurements for all the 473 sites were 2±22 ms (NS), almost all of which were within the range of mean difference ± 2 standard deviations. A significant, positive correlation between the ART and the EOR time was found. The global dispersion of ART was consistent with that of EOR, as was the repolarization sequence measured using these two methods. These findings suggest the usefulness of the ART measurement in evaluation of global sequence and dispersion of ventricular repolarization (Study I).

- Global MAP mapping was performed over both the epicardium and endocardium in 10 healthy open-chest pigs, with 12-lead ECG being recorded simultaneously. The coincidence of the peak and end of the T wave with the full repolarization of the epicardium and endocardium was, for the first time, *in vivo* evaluated.

  The peak of the T wave occurred clearly before the full repolarization of the epicardium, but coincided well with the earliest global EOR, either on the epi- or the endocardium. The end of the T wave was coincident with the full repolarization of the endocardium. These findings suggest that not only the transmural gradients, but also the apico-basal repolarization gradients contribute to the genesis of the T wave (Study II).

  The maximal T_{peak}-T_{end} interval coincided and was positively correlated with the total dispersion of EOR over both the epicardium and endocardium. The mean T_{peak}-T_{end} interval or the T_{peak}-T_{end} interval from a single lead were

significantly smaller than and poorly correlated with the total dispersion of EOR, as were the dispersions in QT_{peak} and QT_{end} intervals. These findings suggest that the maximal T_{peak}-T_{end} interval could serve as a noninvasive index of the global DVR, but not the conventional QT dispersion parameters, nor the mean T_{peak}-T_{end} interval and the T_{peak}-T_{end} intervals from a single lead (Study III).

- Using the MAP mapping technique, global sequence and dispersion of ventricular repolarization under RA pacing, RV endocardial pacing and LV epicardial pacing were evaluated *in vivo* in 10 healthy pigs.

The repolarization sequence followed the activation sequence not only during RA pacing, but also during RV endocardial and LV epicardial pacing, suggesting the importance of the activation sequence in governing the repolarization characteristics (Study IV).

These data provide *in vivo* evidence that pacing site-dependent changes in activation sequence can lead to alterations in ventricular repolarization heterogeneities. Compared to RA and RV endocardial pacing, LV epicardial pacing increases the global DVR and also the QT interval, QT dispersion and T_{peak}-T_{end} interval. These findings may indicate the involvement of exaggeration of global DVR in the incidence of malignant ventricular arrhythmias in a subgroup of patients with biventricular pacing (Study V).

Significant changes in repolarization from an altered activation sequence could happen within a few hours *in vivo*, implying that electrical remodeling of the ventricles may be rapidly induced by an altered activation sequence (Studies IV and V).

REFERENCES

1. Zipes DP. Epidemiology and mechanisms of sudden cardiac death. Can J Cardiol 2005;21 Suppl A:37-40.

2. Myerburg R, Castellanos A. Cardiac arrest and sudden cardiac death. Philadelphia, PA: WB Saunders; 2001.

3. Zipes DP, Camm AJ, Borggrefe M, Buxton AE, Chaitman B, Fromer M, et al. ACC/AHA/ESC 2006 guidelines for management of patients with ventricular arrhythmias and the prevention of sudden cardiac death: a report of the American College of Cardiology/American Heart Association Task Force and the European Society of Cardiology Committee for Practice Guidelines (Writing Committee to Develop Guidelines for Management of Patients With Ventricular Arrhythmias and the Prevention of Sudden Cardiac Death). J Am Coll Cardiol 2006;48(5):e247-346.

4. Camm A, Katritsis D. Risk stratification of patients with ventricular arrhythmias. Philadelphia, PA: WB Saunders; 2000.

5. Nerbonne JM, Kass RS. Molecular physiology of cardiac repolarization. Physiol Rev 2005;85(4):1205-53.

6. Oudit GY, Kassiri Z, Sah R, Ramirez RJ, Zobel C, Backx PH. The molecular physiology of the cardiac transient outward potassium current (I(to)) in normal and diseased myocardium. J Mol Cell Cardiol 2001;33(5):851-72.

7. Shimizu W, Antzelevitch C. Cellular and ionic basis for T-wave alternans under long-QT conditions. Circulation 1999;99(11):1499-507.

8. Efimov IR, Huang DT, Rendt JM, Salama G. Optical mapping of repolarization and refractoriness from intact hearts. Circulation 1994;90(3):1469-80.

9. Yan GX, Antzelevitch C. Cellular basis for the normal T wave and the electrocardiographic manifestations of the long-QT syndrome. Circulation 1998;98(18):1928-36.

10. Shimizu W, Antzelevitch C. Cellular basis for long QT, transmural dispersion of repolarization, and torsade de pointes in the long QT syndrome. J Electrocardiol 1999;32 Suppl:177-84.

11. Drouin E, Charpentier F, Gauthier C, Laurent K, Le Marec H. Electrophysiologic characteristics of cells spanning the left ventricular wall of human heart: evidence for presence of M cells. J Am Coll Cardiol 1995;26(1):185-92.

12. Asano Y, Davidenko JM, Baxter WT, Gray RA, Jalife J. Optical mapping of drug-induced polymorphic arrhythmias and torsade de pointes in the isolated rabbit heart. J Am Coll Cardiol 1997;29(4):831-42.

13. Rosen MR. The electrocardiogram 100 years later: electrical insights into molecular messages. Circulation 2002;106(17):2173-9.

14. Balser JR. The cardiac sodium channel: gating function and molecular pharmacology. J Mol Cell Cardiol 2001;33(4):599-613.

15. Kurokawa J, Abriel H, Kass RS. Molecular basis of the delayed rectifier current I(ks)in heart. J Mol Cell Cardiol 2001;33(5):873-82.

16. Tseng GN. I(Kr): the hERG channel. J Mol Cell Cardiol 2001;33(5):835-49.

17. Anderson ME. Ca2+-dependent regulation of cardiac L-type Ca2+ channels: is a unifying mechanism at hand? J Mol Cell Cardiol 2001;33(4):639-50.

18. Bers DM. Cardiac excitation-contraction coupling. Nature 2002;415(6868):198-205.

19. Marks AR. Ryanodine receptors/calcium release channels in heart failure and sudden cardiac death. J Mol Cell Cardiol 2001;33(4):615-24.

20. Wang Q, Shen J, Splawski I, Atkinson D, Li Z, Robinson JL, et al. SCN5A mutations associated with an inherited cardiac arrhythmia, long QT syndrome. Cell 1995;80(5):805-11.

21. Wang Q, Curran ME, Splawski I, Burn TC, Millholland JM, VanRaay TJ, et al. Positional cloning of a novel potassium channel gene: KVLQT1 mutations cause cardiac arrhythmias. Nat Genet 1996;12(1):17-23.

22. Curran ME, Splawski I, Timothy KW, Vincent GM, Green ED, Keating MT. A molecular basis for cardiac arrhythmia: HERG mutations cause long QT syndrome. Cell 1995;80(5):795-803.

23. Splawski I, Tristani-Firouzi M, Lehmann MH, Sanguinetti MC, Keating MT. Mutations in the hminK gene cause long QT syndrome and suppress IKs function. Nat Genet 1997;17(3):338-40.

24. Abbott GW, Sesti F, Splawski I, Buck ME, Lehmann MH, Timothy KW, et al. MiRP1 forms IKr potassium channels with HERG and is associated with cardiac arrhythmia. Cell 1999;97(2):175-87.

25. Opthof T. In vivo dispersion in repolarization and arrhythmias in the human heart. Am J Physiol Heart Circ Physiol 2006;290(1):H77-8.

26. de Bakker JM, OptHof T. Is the apico-basal gradient larger than the transmural gradient? J Cardiovasc Pharmacol 2002;39(3):328-31.

27. Szentadrassy N, Banyasz T, Biro T, Szabo G, Toth BI, Magyar J, et al. Apico-basal inhomogeneity in distribution of ion channels in canine and human ventricular myocardium. Cardiovasc Res 2005;65(4):851-60.

28. Antzelevitch C, Fish J. Electrical heterogeneity within the ventricular wall. Basic Res Cardiol 2001;96(6):517-27.

29. Antzelevitch C, Sicouri S, Litovsky SH, Lukas A, Krishnan SC, Di Diego JM, et al. Heterogeneity within the ventricular wall. Electrophysiology and pharmacology of epicardial, endocardial, and M cells. Circ Res 1991;69(6):1427-49.

30. Zabel M, Portnoy S, Franz MR. Electrocardiographic indexes of dispersion of ventricular repolarization: an isolated heart validation study. J Am Coll Cardiol 1995;25(3):746-52.

31. Taggart P, Sutton PM, Opthof T, Coronel R, Trimlett R, Pugsley W, et al. Transmural repolarisation in the left ventricle in humans during normoxia and ischaemia. Cardiovasc Res 2001;50(3):454-62.

32. Opthof T, Coronel R, Wilms-Schopman FJ, Plotnikov AN, Shlapakova IN, Danilo P, Jr., et al. Dispersion of repolarization in canine ventricle and the electrocardiographic T wave: T(p-e) interval does not reflect transmural dispersion. Heart Rhythm 2007;4(3):341-8.

33. Lux RL, Green LS, MacLeod RS, Taccardi B. Assessment of spatial and temporal characteristics of ventricular repolarization. J Electrocardiol 1994;27 Suppl:100-5.

34. Kuo CS, Atarashi H, Reddy CP, Surawicz B. Dispersion of ventricular repolarization and arrhythmia: study of two consecutive ventricular premature complexes. Circulation 1985;72(2):370-6.

35. Spach MS, Barr RC. Ventricular intramural and epicardial potential distributions during ventricular activation and repolarization in the intact dog. Circ Res 1975;37(2):243-57.

36. Conrath CE, Wilders R, Coronel R, de Bakker JM, Taggart P, de Groot JR, et al. Intercellular coupling through gap junctions masks M cells in the human heart. Cardiovasc Res 2004;62(2):407-14.

37. Yuan S, Kongstad O, Hertervig E, Holm M, Grins E, Olsson B. Global repolarization sequence of the ventricular endocardium: monophasic action potential mapping in swine and humans. Pacing Clin Electrophysiol 2001;24(10):1479-88.

38. Cheng J, Kamiya K, Liu W, Tsuji Y, Toyama J, Kodama I. Heterogeneous distribution of the two components of delayed rectifier K+ current: a potential mechanism of the proarrhythmic effects of methanesulfonanilideclass III agents. Cardiovasc Res 1999;43(1):135-47.

39. Franz MR, Bargheer K, Rafflenbeul W, Haverich A, Lichtlen PR. Monophasic action potential mapping in human subjects with normal electrocardiograms: direct evidence for the genesis of the T wave. Circulation 1987;75(2):379-86.

40. Antzelevitch C, Sicouri S. Clinical relevance of cardiac arrhythmias generated by afterdepolarizations. Role of M cells in the generation of U waves, triggered activity and torsade de pointes. J Am Coll Cardiol 1994;23(1):259-77.

41. Anyukhovsky EP, Sosunov EA, Rosen MR. Regional differences in electrophysiological properties of epicardium, midmyocardium, and endocardium. In vitro and in vivo correlations. Circulation 1996;94(8):1981-8.

42. Balati B, Varro A, Papp JG. Comparison of the cellular electrophysiological characteristics of canine left ventricular epicardium, M cells, endocardium and Purkinje fibres. Acta Physiol Scand 1998;164(2):181-90.

43. el-Sherif N, Caref EB, Yin H, Restivo M. The electrophysiological mechanism of ventricular arrhythmias in the long QT syndrome. Tridimensional mapping of activation and recovery patterns. Circ Res 1996;79(3):474-92.

44. Li GR, Feng J, Yue L, Carrier M. Transmural heterogeneity of action potentials and Ito1 in myocytes isolated from the human right ventricle. Am J Physiol 1998;275(2 Pt 2):H369-77.

45. Rodriguez-Sinovas A, Cinca J, Tapias A, Armadans L, Tresanchez M, Soler-Soler J. Lack of evidence of M-cells in porcine left ventricular myocardium. Cardiovasc Res 1997;33(2):307-13.

46. Sicouri S, Antzelevitch C. A subpopulation of cells with unique electrophysiological properties in the deep subepicardium of the canine ventricle. The M cell. Circ Res 1991;68(6):1729-41.

47. Sicouri S, Fish J, Antzelevitch C. Distribution of M cells in the canine ventricle. J Cardiovasc Electrophysiol 1994;5(10):824-37.

48. Sicouri S, Quist M, Antzelevitch C. Evidence for the presence of M cells in the guinea pig ventricle. J Cardiovasc Electrophysiol 1996;7(6):503-11.

49. Yan GX, Antzelevitch C. Cellular basis for the electrocardiographic J wave. Circulation 1996;93(2):372-9.

50. Yan GX, Shimizu W, Antzelevitch C. Characteristics and distribution of M cells in arterially perfused canine left ventricular wedge preparations. Circulation 1998;98(18):1921-7.

51. Stankovicova T, Szilard M, De Scheerder I, Sipido KR. M cells and transmural heterogeneity of action potential configuration in myocytes from the left ventricular wall of the pig heart. Cardiovasc Res 2000;45(4):952-60.

52. Morita ST, Zipes DP, Morita H, Wu J. Analysis of action potentials in the canine ventricular septum: No phenotypic expression of M cells. Cardiovasc Res 2007;74(1):96-103.

53. Liu DW, Antzelevitch C. Characteristics of the delayed rectifier current (IKr and IKs) in canine ventricular epicardial, midmyocardial, and endocardial myocytes. A weaker IKs contributes to the longer action potential of the M cell. Circ Res 1995;76(3):351-65.

54. Zygmunt AC, Eddlestone GT, Thomas GP, Nesterenko VV, Antzelevitch C. Larger late sodium conductance in M cells contributes to electrical heterogeneity in canine ventricle. Am J Physiol Heart Circ Physiol 2001;281(2):H689-97.

55. Zygmunt AC, Goodrow RJ, Antzelevitch C. I(NaCa) contributes to electrical heterogeneity within the canine ventricle. Am J Physiol Heart Circ Physiol 2000;278(5):H1671-8.

56. Sicouri S, Moro S, Elizari MV. d-Sotalol Induces Marked Action Potential Prolongation and Early Afterdepolarizations in M but Not Empirical or Endocardial Cells of the Canine Ventricle. J Cardiovasc Pharmacol Ther 1997;2(1):27-38.

57. Litovsky SH, Antzelevitch C. Transient outward current prominent in canine ventricular epicardium but not endocardium. Circ Res 1988;62(1):116-26.

58. Di Diego JM, Sun ZQ, Antzelevitch C. I(to) and action potential notch are smaller in left vs. right canine ventricular epicardium. Am J Physiol 1996;271(2 Pt 2):H548-61.

59. Janse MJ, Capucci A, Coronel R, Fabius MA. Variability of recovery of excitability in the normal canine and the ischaemic porcine heart. Eur Heart J 1985;6 Suppl D:41-52.

60. Burgess MJ, Green LS, Millar K, Wyatt R, Abildskov JA. The sequence of normal ventricular recovery. Am Heart J 1972;84(5):660-9.

61. Burgess MJ. Relation of ventricular repolarization to electrocardiographic T wave-form and arrhythmia vulnerability. Am J Physiol 1979;236(3):H391-402.

62. Bauer A, Becker R, Freigang KD, Senges JC, Voss F, Hansen A, et al. Rate- and site-dependent effects of propafenone, dofetilide, and the new I(Ks)-blocking agent chromanol 293b on individual muscle layers of the intact canine heart. Circulation 1999;100(21):2184-90.

63. Antzelevitch C, Yan GX, Shimizu W. Transmural dispersion of repolarization and arrhythmogenicity: the Brugada syndrome versus the long QT syndrome. J Electrocardiol 1999;32 Suppl:158-65.

64. Taggart P, Sutton P, Opthof T, Coronel R, Kallis P. Electrotonic cancellation of transmural electrical gradients in the left ventricle in man. Prog Biophys Mol Biol 2003;82(1-3):243-54.

65. Hoffman BF. Electrotonic modulation of the T wave. Am J Cardiol 1982;50(2):361-2.
66. Moe GK. Oscillating concepts in arrhythmia research; a personal account. Int J Cardiol 1984;5(1):109-13.

67. Tan RC, Joyner RW. Electrotonic influences on action potentials from isolated ventricular cells. Circ Res 1990;67(5):1071-81.

68. Rohr S. Role of gap junctions in the propagation of the cardiac action potential. Cardiovasc Res 2004;62(2):309-22.

69. Verkerk A, Veldkamp M, de Jonge N, Wilders R, Van Ginneken A. Injury current modulates afterdepolarizations in single human ventricular cells. Cardiovasc Res 2000;47:124-132.

70. Franz MR. The electrical restitution curve revisited: steep or flat slope--which is better? J Cardiovasc Electrophysiol 2003;14(10 Suppl):S140-7.

71. Bass BG. Restitution of the action potential in cat papillary muscle. Am J Physiol 1975;228(6):1717-24.

72. Elharrar V, Surawicz B. Cycle length effect on restitution of action potential duration in dog cardiac fibers. Am J Physiol 1983;244(6):H782-92.

73. Weiss JN, Garfinkel A, Spano ML, Ditto WL. Chaos and chaos control in biology. J Clin Invest 1994;93(4):1355-60.

74. Pastore JM, Girouard SD, Laurita KR, Akar FG, Rosenbaum DS. Mechanism linking T-wave alternans to the genesis of cardiac fibrillation. Circulation 1999;99(10):1385-94.

75. Weiss JN, Garfinkel A, Karagueuzian HS, Qu Z, Chen PS. Chaos and the transition to ventricular fibrillation: a new approach to antiarrhythmic drug evaluation. Circulation 1999;99(21):2819-26.

76. Delmar M, Ibarra J, Davidenko J, Lorente P, Jalife J. Dynamics of the background outward current of single guinea pig ventricular myocytes. Ionic mechanisms of hysteresis in cardiac cells. Circ Res 1991;69(5):1316-26.

77. Koller BS, Karasik PE, Solomon AJ, Franz MR. Prolongation of conduction time during premature stimulation in the human atrium is primarily caused by local stimulus response latency. Eur Heart J 1995;16(12):1920-4.

78. Peterson BZ, Lee JS, Mulle JG, Wang Y, de Leon M, Yue DT. Critical determinants of Ca(2+)-dependent inactivation within an EF-hand motif of L-type Ca(2+) channels. Biophys J 2000;78(4):1906-20.

79. Rosenbaum MB, Blanco HH, Elizari MV, Lazzari JO, Davidenko JM. Electrotonic modulation of the T wave and cardiac memory. Am J Cardiol 1982;50(2):213-22.

80. Patberg KW, Shvilkin A, Plotnikov AN, Chandra P, Josephson ME, Rosen MR. Cardiac memory: mechanisms and clinical implications. Heart Rhythm 2005;2(12):1376-82.

81. Patberg KW, Rosen MR. Molecular determinants of cardiac memory and their regulation. J Mol Cell Cardiol 2004;36(2):195-204.

82. Alessandrini RS, McPherson DD, Kadish AH, Kane BJ, Goldberger JJ. Cardiac memory: a mechanical and electrical phenomenon. Am J Physiol 1997;272(4 Pt 2):H1952-9.

83. Geller JC, Rosen MR. Persistent T-wave changes after alteration of the ventricular activation sequence. New insights into cellular mechanisms of 'cardiac memory'. Circulation 1993;88(4 Pt 1):1811-9.

84. Brandt RR, Shen WK. Bradycardia-induced polymorphic ventricular tachycardia after atrioventricular junction ablation for sinus tachycardia-induced cardiomyopathy. J Cardiovasc Electrophysiol 1995;6(8):630-3.

85. Libbus I, Rosenbaum DS. Transmural action potential changes underlying ventricular electrical remodeling. J Cardiovasc Electrophysiol 2003;14(4):394-402.

86. Costard-Jackle A, Goetsch B, Antz M, Franz MR. Slow and long-lasting modulation of myocardial repolarization produced by ectopic activation in isolated rabbit hearts. Evidence for cardiac "memory". Circulation 1989;80(5):1412-20.

87. Yu H, McKinnon D, Dixon JE, Gao J, Wymore R, Cohen IS, et al. Transient outward current, Ito1, is altered in cardiac memory. Circulation 1999;99(14):1898-905.

88. Patberg KW, Plotnikov AN, Quamina A, Gainullin RZ, Rybin A, Danilo P, Jr., et al. Cardiac memory is associated with decreased levels of the transcriptional factor CREB modulated by angiotensin II and calcium. Circ Res 2003;93(5):472-8.

89. Plotnikov AN, Yu H, Geller JC, Gainullin RZ, Chandra P, Patberg KW, et al. Role of L-type calcium channels in pacing-induced short-term and long-term cardiac memory in canine heart. Circulation 2003;107(22):2844-9.

90. Obreztchikova MN, Patberg KW, Plotnikov AN, Ozgen N, Shlapakova IN, Rybin AV, et al. I(Kr) contributes to the altered ventricular repolarization that determines long-term cardiac memory. Cardiovasc Res 2006;71(1):88-96.

91. Patel PM, Plotnikov A, Kanagaratnam P, Shvilkin A, Sheehan CT, Xiong W, et al. Altering ventricular activation remodels gap junction distribution in canine heart. J Cardiovasc Electrophysiol 2001;12(5):570-7.

92. Turitto G, El-Sherif N. Cardiac resynchronization therapy: a review of proarrhythmic and antiarrhythmic mechanisms. Pacing Clin Electrophysiol 2007;30(1):115-22.

93. Fish JM, Brugada J, Antzelevitch C. Potential proarrhythmic effects of biventricular pacing. J Am Coll Cardiol 2005;46(12):2340-7.

94. Strickberger SA, Conti J, Daoud EG, Havranek E, Mehra MR, Pina IL, et al. Patient selection for cardiac resynchronization therapy: from the Council on Clinical Cardiology Subcommittee on Electrocardiography and Arrhythmias and the Quality of Care and Outcomes Research Interdisciplinary Working Group, in collaboration with the Heart Rhythm Society. Circulation 2005;111(16):2146-50.

95. Medina-Ravell VA, Lankipalli RS, Yan GX, Antzelevitch C, Medina-Malpica NA, Medina-Malpica OA, et al. Effect of epicardial or biventricular pacing to prolong QT interval and increase transmural dispersion of repolarization: does resynchronization therapy pose a risk for patients predisposed to long QT or torsade de pointes? Circulation 2003;107(5):740-6.

96. Fish JM, Di Diego JM, Nesterenko V, Antzelevitch C. Epicardial activation of left ventricular wall prolongs QT interval and transmural dispersion of repolarization: implications for biventricular pacing. Circulation 2004;109(17):2136-42.

97. Bai R, Lu J, Pu J, Liu N, Zhou Q, Ruan Y, et al. Left ventricular epicardial activation increases transmural dispersion of repolarization in healthy, long QT, and dilated cardiomyopathy dogs. Pacing Clin Electrophysiol 2005;28(10):1098-106.

98. Gaita F, Bocchiardo M, Porciani MC, Vivalda L, Colella A, Di Donna P, et al. Should stimulation therapy for congestive heart failure be combined with defibrillation backup? Am J Cardiol 2000;86(9A):165K-158K.

99. Di Cori A, Bongiorni MG, Arena G, Soldati E, Giannola G, Zucchelli G, et al. New-onset ventricular tachycardia after cardiac resynchronization therapy. J Interv Card Electrophysiol 2005;12(3):231-5.

100. Mykytsey A, Maheshwari P, Dhar G, Razminia M, Zheutlin T, Wang T, et al. Ventricular tachycardia induced by biventricular pacing in patient with severe ischemic cardiomyopathy. J Cardiovasc Electrophysiol 2005;16(6):655-8.

101. Guerra JM, Wu J, Miller JM, Groh WJ. Increase in ventricular tachycardia frequency after biventricular implantable cardioverter defibrillator upgrade. J Cardiovasc Electrophysiol 2003;14(11):1245-7.

102. Rivero-Ayerza M, Vanderheyden M, Verstreken S, de Zutter M, Geelen P, Brugada P. Images in cardiovascular medicine. Polymorphic ventricular tachycardia induced by left ventricular pacing. Circulation 2004;109(23):2924-5.

103. Ellenbogen KA, Wood MA, Klein HU. Why should we care about CARE-HF? J Am Coll Cardiol 2005;46(12):2199-203.

104. Daubert JC, Leclercq C, Mabo P. There is plenty of room for cardiac resynchronization therapy devices without back-up defibrillators in the electrical treatment of heart failure. J Am Coll Cardiol 2005;46(12):2204-7.

105. Bristow MR, Saxon LA, Boehmer J, Krueger S, Kass DA, De Marco T, et al. Cardiac-resynchronization therapy with or without an implantable defibrillator in advanced chronic heart failure. N Engl J Med 2004;350(21):2140-50.

106. Cleland JG, Daubert JC, Erdmann E, Freemantle N, Gras D, Kappenberger L, et al. The effect of cardiac resynchronization on morbidity and mortality in heart failure. N Engl J Med 2005;352(15):1539-49.

107. Santangelo L, Ammendola E, Russo V, Cavallaro C, Vecchione F, Garofalo S, et al. Influence of biventricular pacing on myocardial dispersion of repolarization in dilated cardiomyopathy patients. Europace 2006;8(7):502-5.

108. van Huysduynen BH, Swenne CA, Bax JJ, Bleeker GB, Draisma HH, van Erven L, et al. Dispersion of repolarization in cardiac resynchronization therapy. Heart Rhythm 2005;2(12):1286-93.

109. Wilson F, Macleod A, Barker P. The T deflection of the electrocardiogram. Trans Assoc Am Physicians 1931;46:29-38.

110. Lux RL, Ershler PR, Taccardi B. Measuring spatial waves of repolarization in canine ventricles using high-resolution epicardial mapping. J Electrocardiol 1996;29 Suppl:130-4.

111. Autenrieth G, Surawicz B, Kuo CS. Sequence of repolarization on the ventricular surface in the dog. Am Heart J 1975;89(4):463-9.

112. Kharin SN. Depolarisation and repolarisation sequences of ventricular epicardium in chickens (Gallus gallus domesticus). Comp Biochem Physiol A Mol Integr Physiol 2004;137(1):237-44.

113. Cowan JC, Hilton CJ, Griffiths CJ, Tansuphaswadikul S, Bourke JP, Murray A, et al. Sequence of epicardial repolarisation and configuration of the T wave. Br Heart J 1988;60(5):424-33.

114. Toyoshima H, Lux RL, Wyatt RF, Burgess M, Abildskov JA. Sequences of early and late phases of repolarization on dog ventricular epicardium. J Electrocardiol 1981;14(2):143-52.

115. Gepstein L, Hayam G, Ben-Haim SA. Activation-repolarization coupling in the normal swine endocardium. Circulation 1997;96(11):4036-43.

116. Efimov IR, Ermentrout B, Huang DT, Salama G. Activation and repolarization patterns are governed by different structural characteristics of ventricular myocardium: experimental study with voltage-sensitive dyes and numerical simulations. J Cardiovasc Electrophysiol 1996;7(6):512-30.

117. Salama G, Lombardi R, Elson J. Maps of optical action potentials and NADH fluorescence in intact working hearts. Am J Physiol 1987;252(2 Pt 2):H384-94.

118. Kanai A, Salama G. Optical mapping reveals that repolarization spreads anisotropically and is guided by fiber orientation in guinea pig hearts. Circ Res 1995;77(4):784-802.

119. Kongstad O, Xia Y, Liang Y, Hertervig E, Ljungstrom E, Olsson B, et al. Epicardial and endocardial dispersion of ventricular repolarization. A study of monophasic action potential mapping in healthy pigs. Scand Cardiovasc J 2005;39(6):342-7.

120. Kongstad O, Yuan S, Hertervig E, Holm M, Grins E, Olsson B. Global and local dispersion of ventricular repolarization: endocardial monophasic action potential mapping in swine and humans by using an electro-anatomical mapping system. J Electrocardiol 2002;35(2):159-67.

121. Yuan S, Blomstrom-Lundqvist C, Pehrson S, Pripp CM, Wohlfart B, Olsson SB. Dispersion of repolarization following double and triple programmed stimulation. A clinical study using the monophasic action potential recording technique. Eur Heart J 1996;17(7):1080-91.

122. Yuan S, Wohlfart B, Olsson SB, Blomstrom-Lundqvist C. The dispersion of repolarization in patients with ventricular tachycardia. A study using simultaneous monophasic action potential recordings from two sites in the right ventricle. Eur Heart J 1995;16(1):68-76.

123. Weissenburger J, Nesterenko VV, Antzelevitch C. Transmural heterogeneity of ventricular repolarization under baseline and long QT conditions in the canine heart in vivo: torsades de pointes develops with halothane but not pentobarbital anesthesia. J Cardiovasc Electrophysiol 2000;11(3):290-304.

124. Antzelevitch C. Role of transmural dispersion of repolarization in the genesis of drug-induced torsades de pointes. Heart Rhythm 2005;2(2 Suppl):S9-15.

125. Kuo CS, Reddy CP, Munakata K, Surawicz B. Mechanism of ventricular arrhythmias caused by increased dispersion of repolarization. Eur Heart J 1985;6 Suppl D:63-70.

126. Amlie JP, Kuo CS, Munakata K, Reddy PS, Surawicz B. Effect of uniformly prolonged, and increased basic dispersion of repolarization on premature dispersion on ventricular surface in dogs: role of action potential duration and activation time differences. Eur Heart J 1985;6 Suppl D:15-30.

127. Burton FL, Cobbe SM. Dispersion of ventricular repolarization and refractory period. Cardiovasc Res 2001;50(1):10-23.

128. Morgan JM, Cunningham D, Rowland E. Dispersion of monophasic action potential duration: demonstrable in humans after premature ventricular extrastimulation but not in steady state. J Am Coll Cardiol 1992;19(6):1244-53.

129. Dinerman JL, Berger R, Haigney MC, Lawrence JH, Tomaselli GF, Calkins H. Dispersion of ventricular activation and refractoriness in patients with idiopathic dilated cardiomyopathy. Am J Cardiol 1997;79(7):970-4.

130. Kuo CS, Munakata K, Reddy CP, Surawicz B. Characteristics and possible mechanism of ventricular arrhythmia dependent on the dispersion of action potential durations. Circulation 1983;67(6):1356-67.

131. Draisma HH, Schalij MJ, van der Wall EE, Swenne CA. Elucidation of the spatial ventricular gradient and its link with dispersion of repolarization. Heart Rhythm 2006;3(9):1092-9.

132. Coronel R. T wave and dispersion of repolarization. Heart Rhythm 2005;2(2):170-1.

133. Chauhan VS, Downar E, Nanthakumar K, Parker JD, Ross HJ, Chan W, et al. Increased ventricular repolarization heterogeneity in patients with ventricular arrhythmia vulnerability and cardiomyopathy: a human in vivo study. Am J Physiol Heart Circ Physiol 2006;290(1):H79-86.

134. Laurita KR, Girouard SD, Akar FG, Rosenbaum DS. Modulated dispersion explains changes in arrhythmia vulnerability during premature stimulation of the heart. Circulation 1998;98(24):2774-80.

135. Anyukhovsky EP, Sosunov EA, Feinmark SJ, Rosen MR. Effects of quinidine on repolarization in canine epicardium, midmyocardium, and endocardium: II. In vivo study. Circulation 1997;96(11):4019-26.

136. Poelzing S, Dikshteyn M, Rosenbaum DS. Transmural conduction is not a two-way street. J Cardiovasc Electrophysiol 2005;16(4):455.

137. Kurz RW, Xiao-Lin R, Franz MR. Increased dispersion of ventricular repolarization and ventricular tachyarrhythmias in the globally ischaemic rabbit heart. Eur Heart J 1993;14(11):1561-71.

138. Kuo CS, Amlie JP, Munakata K, Reddy CP, Surawicz B. Dispersion of monophasic action potential durations and activation times during atrial pacing, ventricular pacing, and ventricular premature stimulation in canine ventricles. Cardiovasc Res 1983;17(3):152-61.

139. Sedgwick ML, Rasmussen HS, Cobbe SM. Effects of the class III antiarrhythmic drug dofetilide on ventricular monophasic action potential duration and QT interval dispersion in stable angina pectoris. Am J Cardiol 1992;70(18):1432-7.

140. Moubarak JB, Karasik PE, Fletcher RD, Franz MR. High dispersion of ventricular repolarization after an implantable defibrillator shock predicts induction of ventricular fibrillation as well as unsuccessful defibrillation. J Am Coll Cardiol 2000;35(2):422-7.

141. Bazett H. An analysis of the time-relations of electrocardiograms. Heart 1920;7:353-370.

142. Algra A, Tijssen JG, Roelandt JR, Pool J, Lubsen J. QTc prolongation measured by standard 12-lead electrocardiography is an independent risk factor for sudden death due to cardiac arrest. Circulation 1991;83(6):1888-94.

143. Ahnve S. Correction of the QT interval for heart rate: review of different formulas and the use of Bazett's formula in myocardial infarction. Am Heart J 1985;109(3 Pt 1):568-74.

144. Burchell HB. The QT interval historically treated. Pediatr Cardiol 1983;4(2):139-48.

145. Cowan JC, Yusoff K, Moore M, Amos PA, Gold AE, Bourke JP, et al. Importance of lead selection in QT interval measurement. Am J Cardiol 1988;61(1):83-7.

146. Elming H, Brendorp B, Kober L, Sahebzadah N, Torp-Petersen C. QTc interval in the assessment of cardiac risk. Card Electrophysiol Rev 2002;6(3):289-94.

147. de Bruyne MC, Hoes AW, Kors JA, Hofman A, van Bemmel JH, Grobbee DE. Prolonged QT interval predicts cardiac and all-cause mortality in the elderly. The Rotterdam Study. Eur Heart J 1999;20(4):278-84.

148. Okin PM. QT interval prolongation and prognosis: further validation of the quantitative approach to electrocardiography. J Am Coll Cardiol 2004;43(4):572-5.

149. Okin PM, Devereux RB, Howard BV, Fabsitz RR, Lee ET, Welty TK. Assessment of QT interval and QT dispersion for prediction of all-cause and cardiovascular mortality in American Indians: The Strong Heart Study. Circulation 2000;101(1):61-6.

150. Puddu PE, Bernard PM, Chaitman BR, Bourassa MG. QT interval measurement by a computer assisted program: a potentially useful clinical parameter. J Electrocardiol 1982;15(1):15-21.

151. Puddu PE, Jouve R, Mariotti S, Giampaoli S, Lanti M, Reale A, et al. Evaluation of 10 QT prediction formulas in 881 middle-aged men from the seven countries study: emphasis on the cubic root Fridericia's equation. J Electrocardiol 1988;21(3):219-29.

152. Rautaharju PM, Zhang ZM. Linearly scaled, rate-invariant normal limits for QT interval: eight decades of incorrect application of power functions. J Cardiovasc Electrophysiol 2002;13(12):1211-8.

153. Schouten EG, Dekker JM, Meppelink P, Kok FJ, Vandenbroucke JP, Pool J. QT interval prolongation predicts cardiovascular mortality in an apparently healthy population. Circulation 1991;84(4):1516-23.

154. Day CP, McComb JM, Campbell RW. QT dispersion: an indication of arrhythmia risk in patients with long QT intervals. Br Heart J 1990;63(6):342-4.

155. Kors JA, van Herpen G, van Bemmel JH. QT dispersion as an attribute of T-loop morphology. Circulation 1999;99(11):1458-63.

156. Glancy JM, Weston PJ, Bhullar HK, Garratt CJ, Woods KL, de Bono DP. Reproducibility and automatic measurement of QT dispersion. Eur Heart J 1996;17(7):1035-9.

157. Malik M. QT dispersion: time for an obituary? Eur Heart J 2000;21(12):955-7.

158. Malik M, Acar B, Gang Y, Yap YG, Hnatkova K, Camm AJ. QT dispersion does not represent electrocardiographic interlead heterogeneity of ventricular repolarization. J Cardiovasc Electrophysiol 2000;11(8):835-43.

159. Priori SG, Napolitano C, Diehl L, Schwartz PJ. Dispersion of the QT interval. A marker of therapeutic efficacy in the idiopathic long QT syndrome. Circulation 1994;89(4):1681-9.

160. Liang Y, Kongstad O, Luo J, Liao Q, Holm M, Olsson B, et al. QT dispersion failed to estimate the global dispersion of ventricular repolarization measured using monophasic action potential mapping technique in swine and patients. J Electrocardiol 2005;38(1):19-27.

161. Antzelevitch C. T peak-Tend interval as an index of transmural dispersion of repolarization. Eur J Clin Invest 2001;31(7):555-7.

162. Lubinski A, Lewicka-Nowak E, Kempa M, Baczynska AM, Romanowska I, Swiatecka G. New insight into repolarization abnormalities in patients with congenital long QT syndrome: the increased transmural dispersion of repolarization. Pacing Clin Electrophysiol 1998;21(1 Pt 2):172-5.

163. Kleber AG, Janse MJ, Wilms-Schopmann FJ, Wilde AA, Coronel R. Changes in conduction velocity during acute ischemia in ventricular myocardium of the isolated porcine heart. Circulation 1986;73(1):189-98.

164. Franz MR, Bargheer K, Costard-Jackle A, Miller DC, Lichtlen PR. Human ventricular repolarization and T wave genesis. Prog Cardiovasc Dis 1991;33(6):369-84.

165. Antzelevitch C. Transmural dispersion of repolarization and the T wave. Cardiovasc Res 2001;50(3):426-31.

166. Gettes LS. The T wave: a window on ventricular repolarization? J Cardiovasc Electrophysiol 2001;12(11):1326-8.

167. Harumi K, Burgess MJ, Abildskov JA. A theoretic model of the T wave. Circulation 1966;34(4):657-68.

168. Noble D, Cohen I. The interpretation of the T wave of the electrocardiogram. Cardiovasc Res 1978;12(1):13-27.

169. Yan GX, Martin J. Electrocardiographic T wave: a symbol of transmural dispersion of repolarization in the ventricles. J Cardiovasc Electrophysiol 2003;14(6):639-40.

170. Anyukhovsky EP, Sosunov EA, Gainullin RZ, Rosen MR. The controversial M cell. J Cardiovasc Electrophysiol 1999;10(2):244-60.

171. Einthoven W. Galvanometrische registratie van het menschelijk electrocardiogram. Leiden: Eduard Ijdo; 1902.

172. Taran LM SN. The duration of the electrical systol (Q-T) in acute rheumatic carditis in Children. Am Heart J 1947;33:14-26.

173. Dekker JM, Crow RS, Hannan PJ, Schouten EG, Folsom AR. Heart rate-corrected QT interval prolongation predicts risk of coronary heart disease in black and white middle-aged men and women: the ARIC study. J Am Coll Cardiol 2004;43(4):565-71.

174. Priori SG, Schwartz PJ, Napolitano C, Bloise R, Ronchetti E, Grillo M, et al. Risk stratification in the long-QT syndrome. N Engl J Med 2003;348(19):1866-74.

175. Ahnve S. Errors in the visual determination of corrected QT (QTc) interval during acute myocardial infarction. J Am Coll Cardiol 1985;5(3):699-702.

176. McLaughlin NB, Campbell RW, Murray A. Accuracy of four automatic QT measurement techniques in cardiac patients and healthy subjects. Heart 1996;76(5):422-6.

177. Sarma JS, Sarma RJ, Bilitch M, Katz D, Song SL. An exponential formula for heart rate dependence of QT interval during exercise and cardiac pacing in humans: reevaluation of Bazett's formula. Am J Cardiol 1984;54(1):103-8.

178. Malik M. The imprecision in heart rate correction may lead to artificial observations of drug induced QT interval changes. Pacing Clin Electrophysiol 2002;25(2):209-16.

179. Willems JL, Arnaud P, van Bemmel JH, Bourdillon PJ, Brohet C, Dalla Volta S, et al. Assessment of the performance of electrocardiographic computer programs with the use of a reference data base. Circulation 1985;71(3):523-34.

180. Miller J, Zipes D. Management of the patient with cardiac arrhythmias. Philadelphia, PA: WB Saunders; 2001.

181. Gottfridsson C, Sandstedt B, Karlsson T, Edvardsson N. Spectral turbulence and late potentials in the signal-averaged electrocardiograms of patients with monomorphic ventricular tachycardia versus resuscitated ventricular fibrillation. Scand Cardiovasc J 2000;34(3):261-71.

182. Engel G, Beckerman JG, Froelicher VF, Yamazaki T, Chen HA, Richardson K, et al. Electrocardiographic arrhythmia risk testing. Curr Probl Cardiol 2004;29(7):365-432.

183. Estes NA, 3rd, Michaud G, Zipes DP, El-Sherif N, Venditti FJ, Rosenbaum DS, et al. Electrical alternans during rest and exercise as predictors of vulnerability to ventricular arrhythmias. Am J Cardiol 1997;80(10):1314-8.

184. Gold MR, Bloomfield DM, Anderson KP, El-Sherif NE, Wilber DJ, Groh WJ, et al. A comparison of T-wave alternans, signal averaged electrocardiography and programmed ventricular stimulation for arrhythmia risk stratification. J Am Coll Cardiol 2000;36(7):2247-53.

185. Chinushi M, Kozhevnikov D, Caref EB, Restivo M, El-Sherif N. Mechanism of discordant T wave alternans in the in vivo heart. J Cardiovasc Electrophysiol 2003;14(6):632-8.

186. Wilson LD, Wan X, Rosenbaum DS. Cellular alternans: a mechanism linking calcium cycling proteins to cardiac arrhythmogenesis. Ann N Y Acad Sci 2006;1080:216-34.

187. Narayan SM. T-wave alternans and human ventricular arrhythmias: what is the link? J Am Coll Cardiol 2007;49(3):347-9.

188. Choi BR, Salama G. Simultaneous maps of optical action potentials and calcium transients in guinea-pig hearts: mechanisms underlying concordant alternans. J Physiol 2000;529 Pt 1:171-88.

189. Miyoshi S, Miyazaki T, Moritani K, Ogawa S. Different responses of epicardium and endocardium to KATP channel modulators during regional ischemia. Am J Physiol 1996;271(1 Pt 2):H140-7.

190. Kleber AG, Janse MJ, van Capelle FJ, Durrer D. Mechanism and time course of S-T and T-Q segment changes during acute regional myocardial ischemia in the pig heart determined by extracellular and intracellular recordings. Circ Res 1978;42(5):603-13.

191. Dilly SG, Lab MJ. Electrophysiological alternans and restitution during acute regional ischaemia in myocardium of anaesthetized pig. J Physiol 1988;402:315-33.

192. Goette A, Honeycutt C, Langberg JJ. Electrical remodeling in atrial fibrillation. Time course and mechanisms. Circulation 1996;94(11):2968-74.

193. Vassallo JA, Cassidy DM, Kindwall KE, Marchlinski FE, Josephson ME. Nonuniform recovery of excitability in the left ventricle. Circulation 1988;78(6):1365-72.

194. Lee RJ, Liem LB, Cohen TJ, Franz MR. Relation between repolarization and refractoriness in the human ventricle: cycle length dependence and effect of procainamide. J Am Coll Cardiol 1992;19(3):614-8.

195. Witkowski FX, Penkoske PA. A completely automated activation-repolarization interval algorithm for directly coupled unipolar electrograms and its three-dimensional correlation with refractory periods. J Electrocardiol 1988;21(3):273-82.

196. Efimov IR, Cheng YN, Biermann M, Van Wagoner DR, Mazgalev TN, Tchou PJ. Transmembrane voltage changes produced by real and virtual electrodes during monophasic defibrillation shock delivered by an implantable electrode. J Cardiovasc Electrophysiol 1997;8(9):1031-45.

197. Cheng Y, Mowrey KA, Van Wagoner DR, Tchou PJ, Efimov IR. Virtual electrode-induced reexcitation: A mechanism of defibrillation. Circ Res 1999;85(11):1056-66.

198. Efimov I, Biermann M, Zipes D. Fast fluorescent mapping of electrical activity in the heart: practical guide to experimental design and applications. New York: Blackwell publishing; 2003.

199. Chen PS, Moser KM, Dembitsky WP, Auger WR, Daily PO, Calisi CM, et al. Epicardial activation and repolarization patterns in patients with right ventricular hypertrophy. Circulation 1991;83(1):104-18.

200. Steinhaus BM. Estimating cardiac transmembrane activation and recovery times from unipolar and bipolar extracellular electrograms: a simulation study. Circ Res 1989;64(3):449-62.

201. Franz MR, Burkhoff D, Spurgeon H, Weisfeldt ML, Lakatta EG. In vitro validation of a new cardiac catheter technique for recording monophasic action potentials. Eur Heart J 1986;7(1):34-41.

202. Olsson S. Monophasic action potentials of right heart. Suction electrode method in clinical investigations. (Theses). Goteborg: Elanders Boktryckeri Aktiebolag; 1971.

203. Olsson SB, Brorson L, Edvardsson N, Varnauskas E. Estimation of ventricular repolarization in man by monophasic action potential recording technique. Eur Heart J 1985;6 Suppl D:71-9.

204. Franz MR. Current status of monophasic action potential recording: theories, measurements and interpretations. Cardiovasc Res 1999;41(1):25-40.

205. Brorson L, Olsson SB. Atrial repolarization in healthy males. Studies with programmed stimulation and monophasic action potential recordings. Acta Med Scand 1976;199(6):447-54.

206. Brorson L, Olsson SB. Right atrial monophasic action potential in patients with paroxysmal supraventricular tachyarrhythmias. Acta Med Scand 1977;201(1-2):105-10.

207. Shkurovich S, Sahakian AV, Votapka TV, Ji T, Swiryn S. Multi-site dual surface monophasic action potential mapping of atrial repolarization in vivo: is atrial repolarization a two- or three-dimensional process? J Electrocardiol 2000;33 Suppl:127-31.

208. Olsson SB, Cotoi S, Varnauskas E. Monophasic action potential and sinus rhythm stability after conversion of atrial fibrillation. Acta Med Scand 1971;190(5):381-7.

209. Yuan S, Wohlfart B, Rasmussen HS, Olsson S, Blomstrom-Lundqvist C. Effect of dofetilide on cardiac repolarization in patients with ventricular tachycardia. A study using simultaneous monophasic action potential recordings from two sites in the right ventricle. Eur Heart J 1994;15(4):514-22.

210. Franz MR. Long-term recording of monophasic action potentials from human endocardium. Am J Cardiol 1983;51(10):1629-34.

211. Hirsch I, Evardsson N, SB O. Computor based analysis of monophasic action potentials in man. Goteborg: Vasastadens Bokbinderi; 1984.

212. Kondo M, Nesterenko V, Antzelevitch C. Cellular basis for the monophasic action potential. Which electrode is the recording electrode? Cardiovasc Res 2004;63(4):635-44.

213. Nesterenko VV, Kondo M, Antzelevitch C. Biophysical basis for monophasic action potential. Cardiovasc Res 2005;65:942-944.

214. Knollmann BC, Katchman AN, Franz MR. Monophasic action potential recordings from intact mouse heart: validation, regional heterogeneity, and relation to refractoriness. J Cardiovasc Electrophysiol 2001;12(11):1286-94.

215. Knollmann BC, Tranquillo J, Sirenko SG, Henriquez C, Franz MR. Microelectrode study of the genesis of the monophasic action potential by contact electrode technique. J Cardiovasc Electrophysiol 2002;13(12):1246-52.

216. Coronel R, de Bakker JM, Wilms-Schopman FJ, Opthof T, Linnenbank AC, Belterman CN, et al. Monophasic action potentials and activation recovery intervals as measures of ventricular action potential duration: experimental evidence to resolve some controversies. Heart Rhythm 2006;3(9):1043-50.

217. Franz MR. What is a monophasic action potential recorded by the Franz contact electrode? Cardiovasc Res 2005;65(4):940-1; author reply 942-4.

218. Moore HJ, Franz MR. Monophasic Action Potential Recordings in Humans. J Cardiovasc Electrophysiol 2007.

219. Yuan S, Kongstad O, Hertervig E, Holm M, Pripp CM, Olsson SB. Recording monophasic action potentials using a platinum-electrode ablation catheter. Europace 2000;2(4):312-9.

220. Liu S, Yuan S, Hertervig E, Kongstad O, Holm M, Grins E, et al. Monophasic action potential mapping in swine and humans using modified-tip ablation catheter and electroanatomic mapping system. Scand Cardiovasc J 2002;36(3):161-6.

221. Gepstein L, Hayam G, Ben-Haim SA. A novel method for nonfluoroscopic catheter-based electroanatomical mapping of the heart. In vitro and in vivo accuracy results. Circulation 1997;95(6):1611-22.

222. Evardsson N, Hirsch I, SB O. Right ventricular monophasic action potentials in healthy young man. Pacing Clin Electrophysiol 1984;7:813-821.

223. Franz MR, Cohen I, Lee R. Correlation between action potential duration and effective refractory period in vivo: result from 25 patients with normal right ventricular myocardium. (Abstract). Pacing Clin Electrophysiol 1991;14:703.

224. Altman D, Bland J. Measurement in medicine: The analysis of method comparison studies. Statistician 1983;32:307-310.

225. Bland JM, Altman DG. Statistical methods for assessing agreement between two methods of clinical measurement. Lancet 1986;1(8476):307-10.

226. Li Z, Hertervig E, Kongstad O, Holm M, Grins E, Olsson SB, et al. Global repolarization sequence of the right atrium: monphasic action potential mapping in health pigs. Pacing Clin Electrophysiol 2003;26(9):1803-8.

227. Antzelevitch C. Are M cells present in the ventricular myocardium of the pig? A question of maturity. Cardiovasc Res 1997;36(1):127-8.

228. Hamlin RL, Burton RR, Leverett SD, Burns JW. Ventricular activation process in minipigs. J Electrocardiol 1975;8(2):113-6.

229. Antzelevitch C. Cellular Basis for the Repolarization Waves of the ECG. Ann N Y Acad Sci 2006;1080:268-81.

230. Davey PP. QT interval measurement: Q to TApex or Q to TEnd? J Intern Med 1999;246(2):145-9.

231. Nakagawa M, Takahashi N, Watanabe M, Ichinose M, Nobe S, Yonemochi H, et al. Gender differences in ventricular repolarization: terminal T wave interval was shorter in women than in men. Pacing Clin Electrophysiol 2003;26(1 Pt 1):59-64.

232. Zabel M, Lichtlen PR, Haverich A, Franz MR. Comparison of ECG variables of dispersion of ventricular repolarization with direct myocardial repolarization measurements in the human heart. J Cardiovasc Electrophysiol 1998;9(12):1279-84.

233. Osaka T, Kodama I, Tsuboi N, Toyama J, Yamada K. Effects of activation sequence and anisotropic cellular geometry on the repolarization phase of action potential of dog ventricular muscles. Circulation 1987;76(1):226-36.

234. Spach MS, Kootsey JM, Sloan JD. Active modulation of electrical coupling between cardiac cells of the dog. A mechanism for transient and steady state variations in conduction velocity. Circ Res 1982;51(3):347-62.

235. Zubair I, Pollard AE, Spitzer KW, Burgess MJ. Effects of activation sequence on the spatial distribution of repolarization properties. J Electrocardiol 1994;27(2):115-27.

236. Satoh T, Zipes DP. Rapid rates during bradycardia prolong ventricular refractoriness and facilitate ventricular tachycardia induction with cesium in dogs. Circulation 1996;94(2):217-27.

237. Rubart M, Lopshire JC, Fineberg NS, Zipes DP. Changes in left ventricular repolarization and ion channel currents following a transient rate increase superimposed on bradycardia in anesthetized dogs. J Cardiovasc Electrophysiol 2000;11(6):652-64.

238. Libbus I, Wan X, Rosenbaum DS. Electrotonic load triggers remodeling of repolarizing current Ito in ventricle. Am J Physiol Heart Circ Physiol 2004;286(5):H1901-9.

239. Myerburg RJ, Gelband H, Nilsson K, Castellanos A, Morales AR, Bassett AL. The role of canine superficial ventricular muscle fibers in endocardial impulse distribution. Circ Res 1978;42(1):27-35.

240. Wyman BT, Hunter WC, Prinzen FW, McVeigh ER. Mapping propagation of mechanical activation in the paced heart with MRI tagging. Am J Physiol 1999;276(3 Pt 2):H881-91.

241. Wener J, Scherlis L, Sandberg AA. The spread of the excitatory process and the left ventricular cavity potentials in left bundle branch block as studied with exophageal leads. Am Heart J 1951;41(6):864-74.

242. Goyal R, Syed ZA, Mukhopadhyay PS, Souza J, Zivin A, Knight BP, et al. Changes in cardiac repolarization following short periods of ventricular pacing. J Cardiovasc Electrophysiol 1998;9(3):269-80.

243. Ueda N, Zipes DP, Wu J. Epicardial but not endocardial premature stimulation initiates ventricular tachyarrhythmia in canine in vitro model of long QT syndrome. Heart Rhythm 2004;1(6):684-94.

244. Berger T, Hanser F, Hintringer F, Poelzl G, Fischer G, Modre R, et al. Effects of cardiac resynchronization therapy on ventricular repolarization in patients with congestive heart failure. J Cardiovasc Electrophysiol 2005;16(6):611-7.

245. Cazeau S, Leclercq C, Lavergne T, Walker S, Varma C, Linde C, et al. Effects of multisite biventricular pacing in patients with heart failure and intraventricular conduction delay. N Engl J Med 2001;344(12):873-80.

246. Abraham WT, Fisher WG, Smith AL, Delurgio DB, Leon AR, Loh E, et al. Cardiac resynchronization in chronic heart failure. N Engl J Med 2002;346(24):1845-53.

247. Gillis AM, Chung MK. Pacing the right ventricle: to pace or not to pace? Heart Rhythm 2005;2(2):201-6.

248. Sutton PM, Taggart P, Lab M, Runnalls ME, O'Brien W, Treasure T. Alternans of epicardial repolarization as a localized phenomenon in man. Eur Heart J 1991;12(1):70-8.

249. del Balzo U, Rosen MR. T wave changes persisting after ventricular pacing in canine heart are altered by 4-aminopyridine but not by lidocaine. Implications with respect to phenomenon of cardiac 'memory'. Circulation 1992;85(4):1464-72.

ACKNOWLEDGEMENTS

I wish to express my sincere gratitude and appreciation to all those who have helped me to complete this work. I thank especially:

Associate professor **Shiwen Yuan**, my Ph.D. supervisor, through whom the Departments of Cardiology in Dalian, China and in Lund, Sweden, established a cooperative research program, by which I was able to study in Lund and have the opportunity to receive a research education. I thank him for his continuous support and guidance throughout my study, for his critical and thoughtful comments, suggestions, and fruitful discussions during the writing of the five papers and this thesis, and for his profound knowledge of cardiac electrophysiology that has greatly contributed to the completion of this work. Also, I thank him for his caring help in my personal life in Sweden.

Professor **S. Bertil Olsson**, who provided the opportunity for me to study in Sweden and to work for the degree of Ph.D. I thank him for his helpful comments and suggestions on the five papers and this thesis. His comprehensive experience has always been a reliable resource, especially the MAP recording technique, which has become an important tool for the EP society due to his pioneering work in the 1970s. Financial support arranged by Professor Olsson has also provided a solid basis for my Ph.D. projects.

Professor **Yanzong Yang** and professor **Zhihu Lin**, my tutors in China, for giving me the opportunity to study abroad, for their consistently warm inspiration and enthusiastic encouragement, and for their strong support by way of their extensive knowledge in the field of cardiac electrophysiology**.**

My coauthors, **Ole Kongstad**, **Eva Hertervig**, **Pyotr Platonov**, and **Erik Ljungström** and the staff of the EP laboratory at Lund University Hospital, for their help in collecting materials and for all their support of my research work.

Jonas Carlson, our engineer, for his excellent technical support in the study, for solving my computer problems, and for helpful discussions on statistical issues.

Bibi Smideberg, for her kind help and friendship during my stay in Lund, and for the opportunity to enjoy the warmth of her home and some delicious meals.

Monica Magnusson, Lena Lindén, and **Iréne Nilsson** for their secretarial support and friendship during my stay in Lund.

Bjarne Madsen Härdig, for his help and friendship during my stay in Lund.

Zhen Li and **Yaxi Zheng,** for their friendship and the happiness we shared together in Lund. It is a special memory in our lives.

The **staff** of the Department of Cardiology, Lund University Hospital who all supported me.

Shaowen Liu, **Lianjun Gao**, **Shulong Zhang**, **Donghui Yang,** and all my colleagues in Dalian, for their help, support, and encouragement throughout this work. Especially for their warm help in my clinical work, daily life, and for the happiness they shared with me during my difficult task of writing this thesis.

All my friends, for their friendship and the happiness we shared together. Too many names come to mind, and they cannot all be listed here due to the limited spaces. My friends know my heart. With their companionship, I can enjoy those many cheerful activities, including pleasant journey by *Nature Bus*; watching Chinese Kungfu and art show by foreigner; celebrating the *China National Day* on Swedish old merchant ship *Goteborg*; being the interpreter on the press in Copenhagen; the organizing work for the *Lund Chinese Association* and so on. This is not only scientific Ph.D. work, but has also involved experiencing a different culture, and a wonderful and memorable life abroad. Life would have been completely different without their friendship.

In addition to the Ph.D. project, I have luckily got the opportunities to be involved in the following scientific events during these years: the *Pfizer Fellowship* trip to *Cambridge, Oxford,* and *London*; the academic visit to *St. Georg Hospital, Hamburg, Germany,* and *Hopital Haut-Leveque, Bordeaux, France*; the experience of organizing the *'China Atrial Fibrillation Symposium 2006'*; being the Chinese coordinator for the *'World Wide Online Atrial Fibrillation Symposium II'*; and the *'12th Congress of the International Society for Holter and Noninvasive Electrocardiology (ISHNE)',* on which I will receive the *'Junior Investigator Award'* by June 9th, 2007. I am really grateful to all who provided me the opportunities and made my life more colorful and fruitful.

Dr. **Alistair Hugh Kidd**, for his linguistic corrections of the five papers and this dissertation.

My parents**, Hua Xia** and **Guizhen Liang**, for their understanding and all kinds of support in my life. My brother, **Yunping Xia**, my sister in law, **Chunrong Li**, and their lovely daughter, **Ji Xia**, for their continuous and unending support, trust, and love.

My wife, **Ling Fan,** for always being there with me and for your love, support, patience, and understanding. Without you the completion of this work and full enjoyment of life would never have been possible. Thank you!

FINANCIAL SUPPORT

This work was supported by funds from the Swedish Heart-Lung Foundation, the Lund University Hospital donation funds, the Franke and Margaretha Bergqvist Foundation and Biosense Webster, Johnson & Johnson, Inc.

APPENDIX: ORIGINAL PAPERS I-V

I. **Xia Y,** Kongstad O, Hertervig E, Holm M, Olsson B, Yuan S. Activation Recovery Time Measurements in Evaluation of Global Sequence and Dispersion of Ventricular Repolarization.

II. **Xia Y,** Liang Y, Kongstad O, Liao Q, Holm M, Olsson B, Yuan S. *In Vivo* Validation of the Coincidence of the Peak and End of the T Wave with the Full Repolarization of the Epicardium and Endocardium in Swine.

III. **Xia Y,** Liang Y, Kongstad O, Liao Q, Holm M, Olsson B, Yuan S. T(peak)-T(end) Interval as an Index of Global Dispersion of Ventricular Repolarization: Evaluations Using Monophasic Action Potential Mapping of the Epi- and Endocardium in Swine.

IV. **Xia Y,** Kongstad O, Platonov P, Holm M, Olsson B, Yuan S. Ventricular Repolarization Sequence During Right Ventricular Endocardial and Left Ventricular Epicardial Pacing: Monophasic Action Potential Mapping in Swine.

V. **Xia Y,** Kongstad O, Platonov P, Holm M, Olsson B, Yuan S. Increased Global Dispersion of Ventricular Repolarization during Left Ventricular Epicardial Pacing: *In Vivo* Evaluation by Monophasic Action Potential Mapping in Swine.